

Conceptual Design of a Solar-Thermal Heating System
with Seasonal Storage for a Vashon Greenhouse

Anna Henson

A thesis
submitted in partial fulfillment of the
requirements of the degree of

Master of Science in Mechanical Engineering

University of Washington

2006

Program Authorized to Offer Degree:
Mechanical Engineering

University of Washington
Graduate School

This is to certify that I have examined this copy of a master's thesis by

Anna Henson

and have found that it is complete and satisfactory in all respects, and that any and all
revisions required by the final examining committee have been made.

Committee Members:

Philip Malte

Rita Schenck

Joyce Cooper

Date: _____

In presenting this thesis in partial fulfillment of the requirements for a master's degree at the University of Washington, I agree that the Library shall make its copies freely available for inspection. I further agree that extensive copying of this thesis is allowable only for scholarly purposes, consistent with "fair use" as prescribed in the U.S. Copyright Law. Any other reproduction for any purposes or by any means shall not be allowed without my written permission.

Signature _____

Date _____

TABLE OF CONTENTS

List of Figures	iii
List of Tables	iv
Chapter 1: Introduction	1
1.1 Objective	1
1.2 Justification for Research	1
1.3 Background	1
1.4 Seasonal Storage Review	2
1.5 System Design Requirements	5
1.6 Approach and Methodology	6
Notes to Chapter 1	9
Chapter 2: Heating Load and System Capacity Estimate	10
2.1 Assumptions and Boundary Conditions	12
2.2 Calculations and Results	13
2.2.1 Greenhouse Heat Loss	13
2.2.2 Greenhouse Heat Gain	16
2.2.3 Greenhouse Heat Demand	23
2.2.4 Storage System	24
2.2.5 Collector System	26
2.3 Conclusions	29
Notes to Chapter 2	31
Chapter 3: Comparative Life Cycle Study	32
3.1 Goal	34
3.2 Scope	34
3.2.1 Function, Functional Unit, and Reference Flows	34
3.2.2 System Boundaries	35
3.2.3 Impact Assessment Data Categories	37
3.2.4 Criteria for Inclusion of Inputs/Outputs	38
3.2.5 Data Quality Requirements	38
3.3 Inventory Analysis	38
3.3.1 Data Collection Procedure	38
3.3.2 Unit Process Description	47
3.3.3 Calculation Procedure	49
3.3.4 Results	51
3.4 Impact Assessment	53
3.4.1 Classification	54
3.4.2 Characterization	54
3.4.3 Normalization	56
3.4.4 Results	57
3.5 Interpretation	60
3.5.1 Contribution Analysis	61
3.5.2 Perturbation Analysis	63
3.5.3 Discernibility	63
3.6 Conclusions	65
Notes to Chapter 3	67

Chapter 4: Heat Transfer Simulation	70
4.1 Physical Model.....	71
4.1.1 Component Selection.....	71
4.1.2 Assumptions.....	72
4.1.3 Operating Parameters.....	73
4.2 Heat Transfer Equations	74
4.2.1 Greenhouse Hourly Heat Loss.....	74
4.2.2 Greenhouse Hourly Solar Heat Gain	75
4.2.3 Greenhouse Hourly Heat Demand	78
4.2.4 Collector Hourly Heat Gain.....	82
4.2.5 Storage System Hourly Temperatures	84
4.2.6 Heat Delivery System	87
4.3 Simulation Code Description.....	90
4.3.1 Input Parameters	90
4.3.2 Storage Geometry	91
4.3.3 Energy Balance	92
4.3.4 Storage Size Minimization.....	93
4.3.5 Cost Minimization	94
4.4 Simulation Code Results and Final Design	97
Notes to Chapter 4	102
Chapter 5: Economic Analysis.....	104
5.1 Calculation of Specific Cost per kWh	104
5.2 Economic Feasibility	106
5.3 Cost Reduction Opportunities.....	107
5.3.1 Cost breakdown	107
5.3.2 Economy of Scale	108
5.3.3 Supplemental heating.....	109
Notes to Chapter 5	110
Chapter 6: Conclusions.....	111
Bibliography	114
Appendix A: LCA Matrices.....	118
Appendix B: UWME DFE laboratory scoring method.....	120
Appendix C: SRCC Collector Certification Page.....	121
Appendix D: Heat Transfer Simulation Code.....	122
Storage Geometry Function Code.....	127
Specific Heat Function Code	128
Heat Collected Function Code.....	128
Heat Load Function Code.....	129
Greenhouse Heat Transfer Function Code.....	129

LIST OF FIGURES

Figure 2.1 Physical model of solar-thermal heating system.....	11
Figure 2.2 Greenhouse annual load profile.....	24
Figure 2.3 Annual profile of collector heat gain.....	28
Figure 3.1 Geometry of the two applicable seasonal storage design options.	33
Figure 3.2 Materials layout of the two seasonal storage design options.	34
Figure 3.3 Life cycle process flow diagram for Seasonal Storage System.....	37
Figure 3.4 Normalized heating system comparison for each insulation data set.....	58
Figure 3.5 Normalized impact comparison to Diesel.	60
Figure 3.6 Global warming contribution analysis of gravel-water pit storage.	62
Figure 3.7 Global warming contribution analysis of concrete tank heat storage.....	62
Figure 3.8 Energy use and global warming comparison with 30% uncertainty.	64
Figure 3.9 Environmental impact with 10% uncertainty range shown.....	65
Figure 4.1 Diagram of physical model with temperature nodes.....	71
Figure 4.2 Greenhouse heat profile during the 24 hour period of January 7th.....	81
Figure 4.3 Hourly greenhouse heat profile over 5 days in October.....	82
Figure 4.4 Collector heat gain as a function of the tilt angle, beta.	83
Figure 4.5 Storage tank stratification showing heat and water flow.....	85
Figure 4.6 Annual temperature change and energy balance.....	93
Figure 4.7 Heating system cost versus insulation thickness.....	95
Figure 4.8 Physical model of solar-thermal heating system.....	97
Figure 4.9 Temperature profile of storage tank throughout year.....	100
Figure 4.10 Heat gain and loss from storage system throughout year in kJ.	101
Figure 5.1 Cost breakdown of final solar heating system.....	108
Figure 5.2 Cost of Solarthermie-2000 seasonal storage system per m ³ water equivalent.....	109

LIST OF TABLES

Table 2.1	List of Assumptions.....	13
Table 2.2	Calculation of Heat Loss from Greenhouse.....	15
Table 2.3	Greenhouse Heat Loss Coefficient, $(UA)_h$ calculation.....	16
Table 2.4	Calculation of specific absorbed radiation gain on south roof in MJ/m^2	18
Table 2.5	Calculation of specific absorbed radiation on south wall in MJ/m^2	18
Table 2.6	Calculation of transmittance-absorptance products for diffuse and ground reflected radiation.....	22
Table 2.7	Calculation Total Heat Gain.....	23
Table 2.8	Heat Demand for Greenhouse in MJ.....	23
Table 2.9	Calculation of specific absorbed radiation on collector.....	27
Table 2.10	Calculation of useful heat gain to collector.....	28
Table 3.1	Materials and processes required for each storage system.....	35
Table 3.2	Original and modified input data for low density polyethylene production process.....	40
Table 3.3	Original and modified output data for low density polyethylene production process.....	41
Table 3.4	Original and modified data for BEES mineral wool production process.....	42
Table 3.5	Average US Electricity production mix and conversion efficiency.....	42
Table 3.6	Specific costs for construction of the storage system designs.....	43
Table 3.7	Calculation example of transportation requirements for LDPE pipes.....	44
Table 3.8	Transportation requirements from Commodity Flow Survey in ton-miles per kg.....	45
Table 3.9	Local transportation calculations for construction process materials in miles.....	46
Table 3.10	Total transportation requirements for 1 st phase materials in ton-miles/kg.....	46
Table 3.11	Data Quality Scores for Processes (scale 1 to 5 with 1 being best).....	49
Table 3.12	Inventory analysis results for required inputs.....	52
Table 3.13	Inventory analysis results for outputs.....	53
Table 3.14	Classification of inventory flow outputs to each impact category.....	54
Table 3.15	Equivalency factors from TRACI database (q matrix).....	56
Table 3.16	Life cycle impact assessment normalization and characterization results.....	57
Table 3.17	Life cycle impact assessment normalization and characterization results.....	57
Table 3.19	Global Warming Impact to supply 400 MWh for 20 years in kg CO_2 Equivalents.....	59
Table 3.20	Percent change of inventory vector with 1% increase of each required input.....	63
Table 4.1	Heating system component selection and justification.....	72
Table 4.2	Temperature point operating parameters.....	74
Table 4.3	Heat Loss for January 7th.....	75
Table 4.4	Hourly heat gain on south roof and wall for January 7th.....	78
Table 4.5	Heat Demand for January 7 th	81
Table 4.6	Specific costs of heating components.....	96
Table 4.7	Simulation Results.....	98

Table 5.1 Capital cost in US dollars.	105
Table 5.2 Economic analysis of solar-thermal heating system in thousands of US dollars.....	105
Table 5.3 Price comparison of solar to natural gas heating with carbon sequestration in US \$.	107

ACKNOWLEDGEMENTS

The author wishes to express sincere appreciation to the Department of Mechanical Engineering for the generous financial and educational support provided to me; Professor Joyce Cooper for imparting her extensive resources and knowledge of Life Cycle Assessment; Dr. Rita Schenck for her thoughtful involvement; and my advisor Professor Philip Malte, without whose comprehensive feedback I could not have completed this project.

Chapter 1: Introduction

1.1 Objective

The objective of this study is to design and optimize a solar-thermal heating system with seasonal storage for a large historic greenhouse on Vashon Island, in the Puget Sound of Washington state. The heating system design is optimized for environmental impact, thermal efficiency, and cost.

1.2 Justification for Research

Global climate change and fossil fuel shortages are increasingly at the forefront of US and international concerns. Solar-thermal systems are a viable alternative to burning fossil fuels for heating. The major problem arises in the fact that the solar resource is abundant during the spring and summer months while heating demand is greatest in the winter. This project will examine the feasibility of using seasonal storage to solve this problem as well as design a 100% solar heating system for a suitable application.

1.3 Background

The historic Harrington-Beall greenhouses produced high quality flowers on Vashon Island for a century, but the operations were forced to relocate to warmer climates during the 1970's oil crisis due to the high cost of heating. The Harrington-Beall greenhouses were the largest suppliers of roses in the entire United States and produced world-renowned orchids.¹

The current owners of the Harrington-Beall Greenhouse Historic District, the Institute for Environmental Research and Education, plan to restore the oldest greenhouse and want to heat it using 100% solar energy. Normally, this is accomplished by designing a “solar

greenhouse.” Modern “solar greenhouses” usually have a relatively small heating demand, mostly in the winter or during long periods of overcast. A “solar greenhouse” is basically a greenhouse designed to passively use the sun as its primary source of heating.² This is accomplished by designing the greenhouse with a large, transparent, south-facing wall tilted at the optimum angle for solar gain, with all surfaces having proper insulation, and to contain large heat capacity to store the radiation overnight (usually in the form of water in black containers). The historic Vashon greenhouses are not “solar greenhouses.” The existing structure is only moderately situated for solar gain, and for historic restoration purposes, the glass must match the original, which has poor insulation qualities. Therefore, in order for the high heating load of the Vashon greenhouses to be met by solar energy, an external system must be designed.

Given the high heating load as well as the moderate to low solar radiation in the northwest, heating the greenhouse using only solar energy is not trivial. The only way to accomplish it is to use a seasonal storage system to store the summer radiation to be used in the darker colder months from October to February. Seasonal heating systems are being developed, tested, and successfully demonstrated in Scandinavia, Germany, and Canada.

1.4 Seasonal Storage Review

The “European Large-Scale Solar Heating Network,” a “non-profit-making network of European institutes and companies researching Central Solar Heating Plants (CSHP),” was created to “enhance the development of large-scale solar heating technologies through knowledge transfer between participating countries.”³ This international network

provided an overview of the existing large-scale solar heating (a system with more than 500m² collector area) research in Europe through 1997.³ This overview lists all the large-scale plants that were operating or were planned to be built in 1997. Most of the plants supply heat to residential buildings using a central heating plant. Approximately a third of these are combination systems with wood fuel fired heating plants, especially in Sweden and Austria. Eleven of the fifty one large-scale solar heating plants listed in the overview use seasonal storage, seven of which use water as the storage medium and three use ground.⁴ All of the large-scale solar heating plants reviewed are designed to provide a fraction of the heating supplied by the system. In 1997, Sweden had the most large-scale solar heating plants in Europe, 18 out of 51. However, the interest in large-scale solar heating has increased significantly in Germany and Austria. Sweden is no longer emphasizing research in CSHP with or without seasonal storage, although most of the plants are still in use with very low operation and maintenance costs.⁵ Typical minimum values for a central solar heating plat with diurnal storage are at least 60 m² collector area and 3000 to 6000 liters of storage volume. Typical minimum values for a central solar heating plat with seasonal storage are at least 300 m² collector area and 450 m³ of storage volume.⁶ The most important characteristic differentiating seasonal storage heating systems from large diurnal heating systems is the solar fraction of demand met by the solar heating system. Large diurnal systems are designed to provide around 90% of the demand during July and August, resulting in an overall solar fraction usually around 20-30%, generally for only hot water heating. Heating systems with seasonal storage aim for a solar fraction above 50% and usually supply both hot water and space heating.

The most current research and development program of large-scale solar heating systems with seasonal storage is Germany's "Solarthermie-2000." This program has 12 plants in operation and 4 plants currently under study. Five of the twelve plants use hot-water as the heat storage medium and four use gravel-water. Of the remaining three seasonal heat stores in operation, one is an aquifer heat store, one is a duct heat store, and one is a combination hot-water and duct heat store. One of the most significant issues these programs have faced is decreased storage efficiency due to higher return temperatures from the heating network than expected.⁷ This is considered when designing the heat delivery system to the greenhouse.

All of the existing seasonal solar-thermal heating systems use supplemental fossil fuel heating to cut down on the size of the solar-thermal components. The existing system with the highest solar fraction is the Drake Landing Solar Community in Okotoks, Alberta, Canada, where 90% of the space heating requirements will be met by the large-scale solar heating system with borehole field storage (duct).⁸ Borehole fields have proven the most cost effective of the seasonal storage systems. This technology accomplishes such low cost because the thermal mass used for storage is the ground itself resulting in lower construction costs. Borehole heat exchangers (BHEs) are installed in the rock 30 to 100 meters deep and 1.5 to 3 meters apart. The BHE consists of the borehole, a single or double U-pipe or a concentric pipe with the thermal fluid (usually water) flowing from top to bottom and back up, and grouting material filled for better conduction between the pipes and the borehole wall. Another advantage of borehole field

storage is its easy expandability. However, the borehole field technology is only viable where solid ground can be drilled at least 100 feet without running into ground water flow.⁹ These conditions are not met at the Vashon site.

The two types of seasonal storage design options that are applicable to the Vashon greenhouses are a gravel-water pit or a concrete-steel hot-water tank. Both of these concepts have been designed, tested, and redesigned by “Solarthermie-2000,” the research and development program in Germany.¹⁰ The designs in this study are based on the latest systems of each type: the gravel-water pit in Steinfurt and the hot-water tank in Friedrichshafen. The 110 MWh per year Steinfurt pilot plant has a collector area of 510 m² and a storage volume of 1500 m³ (water equivalent). The 1.4 GWh per year Friedrichshafen plant has a collector area of 3500 m² and a storage volume of 12,000 m³.⁶

1.5 System Design Requirements

The Institute for Environmental Research and Education (IERE) is interested in restoring and operating their oldest greenhouse with as little environmental impact as possible.

This study examines the feasibility of heating one single greenhouse, with entirely solar energy, and containing the storage system within the footprint of the greenhouse.

Limiting land use of the system emphasizes the importance of a self-sustaining system that does not depend on land, energy, or materials outside of the system. The design requirements provided by IERE are:

1. Provide 100% solar heat to greenhouse
2. Limit the size of the storage to fit within the footprint of the greenhouse
3. Minimize environmental impact and cost

4. Maintain greenhouse temperatures ideal for optimum growing
5. Maintain historic greenhouse structure

1.6 Approach and Methodology

The bulk of the design of the greenhouse heating system is to optimize the size of each sub-system (solar collector system, storage system, and heat delivery system) to meet the design requirements listed above and stay within the operating parameters of the materials and components of the system. The selection of specific components and materials for each sub-system is also critical.

The solar resource and heating demand is preliminarily assessed in chapter 2 in order to estimate the required size of each sub-system. This analysis is simplified as much as possible and assumes typical properties for generic components. Monthly average solar radiation is used to estimate the solar heat gain to the greenhouse and average air temperatures are used to estimate the heat loss from the greenhouse. These estimates determine the final heat load that the solar-thermal heating system needs to deliver to the greenhouse. Based on this heating demand, the size of the storage and collector sub-systems can be approximated. The results of the preliminary assessment provide a solid basis for component selection and a clear approximation with which to compare final results.

A comparative life cycle study, presented in chapter 3, is performed in order to select the type of storage system, gravel-water pit or concrete water tank. The amount of materials needed for each design option is determined based on the size estimate for the storage sub-system obtained in chapter 2. The study compares the life cycle environmental

impact of building each storage design. The emissions from constructing the storage unit, manufacturing the materials in the storage unit, and all the upstream processes required to manufacture those materials are calculated in the life cycle inventory analysis. The environmental impact from the emissions of each design option is compared in the impact assessment. Finally, the significance of the impact assessment is discussed in the interpretation section. The life cycle study results provide an environmental impact and cost comparison of the two systems to determine which design option is most suitable for the Vashon application.

Chapter 4 presents a detailed heat transfer simulation, modeling the specific characteristics of each sub-system. The specific storage sub-system is determined in chapter 3 and the selection of the other sub-systems is presented at the beginning of chapter 4. The calculations performed in the detailed analysis are similar to those performed in the preliminary assessment. The most significant difference is the use of hourly rather than monthly radiation and meteorological data. This means that the set of heat transfer equations is solved 8,760 times (once for each hour) to simulate one year, instead of 12 times (once for each month) as in chapter 2. Because of the large number of calculations, MatLab is used to solve the heat transfer equations instead of the Excel spreadsheet used in chapter 2. The modeling of each sub-system is also more detailed than in chapter 2 because the characteristics of each sub-system are taken into account. This simulation optimizes the size of each component to finalize the entire system design to meet the specific needs of the Vashon greenhouse. The heating system is designed to minimize the specific cost per kWh of heat provided.

In chapter 5, a final economic analysis is performed on the heating system to determine if it is economically feasible. The specific cost per kWh is calculated based on the capital cost of the final, optimized design. Opportunities for cost reduction are also identified and discussed.

Notes to Chapter 1

¹ HistoryLink, “King County Landmarks: Harrington-Beall Greenhouse Company Historic District (ca. 1885-1989), Vashon, Vashon Island.” 5 July 2005 <www.historylink.org>.

² Magee, Tim with Ectotope Group, A solar greenhouse guide for the Pacific Northwest, (Seattle: the Group, 1979) 1.

³ European Large-Scale Solar Heating Network, “Information Brochure on Large-Scale Solar Heating: Thermie B – Contract no DIS/1164/97” (Göteborg, Sweden: CIT Energy Management AB, 1999) 4, 30 March 2005 <<http://main.hvac.chalmers.se/cshp/ELSSHN.pdf>>.

⁴ European Large-Scale Solar Heating Network, 3.

⁵ European Large-Scale Solar Heating Network, 9.

⁶ Schmidt, T., D. Mangold, H. Müller-Steinhagen, “Central solar heating plants with seasonal storage in Germany,” Solar Energy 76 (2004) 165-174.

⁷ Schmidt, T. 173.

⁸ Canada, Natural Resources Canada (NRCan), “Solar Energy Heating it up in Alberta: Homeowners will benefit from the sun’s warmth on cold, cloudy winter days,” Natural Elements 2, 27 June 2005, 10 Oct 2005 <http://www.rncan.gc.ca/elements/issues/02/cetc_e.html>.

⁹ Schmidt, T., D. Mangold, H. Müller-Steinhagen. “Seasonal Thermal Energy Storage in Germany.” paper delivered to ISES Solar World Congress sponsored by the German Federal Ministry for Economy and Technology. Göteborg, Sweden (2003) 4-5.

¹⁰ Schmidt, T. “Seasonal Thermal Energy Storage” 5.

Chapter 2: Heating Load and System Capacity Estimate

The preliminary assessment of the heating system in this chapter is performed in order to determine approximate storage capacity required to meet the greenhouse heating load. This capacity size is used to perform a comparative life cycle study on two storage designs in chapter 3 in order to determine the lowest environmental impact option. The preliminary assessment also gives a simple approximation with which to compare the detailed heat transfer simulation performed in chapter 4. All data for this section are based on monthly daily averages of incident solar radiation, temperature, and atmospheric conditions; therefore, the diurnal behavior is ignored. All data and equations used in this section come from Solar Engineering of Thermal Processes by Duffie and Beckman.¹

The physical model of the heating system is divided into three sub-systems: the greenhouse heat delivery system, the seasonal storage system, and the solar collector system. Figure 2.1 shows the three sub-systems, the heat transfer to or from them, and the thermal fluid flow between the systems.

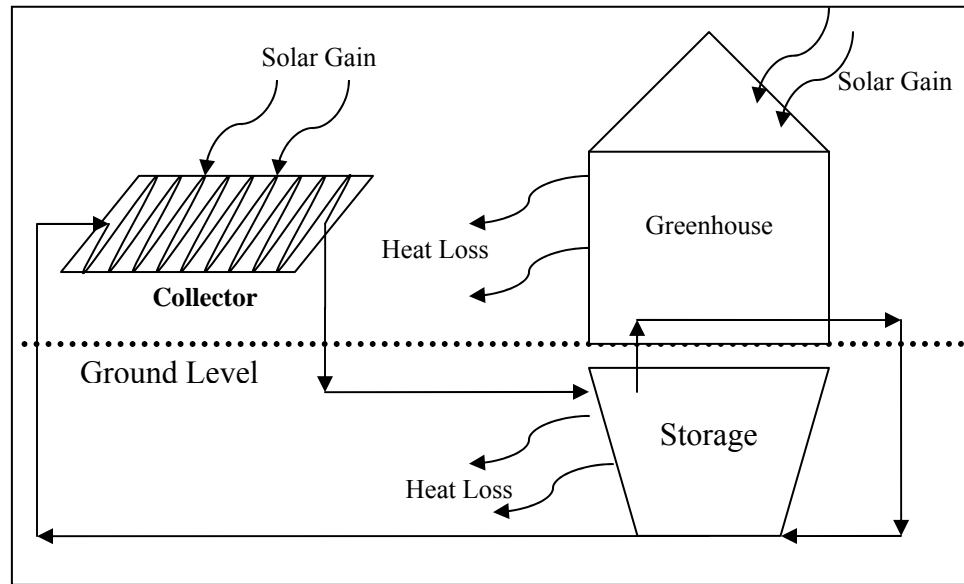


Figure 2.1 Physical model of solar-thermal heating system.

The heating load that the solar-thermal heating system needs to supply to the greenhouse is approximated by first calculating the monthly heat loss based on the outdoor temperature, indoor temperature, and heat conduction properties of the greenhouse materials in section 2.2.1 . This heat loss is partly offset by the solar heat gain through the greenhouse windows; therefore the monthly solar heat gain to the greenhouse is estimated in section 2.2.2 . Finally the heating load is determined by subtracting the solar heat gain from the heat loss in section 2.2.3 . If the monthly solar heat gain is larger than the monthly heat loss, the heating demand for the month is assumed to be zero.

Based on the heat load estimate, the size (volume of water used as thermal storage) of the seasonal storage system is estimated in section 2.2.4 . The insulation required to limit the heat loss from the storage system to 10% is also calculated. The necessary heat capacity of the storage system is assumed to be the yearly heat load plus the 10% heat loss through the storage walls.

The collector area required to supply the necessary amount of heat to the storage system is calculated in section 2.2.5. Typical collector properties, average inlet temperatures, and tilt angle equal to the latitude are assumed in order to estimate the collector efficiency for each month. This efficiency and incident solar radiation are used to calculate the monthly solar heat gain from the collectors. The collector area is solved for the yearly heat gain to equal the required heat capacity of the storage system.

2.1 Assumptions and Boundary Conditions

The heat transfer analysis involved in this preliminary assessment is simplified as much as possible while maintaining good accuracy. This is done by making appropriate assumptions and using monthly daily average meteorological data for Seattle. The detailed heat transfer simulation presented in chapter 4 eliminates many of these assumptions. The solar radiation on Vashon Island, which is geographically very close to Seattle, is thought to be higher than in Seattle, so using data for Seattle provides a conservative estimate. The amount of heat demanded by the greenhouse from the solar-thermal heating system is calculated with a steady-state energy balance:

$$\begin{aligned}
 Energy_{in} &= Energy_{out} \\
 HeatLoad + SolarHeatGain &= HeatLoss \\
 HeatLoad &= HeatLoss - SolarHeatGain
 \end{aligned}$$

Equation 2.1

This *HeatLoad* term is the amount of heat that the seasonal storage heating system needs to collect, store, and then supply to the greenhouse. The monthly daily average meteorological data provides:

\bar{H} = monthly average daily radiation on a horizontal surface in MJ/m²

\bar{K}_T = monthly average clearness index

T_a = 24-hour monthly daily average ambient temperature in C

DD_m = average number of degree days in the month to the base temperature of 18.3 C

Table 2.1 List of Assumptions.

Assumption	Justification
Monthly average daily metrological data for Seattle applies.	Simplifies estimation and provides a good approximation.
Diurnal temperature changes are ignored	Allows the calculation of one set of heat transfer equations for each month using one set of meteorological data.
The indoor air temperature of the greenhouse is maintained at 20 C.	Typical greenhouse indoor air temperature.
Cooling loads are met by increased ventilation and shading.	Standard practice in greenhouse management. ²
The heat gain from solar radiation is entirely from the south roof and the south wall.	High latitude and monthly averages result in negligible incident radiation on the north roof and other walls. Walls have small area.
The heat transfer to or from the greenhouse is steady-state.	Simplifies estimation and corresponds with using monthly average data.
There is negligible internal generation.	There are very few sources of internal generation in a greenhouse.
The greenhouse roof and windows are 8mm twin walled polycarbonate.	Information from IERE.
Heat is stored in a large seasonal storage water tank that heats to 85 C and discharges to 35 C.	Typical range for seasonal storage systems. ³ The low is limited by the return temperature from the greenhouse and the high is limited by the storage materials.
Heat loss through wall of tank is limited to 10% of the heat stored with insulation.	Insulation thickness is typically sized for about a 10% heat loss.
Storage tank is a rectangular prism sized to fit within the greenhouse footprint.	A generic geometry is used to make estimates.
Properties for water in storage system taken at 60 C.	60C is the expected average storage temperature.
Typical absorption, transmittance, and efficiency properties for the collectors apply.	A generic collector system is used to simplify the analysis.
Optimum tilt angle is equal to the latitude (47.5°).	Optimum tilt is equal to latitude when discounting weather factors. ⁴ Tilt angle will be optimized for this system in chapter 4.

2.2 Calculations and Results

2.2.1 Greenhouse Heat Loss

The heat loss rate from the greenhouse is defined as the building heat loss coefficient multiplied by the indoor-outdoor temperature difference.⁵

$$\dot{HL} = (UA)_h (Th - Ta)$$

Equation 2.2

where

\dot{HL} = rate of heat loss in Watts

$(UA)_h$ = building heat loss coefficient, 11299 W/C

Th = indoor temperature, 20 C

Ta = outdoor temperature in C

Similarly, the total heat loss for each month from the greenhouse can be defined as the building heat loss coefficient multiplied by the number of degree days for each month: ⁵

$$HL_m = \frac{MJ}{10^6 J} \frac{86400s}{day} (UA)_h DD_{h,m}$$

Equation 2.3

where

HL_m = monthly heat loss in MJ

$DD_{h,m}$ = monthly degree days for greenhouse in degrees Celsius-days

A standard degree day is the difference between the base temperature and the average outdoor temperature for each day measured in degrees. To get the number of degree days in one month each day's temperature difference is summed for the days in that month: ⁶

$$DD_m = \sum_{mo} abs(Tb - Tav)$$

Equation 2.4

where

DD_m = standard monthly degree days

Tb = base temperature or balance temperature

Tav = average outdoor temperature

Calculating the heat loss with the available monthly degree day data is preferred, because it is more accurate than using the average daily temperature for the entire month.

However, the standard degree day uses a base temperature rather than the indoor temperature in order to account for internal generation and incoming solar radiation. For

the greenhouse heat demand assessment, internal generation is assumed to be negligible and solar radiation is accounted for separately, so the degree day value must be adjusted. The standard degree day uses a base temperature of 18.3 degrees Celsius, which is typical for buildings built before 1940 with an indoor temperature of 24 Celsius.⁷ The adjusted degree days replace the base temperature, T_b , with the actual indoor temperature T_h of 20 degrees Celsius. As shown in Table 2.2, the adjusted degree days correspond to a 1.7 degree increase per day of the month.

Table 2.2 Calculation of Heat Loss from Greenhouse.

Month	T_{ave} (C) ⁸	Standard Degree Days ⁸	Adjusted Degree Days	Heat Loss (MJ)
January	3	465	518	505,416
February	6	355	403	393,462
March	7	364	417	406,812
April	9	279	330	322,169
May	13	194	247	240,846
June	15	123	174	169,871
July	18	74	127	123,694
August	18	81	134	130,527
September	15	126	177	172,800
October	11	234	287	279,897
November	7	344	395	385,627
December	5	424	477	465,388

The monthly heat loss shown in the far right column of Table 2.2 is calculated from Equation 2.3 with DD_h from the column headed “adjusted degree days” and the total building heat loss coefficient $(UA)_h$ of 11,299 W/C shown in Table 2.3. The total building heat loss coefficient is the sum of the heat loss coefficients multiplied by the surface area for each type of construction material:

$$(UA)_h = \sum_{mat} (UA)_{mat}$$

Equation 2.5

Table 2.3 Greenhouse Heat Loss Coefficient, (UA)_h calculation.

Greenhouse component	Area (m²)	U value (W/m²C)⁹	UA (W/C)
Ground	1783.74	0.5	892
Wall windows	237.83	3.35	797
Knee wall	148.64	1.48	220
Roof	2140.49	3.35	7,171
Air changes per hour	2		2,220
Total			11,299

The UA value for the air changes per hour accounts for the heat loss from the temperature difference between air leaving the building and air entering the building. It is calculated with the equation:

$$UA_{eq} = NV\rho c_p / 3600$$

Equation 2.6

where

UA_{eq} = UA equivalent for air changes, 2220 W/C

N = number of air changes per hour, 2

V = volume of interior of greenhouse, 3980 m³

ρ = density of air at 20 C, 1009 kg/m³

c_p = specific heat of air at 20 C, 0.995 J/kg-C

2.2.2 Greenhouse Heat Gain

The greenhouse monthly heat gain is approximated by first calculating the specific monthly average absorbed radiation, in MJ/m², for each south-facing surface (wall and roof). The calculation of the specific monthly absorbed radiation for the south surfaces are shown in Table 2.4 and Table 2.5 and are determined according the isotropic diffuse assumption developed by Liu and Jordan and extended by Klein:¹⁰

$$\bar{S} = \bar{H}_B \bar{R}_B (\bar{\tau\alpha})_B + \bar{H}_D (\bar{\tau\alpha})_D \frac{1 + \cos \beta}{2} + \bar{H} \rho_G (\bar{\tau\alpha})_G \frac{1 - \cos \beta}{2}$$

Equation 2.7

where

\bar{S} = monthly average daily absorbed radiation on tilted surface in MJ/m²

\bar{H} = monthly average daily radiation on a horizontal surface in MJ/m²

\bar{R}_B = monthly average ratio of beam radiation on a tilted to horizontal surface

$(\bar{\tau\alpha})$ = monthly average transmittance-absorptance product

β = tilt angle of surface from horizontal in degrees

ρ_G = ground reflectance, 0.2

This form of the absorbed radiation equation often slightly underestimates the total gain because it does not account for circumsolar diffuse or horizon brightening.¹¹ This likely underestimation results in a conservative estimate. The only difference in the calculations for the radiation value on the south roof and the south wall is the tilt angle, which is 60 degrees for the roof and 90 degrees for the wall. However, the \bar{R}_B value and the $(\bar{\tau\alpha})$ values depend on this angle. Therefore, columns 8 through 10 of Table 2.4 need to be recalculated for the vertical wall and are shown in Table 2.5.

Table 2.4 Calculation of specific absorbed radiation gain on south roof in MJ/m².

1	2	3	4	5	6	7	8	9	10	11
Month	\bar{H}^8	\bar{K}_T^8	δ	ω_s	\bar{H}_D	\bar{H}_B	\bar{R}_B	$\frac{(\bar{\tau}\alpha)_B}{(\bar{\tau}\alpha)_n}$	$(\bar{\tau}\alpha)_B$	\bar{S}_{SR}
J	2.98	0.28	-20.9	65.4	1.48	1.50	3.155	0.96	0.676	4.07
F	5.62	0.35	-13	75.4	2.73	2.89	2.65	0.97	0.683	6.85
M	9.64	0.41	-2.4	87.4	4.65	4.99	1.6	0.97	0.683	8.21
A	14.69	0.45	9.4	100.4	7.23	7.46	1.12	0.97	0.683	9.98
M	19.46	0.5	18.8	111.8	9.41	10.05	0.83	0.96	0.676	11.22
J	20.46	0.49	23.1	117.7	10.43	10.03	0.71	0.95	0.669	10.88
J	25.52	0.63	21.2	115.0	10.05	15.47	0.76	0.95	0.669	14.12
A	18.34	0.53	13.5	105.2	8.08	10.26	0.99	0.97	0.683	11.83
S	13.03	0.49	2.2	92.4	5.67	7.36	1.39	0.98	0.690	10.50
O	7.45	0.41	-9.6	79.4	3.38	4.07	2.015	0.97	0.683	7.63
N	3.83	0.32	-18.9	68.1	1.83	2.00	2.88	0.96	0.676	4.98
D	2.4	0.26	-23	62.4	1.19	1.21	3.73	0.95	0.669	3.71

Table 2.5 Calculation of specific absorbed radiation on south wall in MJ/m².

Month	\bar{R}_B	$\frac{(\bar{\tau}\alpha)_B}{(\bar{\tau}\alpha)_n}$	$(\bar{\tau}\alpha)_B$	\bar{S}_{SW}
J	3.35	0.98	0.58	3.43
F	2.16	0.96	0.57	4.51
M	1.25	0.92	0.55	5.04
A	0.65	0.86	0.51	5.00
M	0.37	0.73	0.43	4.91
J	0.28	0.66	0.39	4.67
J	0.32	0.68	0.41	5.72
A	0.52	0.79	0.47	5.39
S	0.97	0.87	0.52	5.74
O	1.81	0.94	0.56	5.33
N	2.98	0.97	0.58	4.08
D	3.83	0.98	0.58	3.11

In this model the incoming radiation is separated into beam, diffuse, and ground-reflected radiation terms. The subscripts B, D, G, refer to beam, diffuse, and ground. Each form of radiation has a geometric factor and a transmittance-absorptance factor associated with it.

The geometric factors account for the incident angle of each type of radiation. The

transmittance-absorptance factors account for the amount of radiation that passes through the window glazing.

Determining Radiation Values

The total radiation, the \bar{H} values in Table 2.4, column 2, are obtained from radiation data, but the distribution of this total radiation term into the diffuse and beam components must be estimated based on the sun angle and the clearness of the sky according to the Collares-Pereira and Rable correlation:¹²

$$\frac{\bar{H}_D}{\bar{H}} = 0.775 + 0.00606(\omega_s - 90) - [0.505 + 0.00455(\omega_s - 90)] \cos(115\bar{K}_T - 103)$$

Equation 2.8

where

ω_s = sunset hour angle

\bar{K}_T = monthly average clearness index

The clearness index shown in Table 2.4, column 3 also comes from radiation data. The sunset hour angle is the angular displacement of the sun at sunset from the local meridian. It is an indication of how long the sun is up during the day. It can be calculated with the equation below, the results of which are shown in Table 2.4, column 6:¹³

$$\omega_s = -\tan(\phi) \tan(\delta)$$

Equation 2.9

where

ϕ = latitude

δ = declination, angular displacement of the sun at solar noon

The latitude of the greenhouse site on Vashon is 47.5 degrees. The average declination angles for each month shown in Table 2.4, column 5 are for the recommended average days for months from Duffie-Beckman.¹⁴ With the input of H , K , and δ and the

calculation of ω_s , the results of equation 2.6 for H_D are shown in Table 2.4, column 6.

The H_B values in the adjacent column are determined from H_D :

$$\bar{H}_B = \bar{H} - \bar{H}_D$$

Equation 2.10

Determining Geometric Factors

The geometric factor for the beam radiation is the \bar{R}_B term. This value is the ration of the angle of the sun on the tilted surface compared to the angle on a horizontal surface.

During winter the sun is low in the sky so a surface tilted toward the south would get more sun than a horizontal surface and \bar{R}_B would be greater than one. Conversely in the summer when the sun passes overhead \bar{R}_B would be less than one. The \bar{R}_B values in column 4, Table 2.4 calculated with the equation:¹⁵

$$\bar{R}_B = \frac{\cos(\phi - \beta) \cos(\delta) \sin(\omega_s') + (\pi / 180) \omega_s' \sin(\phi - \beta) \sin(\delta)}{\cos(\phi) \cos(\delta) \cos(\omega_s) + (\pi / 180) \omega_s \sin(\phi) \sin(\delta)}$$

Equation 2.11

where

$$\omega_s' = \min \left[\begin{array}{l} \arccos(-\tan(\phi) \tan(\delta)) \\ \arccos(-\tan(\phi - \beta) \tan(\delta)) \end{array} \right]$$

Equation 2.12

The geometric factors for the diffuse and ground radiation values depend only on the tilt angle; therefore they remain constant throughout the year. The diffuse sky model assumes that the diffuse radiation is received uniformly from the entire sky dome,¹⁶

which results in a view factor from the surface to the sky of $\frac{1 + \cos \beta}{2}$. Likewise, the

reflected ground radiation is assumed to reflect uniformly from a horizontal flat surface,

so the view factor from the surface to the ground is used: $\frac{1 - \cos \beta}{2}$.

Determining Transmittance-Absorptance Products

The monthly average transmittance-absorptance products are determined by first calculating the transmittance-absorptance product with incident radiation normal to the surface, $(\tau\alpha)_n$, and then using the ratio of the true transmittance-absorptance product to the normal transmittance-absorptance product, $\frac{(\overline{\tau\alpha})}{(\overline{\tau\alpha})_n}$. The absorptance is approximated

with the equation:¹⁷

$$\alpha = \frac{\alpha_i}{\alpha_i + (1 + \alpha_i)\tau_d * A_a / A_i}$$

Equation 2.13

where

α_i = Average absorptivity of 0.7 for the interior material of the greenhouse

τ_d = Diffuse transmittance of the reflected radiation through polycarbonate, 0.74

A_a = Area of the aperture, total area of roof and windows, 2378 m²

A_i = Area of interior surface of greenhouse (not including windows), 1932 m²

Combining the resulting absorptivity of 0.719 from this equation and the transmittance value for 8mm twin walled polycarbonate of 0.81,¹⁸ the monthly average normal transmittance-absorptance product, $(\overline{\tau\alpha})_n$ is 0.596 according to the equation:¹⁹

$$(\overline{\tau\alpha})_n = 1.01\tau\alpha$$

Equation 2.14

The ratios of $\frac{(\overline{\tau\alpha})}{(\overline{\tau\alpha})_n}$ are given as a function of the incident angle θ on figure 5.6.1 on page

230 of Duffie-Beckman adapted from Klein. For the diffuse and ground radiation this value remains constant throughout the year since the incident angle does not depend on the path of the sun. The effective incident angles for the isotropic diffuse and ground-reflected radiation are determined from figure 5.4.1 on page 227 of Duffie and Beckman.

The incident angle for the beam radiation is determined from figure 5.10.1b on page 240 of Duffie-Beckman for each month based on the tilt angle and the latitude. The transmittance-absorptance ratios and final transmittance-absorptance values for beam radiation for each month are shown in Table 2.4, columns 9 and 10 for the south roof and Table 2.5, columns 3 and 4 for the south wall. The effective incident angles, transmittance-absorptance ratios, and the final transmittance absorptance products for ground and diffuse radiation are shown in Table 2.6.

Table 2.6 Calculation of transmittance-absorptance products for diffuse and ground reflected radiation.

	S Roof at 60°	S Wall at 90°
$\theta_{e,D}$	56.5°	59°
$\theta_{e,G}$	65°	59°
$\frac{(\overline{\tau\alpha})_D}{(\overline{\tau\alpha})_n}$	0.86	0.83
$\frac{(\overline{\tau\alpha})_G}{(\overline{\tau\alpha})_n}$	0.725	0.83
$(\overline{\tau\alpha})_D$	0.512	0.494
$(\overline{\tau\alpha})_G$	0.432	0.494

Determining Total Heat Gain

The calculation of the total solar heat gain to the greenhouse for each month is shown in Table 2.7. The specific absorbed radiation results from Table 2.4 for the south roof and Table 2.5 for the south wall are in columns 2 and 4 respectively of Table 2.7. Each specific absorbed radiation value is multiplied by the area of each surface to obtain the radiation heat gain on each surface in MJ for each month. These two values are summed to obtain the total solar heat gain for each month shown in the far right column of Table 2.7.

Table 2.7 Calculation Total Heat Gain

Month	\bar{S}_{SR}	Heat Gain _{SR}	\bar{S}_{SW}	Heat Gain _{SW}	Total Heat Gain (MJ)
January	4.07	135,104	5.77	15,963	151,067
February	6.85	207,055	7.60	18,973	226,028
March	8.21	272,494	8.50	23,500	295,995
April	9.98	320,399	8.44	22,594	342,993
May	11.22	372,304	8.30	22,946	395,250
June	10.88	349,430	7.94	21,248	370,678
July	14.12	468,544	9.57	26,466	495,010
August	11.83	392,559	9.07	25,080	417,639
September	10.50	337,205	9.66	25,836	363,041
October	7.63	253,179	8.95	24,757	277,936
November	4.98	159,811	6.86	18,363	178,174
December	3.71	123,183	5.23	14,463	137,646

2.2.3 Greenhouse Heat Demand

The results for heat loss and heat gain for each month from Table 2.2 and Table 2.7 are used in Equation 2.1 to calculate the greenhouse heat demand. Negative answers to the equation would indicate a cooling load and therefore only positive values result in heat demand values. Increased ventilation is assumed to prevent overheating during the summer. The results are shown in Table 2.8 and Figure 2.2. The greenhouse monthly heating requirements range from 47 GJ in October to a maximum of 373 GJ in January. The total heating demand for the year is 1,439 GJ.

Table 2.8 Heat Demand for Greenhouse in MJ.

Month	Heat Loss	Heat Gain	Heat Demand
January	505,416	132,019	373,396
February	393,462	172,031	221,431
March	406,812	240,729	166,083
April	322,169	272,115	50,054
May	240,846	313,262	0
June	169,871	296,828	0
July	123,694	391,793	0
August	130,527	326,375	0
September	172,800	288,270	0
October	279,897	232,436	47,461
November	385,627	154,003	231,624
December	465,388	116,253	349,136
Total			1,439,185

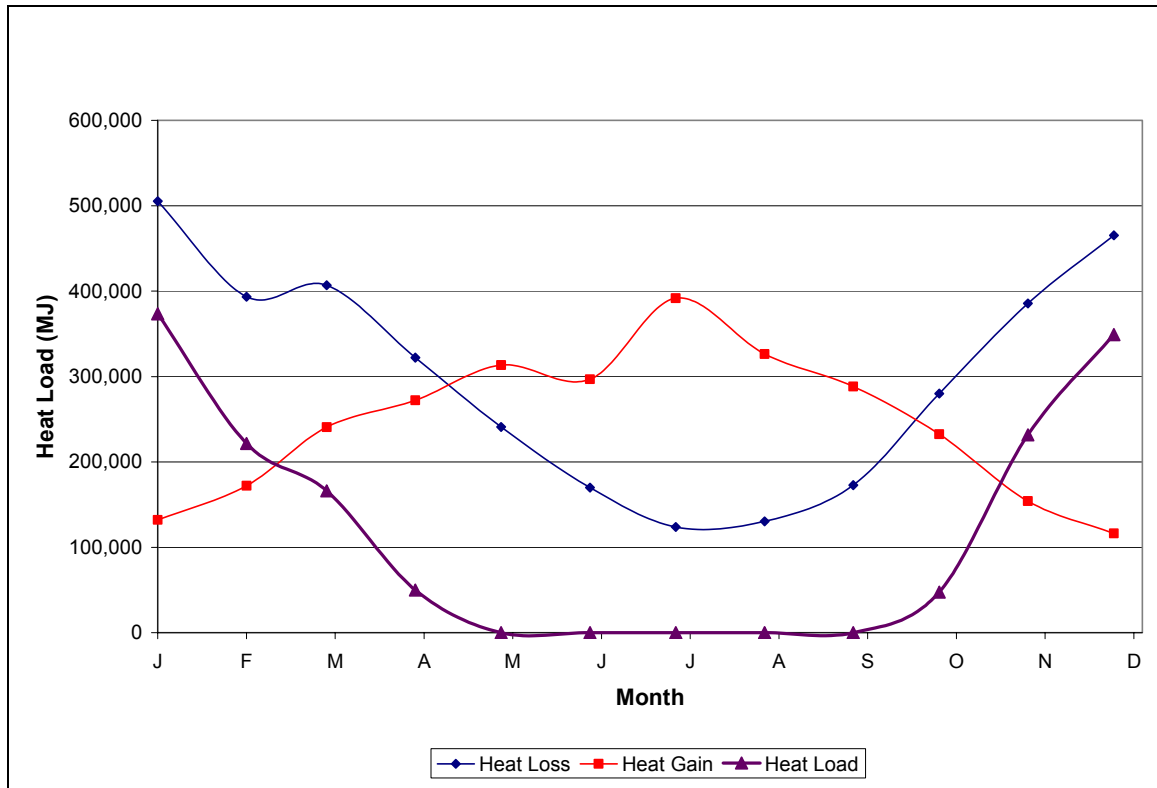


Figure 2.2 Greenhouse annual load profile.

2.2.4 Storage System

In Figure 2.2, it can be seen that the largest solar gain to the greenhouse occurs at the same time of year as the lowest heat losses (during the summer). It is for this reason that a solar-thermal heating system requires seasonal storage: to utilize the high solar radiation in the summer by capturing and storing it to later heat the greenhouse in the winter. The summer radiation heat is stored by heating water in a large storage tank. The storage capacity of the tank is determined from the total annual heating demand, but there will be heat loss from the heat storage system. This is accounted for by assuming enough insulation is added to limit the heat loss to 10% of the heat stored:

$$Cap - 0.1Cap = HeatDemand$$

$$Cap = 1.11HeatDemand$$

$$Cap = 1,597 \text{ GJ}$$

Equation 2.15

The required insulation thickness can be estimated with Fourier's law for heat flow through the insulated storage walls by assuming steady state, one-dimensional conduction. The change in temperature between the storage tank water and the ground is assumed to be an average of 40 C; the surface area of the tank is calculated based on rectangular prism geometry; and the heat rate is multiplied by the seconds in a year to get the total heat loss over one year's time. Solving for the thickness, the equation becomes:

$$q = \frac{kAdT}{dx}$$

$$HL_{st} = 0.1Cap = \frac{k_{ins} SA_{st} \Delta T_{st-g} 3.156 \times 10^7 \frac{\text{seconds}}{\text{year}} \frac{\text{GJ}}{10^9 \text{ J}}}{th_{ins}}$$

$$th_{ins} = \frac{k_{ins} SA_{st} \Delta T_{st-g} 3.156 \times 10^7 \frac{\text{seconds}}{\text{year}} \frac{\text{GJ}}{10^9 \text{ J}}}{HL_{st}}$$

Equation 2.16

where

HL_{st} = heat loss from storage, 158 GJ

k_{ins} = conductivity of mineral wool, 0.0389 W/m-C²⁰

ΔT_{st-g} = average temperature difference between storage water and ground, 40 C.

SA_{st} = surface area of storage tank, 4,098m²

th_{ins} = insulation thickness, result of 1.27m

The volume of water required to reach this storage capacity is calculated with the equation:

$$V_{st} = \frac{26 \text{ Cap}/10^9}{Cp_w \rho_w \Delta T_w}$$

Equation 2.17

where

V_{st} = storage volume in m³

Cp_w = specific heat of storage water, 4.19 J/kg-C

ρ_w = density of storage water, 975 kg/ m³

ΔT_w = temperature change of storage water, 50 C from fully heated to fully cooled

The resultant storage volume is 7,821 m³. This is the value used to determine the amounts of material required to build each storage design option that is compared in the life cycle study described in chapter 3.

2.2.5 Collector System

The same equations to calculate the specific absorbed solar radiation to the greenhouse are used to calculate the solar gain to the collectors. The absorbed radiation results for the collectors are shown in Table 2.9. Typical solar-thermal collectors are located on the roof of the building for which they supply heat. However, in this case, the greenhouse roof must be transparent to allow natural light and heat to pass through to the plants. There are no existing structures on the property appropriate for mounting the collectors, so they will be field-mounted on free-standing frames set at the optimum tilt angle assumed to be equal to the latitude of 47.5 degrees. As with the absorbed radiation calculation for the south wall, \bar{R}_B and $(\tau\alpha)_B$ must be recalculated for each month based on the new tilt angle. The transmittance and absorptance are also different for the collector. Generic collector properties are assumed in order to calculate typical collector performance. The transmittance is assumed to be 0.91, which is for 1 cover with a KL

value of 0.0125.²¹ The absorptance is assumed to be 0.9, which is typical for a collector.²²

Table 2.9 Calculation of specific absorbed radiation on collector

Month	\bar{R}_B	$\frac{(\bar{\tau}\alpha)_B}{(\bar{\tau}\alpha)_n}$	$(\bar{\tau}\alpha)_B$	\bar{S} (MJ/m ²)
January	3.155	0.96	0.7941	4.96
February	2.65	0.97	0.80237	8.37
March	1.6	0.97	0.80237	10.20
April	1.12	0.97	0.80237	12.58
May	0.83	0.96	0.7941	14.30
June	0.71	0.95	0.78583	14.00
July	0.76	0.95	0.78583	17.91
August	0.99	0.97	0.80237	14.91
September	1.39	0.98	0.81065	13.05
October	2.015	0.97	0.80237	9.38
November	2.88	0.96	0.7941	6.07
December	3.51	0.95	0.78583	4.29

To calculate the heat gain to the tank from the collector, the efficiency of the collector must be taken into account. This is done by assuming typical collector characterization values. The collector overall loss coefficient is assumed to be 5 W/m²-C and the collector heat removal factor to be 0.75.²³ The final useful heat gain can then be calculated with the equation:²⁴

$$Q_U = A_c F_R [S - U_L (T_i - T_a)]$$

Equation 2.18

where

Q_U = Useful heat gain in MJ/day

A_c = Area of collector, **929 m²**

F_R = Heat removal factor

U_L = Overall loss coefficient of collector in W/m²-C

T_i = Fluid inlet temperature, assumed to be the average storage tank temperature of 45 C

T_a = Ambient temperature, from meteorological data in C

The results of this calculation are shown in Table 2.10 where the column entitled “Coll Loss” shows the $U_L(T_i - T_a)$ term. The area of the collector is set for the total annual heat gain to equal the total capacity of the storage system.

Table 2.10 Calculation of useful heat gain to collector.

Month	\bar{S} (MJ/m ² -day)	Coll. Loss (MJ/day)	Q _u (MJ/day)	Heat Gain (MJ)
January	4.96	5.33	0	0
February	8.37	4.90	2421	67,788
March	10.20	4.75	3799	117,758
April	12.58	4.46	5653	169,604
May	14.30	3.89	7257	224,979
June	14.00	3.60	7245	217,347
July	17.91	3.17	10274	318,504
August	14.91	3.17	8179	253,546
September	13.05	3.60	6584	197,512
October	9.38	4.18	3626	112,420
November	6.07	4.75	917	27,497
December	4.29	5.04	0	0
Total				1,706,955

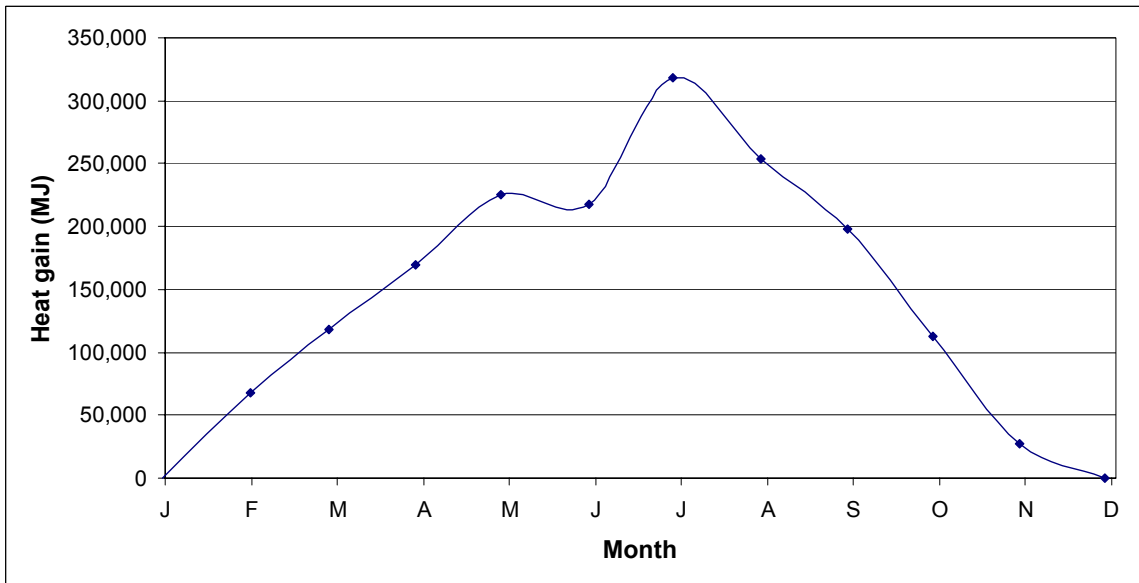


Figure 2.3 Annual profile of collector heat gain.

2.3 Conclusions

The estimates of the greenhouse heating demand, storage size, and collector size performed in this preliminary analysis provide simple, clear approximations on which to base the design decisions in chapters 3 and 4. The heat storage size estimate and insulation requirements are used to calculate the amount of materials necessary to build the two types of storage systems compared in the life cycle study presented in chapter 3. The results of the life cycle study are used to select the type of seasonal heat storage system in the final design. The heating demand and collector size calculations in this chapter provide insight on which to base the component selection of the collector and heat delivery systems. The results from this chapter are also compared with the results of the detailed thermal analysis in chapter 4 to ensure reasonable values.

Even though the analysis performed in this section is valid to predict the general heating demand through the year, the total heating demand is likely underestimated. Using monthly averages and making the steady-state assumption in the energy balance results in a heating load equation that does not account for excess solar gain during the day. It is inherently assumed that the extra heat is stored and available for heating during the night when there is higher heat loss. Passive thermal storage in water and other thermal mass receiving direct sunlight would make this possible, but a finite thermal mass results in diurnal temperature changes. These transient effects need to be modeled to see how much of the collected heat can be stored while maintaining appropriate greenhouse temperatures. Along with the indoor greenhouse temperatures, actual solar radiation and outdoor temperature values cycle daily and vary significantly from one day to the next.

It is important to simulate this diurnal behavior to obtain a more accurate model of the heating demands and heating system requirements. A more detailed simulation using hourly solar and meteorological data is described in chapter 4. In order to perform a detailed analysis, each component of the heating system needs to be specified in order to model its specific characteristics. The storage sub-system component has two viable design options. Chapter 3 presents a comparative life cycle study performed to determine which design option presents the lowest environmental impact at reasonable cost.

Notes to Chapter 2

¹ Duffie, John A. and William A. Beckman, Solar Engineering of Thermal Processes 2nd ed. (New York: John Wiley & Sons, 1991).

² Canada, agriculture Canada, Research Branch, Energy-conserving urban greenhouses for Canada (Publication 1814E 1987)

³ Tmp range of storage

⁴ Duffie about $\beta = \gamma$

⁵ Duffie 417.

⁶ Duffie 418.

⁷ Duffie 843.

⁸ Duffie 878.

⁹ Duffie 421.

¹⁰ Duffie 109, 239.

¹¹ Duffie 96.

¹² Duffie 86.

¹³ Duffie 19.

¹⁴ Duffie 14.

¹⁵ Duffie 109.

¹⁶ Duffie 91.

¹⁷ Duffie 246.

¹⁸ Macrolux. "Macrolux plastics" 8 Jan 2006
<<http://www.tapplastics.com/uploads/pdf/Coex8mm.pdf>>.

¹⁹ Duffie 230.

²⁰ Conductivity of mineral wool

²¹ Duffie coll transmittance

²² Typical absorptance for collector

²³ Duffie 266, 313; Stine, William and Michael Geyer, "Flat-Plate Collectors," Power From The Sun, fig 6.4, 12 Jan 2006 <
<http://www.powerfromthesun.net/Chapter6/Chapter6.htm>>.

²⁴ Duffie 278.

Chapter 3: Comparative Life Cycle Study

Life cycle assessment (LCA) is defined by the International Standards Organization (ISO) as “a systematic set of procedures for compiling and examining the inputs and outputs of materials and energy and the associated environmental impacts directly attributable to the functioning of a product or service system throughout its life cycle.”¹

The overall goal of this paper is to present and evaluate an ecologically responsible heating system design using solar-thermal energy. Using renewable energy as a heat source does not guarantee that the heating system actually has a lower overall environmental impact than a traditional heating system. Because so much material is required to construct the heating system, the life cycle emissions associated with building the heating system may be higher than those of burning traditional heating fuels. This chapter presents the following sections according to ISO 14040 and 14041 standards:^{1,2}

1. **Goal and Scope:** A clear formulation of the research question and intended application of the results with the definition of the function and functional unit of the system to be studied.
2. **Inventory Analysis:** Inventory collection of the input and output data necessary to meet the goals of the study.
3. **Impact Assessment:** Evaluation of the potential environmental impacts resulting from the inventory inputs and outputs.
4. **Interpretation:** Evaluation of the quality of the impact assessment results with relation to the goal and scope of the study.

The largest and least studied of the three sub-systems of the heating system (collector, heat delivery, and storage) is the seasonal heat storage system.³ The life cycle study presented in this chapter attempts to determine the type of heat storage system that will

meet the goal of minimizing the environmental impact while maintaining reasonable cost values. Several demonstration plants have been in operation in Germany under the “Solarthermie-2000” program to demonstrate the technical and economic feasibility of the most promising storage concepts.⁴ The two applicable storage concepts, the plastic-lined gravel-water pit and the concrete water tank, are scaled to create two storage design options for the life cycle study. Figure 3.1 shows the basic geometry and layout of the two systems.

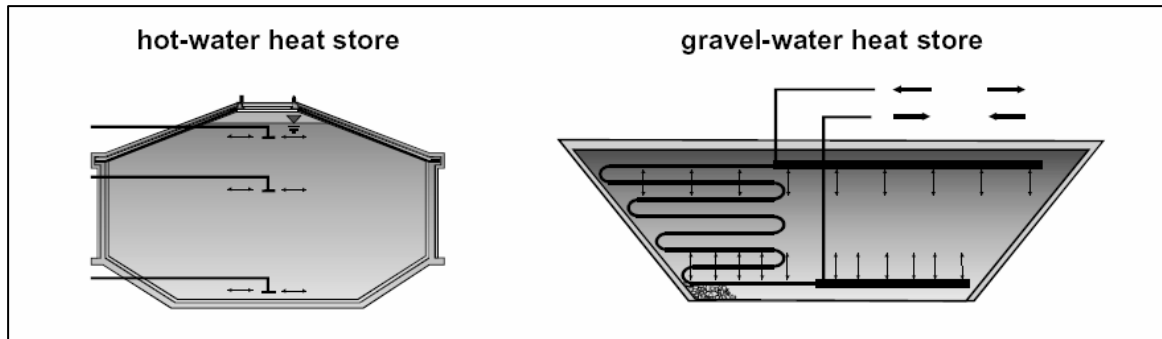


Figure 3.1 Geometry of the two applicable seasonal storage design options.⁵

The cross-sectional views of the two storage types shown above correspond to the width of the greenhouse and the depth below the greenhouse where the storage systems will be located. The widest section of each design option, plus insulation, equals the width of the greenhouse (80 feet). The storage unit length, including insulation, extends the length of the greenhouse (240 feet). Figure 3.2 gives the detailed layout of the materials required for each design option. The hot-water heat storage holds the water without leaking using 1.25 mm thick stainless steel. The steel is supported with concrete, and the heat is contained using mineral wool insulation outside the concrete. The gravel pit heat storage holds the gravel-water with a polyethylene liner, and also contains the heat using mineral wool insulation.

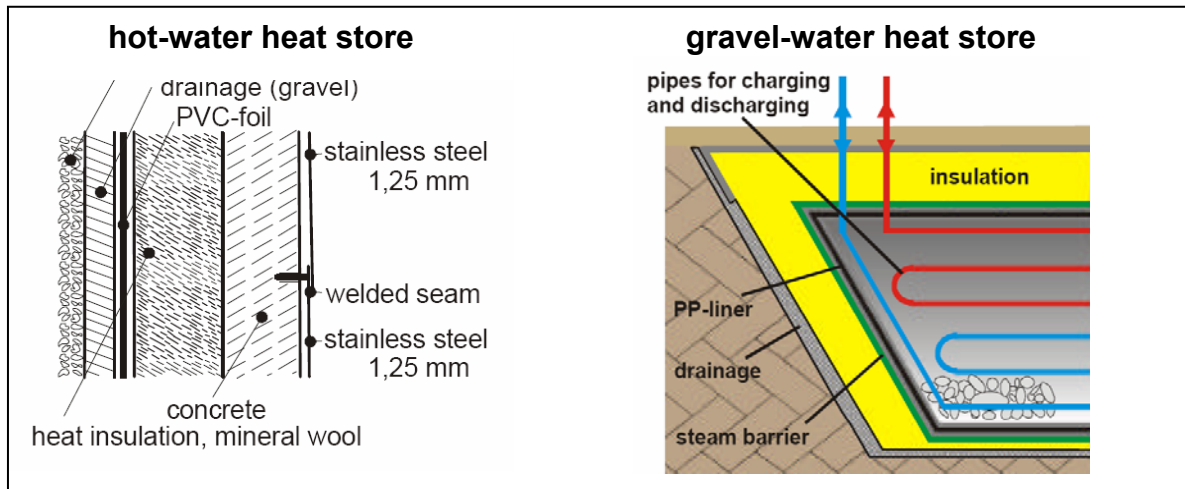


Figure 3.2 Materials layout of the two seasonal storage design options.⁶

3.1 Goal

The purpose of this study is to compare the life cycle environmental impacts and costs of the gravel-water pit versus the concrete-steel water tank seasonal heat storage design options based on LCA. The results of the study are used to decide which storage option is incorporated into the final heating system design described in chapter 4. The methodology and information presented will follow ISO 14040 and 14041 standards,¹ and the textbook “The Computational Structure of Life Cycle Assessment.”⁷

3.2 Scope

3.2.1 Function, Functional Unit, and Reference Flows

The function of the solar-thermal system is to provide 100% of the heat demand for the greenhouse using solar energy, approximately 400,000 kWh per year. The function of the storage sub-system is to store the summer heat through the fall and winter to supply the winter and spring loads to the greenhouse. The functional unit requirements for this sub-system is to store the 400,000 kWh for 5 months after 10% heat loss (through insulated tank walls), resulting in a 443,750 kWh total capacity. The reference flows for

this sub-system are the volume of water or water-gravel mixture required for the total capacity (approximately 8,000 m³ of water from Equation 2.17) and the mass of materials (concrete, steel, plastic, insulation, etc.) required to contain the heat and storage medium for a life of 20 years.

The materials and processes needed to construct each storage system (the first phase processes) are shown in Table 3.1. The first phase processes are those that are required to construct the storage system; the second phase processes are those that are required to produce the inputs required by the first phase processes; the third phase processes are those that are required to produce the inputs required by the second phase processes; and so on. The materials themselves are considered a process because a production process is necessary in order to manufacture the materials.

Table 3.1 Materials and processes required for each storage system.

Gravel-Water Pit		Concrete Water Tank	
Gravel (kg)	6.29E+06	Gravel (kg)	1.10E+06
Pipe (kg)	4.39E+03	Stainless Steel (kg)	3.61E+04
PP Liner (kg)	1.51E+04	Concrete (kg)	1.10E+03
Rock Wool (kg)	2.28E+05	Rock Wool (kg)	1.68E+05
Hydraulic Digging (m ³)	1.60E+04	Hydraulic Digging (m ³)	1.58E+04

3.2.2 System Boundaries

Figure 3.3 shows the process flow diagram for the seasonal storage sub-system. The sub-system includes the storage medium, tank, insulation, and any necessary piping to exchange heat with the tank. The storage system maintenance during the use phase of the life-cycle is assumed to be negligible. Little or no materials or equipment will need to be

added to the system during its use. The disposal and recovery phase are also assumed to be outside the system boundaries since neither system will likely be moved or recovered at end-of-life. Therefore, only the materials extraction and processing, electricity production, fuel production, and construction stages of the life cycle are considered in this study (shown by the dashed line in

Figure 3.3). For simplicity in the figure, all materials processing upstream of the materials production are represented as one process, and fuel production represents all processes to produce all the required fuels. However, detailed data for sub-processes (from extraction to point of use) have been assessed for each of these process groups. The raw material inputs are shown as arrows crossing the top of the system boundary. These are the only environmental flows, flows that cross the system boundary, represented in the figure. The other environmental flows, raw energy inputs and emission outputs, are too numerous to be included in the figure. The economic flows, flows that do not cross the system boundary, are represented as arrows traveling from one process to another within the dashed system boundary line.

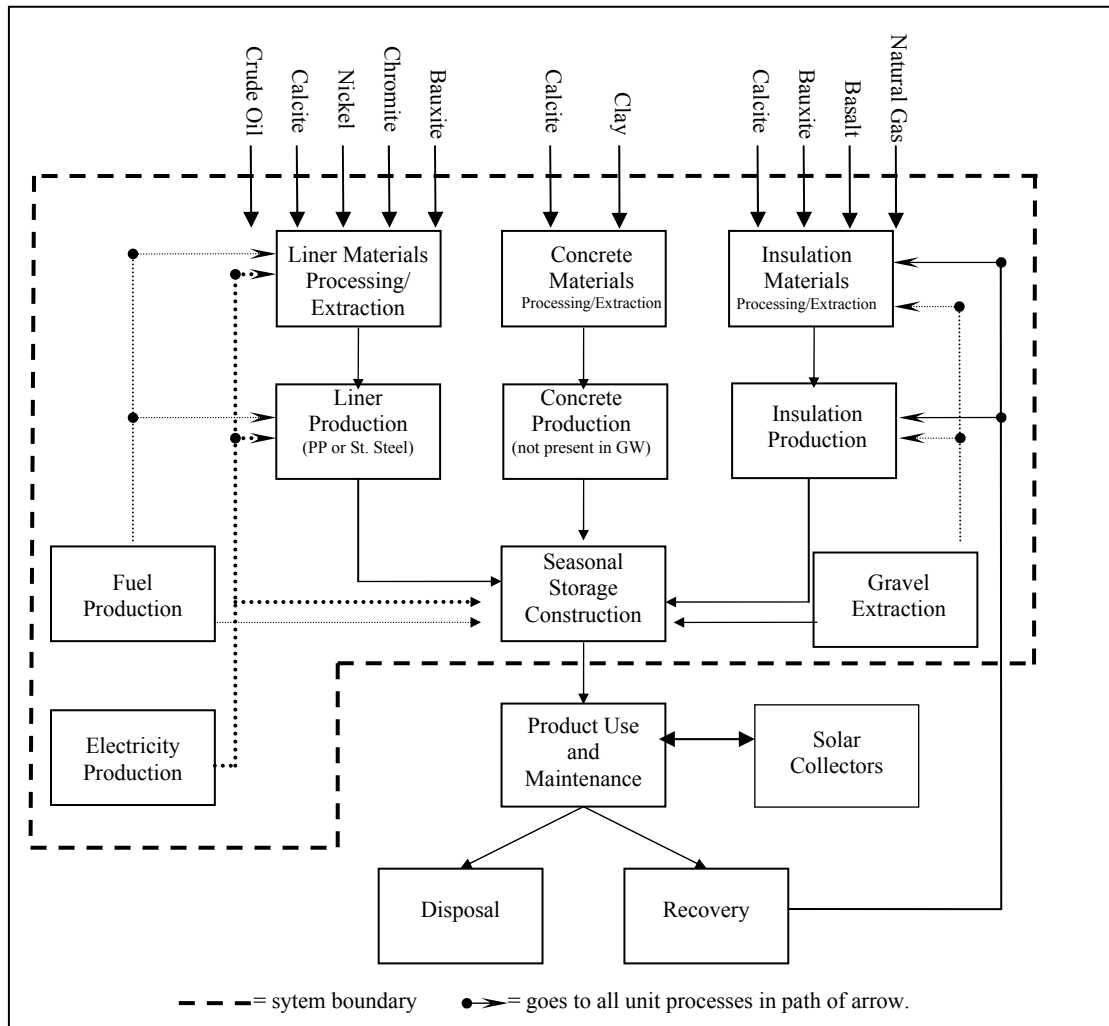


Figure 3.3 Life cycle process flow diagram for Seasonal Storage System.

3.2.3 Impact Assessment Data Categories

The primary metrics used to evaluate the impact of the systems are total energy use and global warming impact; other impact categories from the US EPA TRACI database:⁸ photochemical smog and acidification are also assessed. This study does not track the flows required to assess the remaining TRACI impact categories. Construction cost is also compared; however minimizing the environmental impacts has a higher priority than minimizing cost. The construction costs are estimated in this study to ensure that

selecting the design with lower environmental impact does not result in significantly higher costs. The US electricity grid mix is used for electricity input.

3.2.4 Criteria for Inclusion of Inputs/Outputs

Inputs are included if they comprise more than 5% of the total mass or energy use of each process, or present significant environmental impact potential. No disposal, treatment, factories (includes plants, storage facilities, furnaces, machines, etc.), or storage processes are included because these processes contribute a small percentage to the total life cycle emissions and require several phases of upstream processes. All cut-off (deleted) inputs are tracked in order to be included in future work. All outputs provided by the US Greenhouse Gases, Regulated Emissions, and Energy Use in Transportation (GREET) database are included: CO₂, CH₄, N₂O, VOC, CO, NO_x, PM10, and SO_x.⁹

3.2.5 Data Quality Requirements

The data quality must receive an average score of 3 or better on the UWME DFE laboratory scoring method based on the ISO standards: time; geography; technological relevance; representativeness, sources, and uncertainty of data; and consistency and reproducibility of the methods.¹⁰ This score indicates the quality and applicability of the each process data set used in the life cycle study. If any process data set fails the scoring method, the process is replaced with alternative process data from another source.

3.3 Inventory Analysis

3.3.1 Data Collection Procedure

Two demand vectors, set of economic flows of which the system is required to produce,¹¹ for constructing each storage unit design option are created. These demand vectors are

based on the amount of material required to build each storage system sized to meet the required capacity shown in Table 3.1. The majority of the material processing data are collected from EcoInvent, which is copyright protected and whose raw data may not be published.¹² The plastics process data are from the Association of Plastics Manufacturers in Europe (APME) LCA data sets.¹³ The insulation process data are taken from the life cycle inventory (LCI) data from the BEES (Building for Environmental and Economic Sustainability) software program published by the National Institute of Standards and Technology.¹⁴ The electricity data come from the US GREET database for an average US energy mix.⁹ The transportation process data also come from GREET,^{9,15} and EcoInvent. The transportation requirement data come from the 2002 US census Commodity Flow Survey.¹⁶ The cost data come mostly from the construction costs of existing “Solarthermie-2000” program storage systems.¹⁷

APME Plastic Production Process Data

The APME plastic production data are presented as an entire LCI, so no upstream processes are required. It incorporates all the processes and infrastructure to create 1 kg of the specified polymer. However, since this study is for the US rather than Europe, it would be advantageous to use US electricity process data from GREET rather than that used in the European LCI. Therefore, upstream processes for energy use are included rather than the total APME LCI. Table 3.2 shows the original APME LCI data and the modified data of energy use for the production process of low density polyethylene. The APME data present energy use broken up into four categories. The “energy content of delivered fuel” and “energy use in transport” values are summed to obtain the modified

energy input required for the plastic production processes in this study. The delivered fuels are listed as electricity, oil fuels, and other fuels. The electricity is entered as a required input for electricity (converted from MJ to kWh), oil fuels as that for heavy fuel oil, and other fuels as that for diesel. The last two assumptions are made as a conservative estimate resulting in emissions values in the high end of the possible range.

Table 3.2 Original and modified input data for low density polyethylene production process.

APME Original Data						Modified Data	
Fuel type	Fuel prod'n & delivery energy (MJ)	Energy content of delivered fuel (MJ)	Energy use in transport (MJ)	Feedstock energy (MJ)	Total energy (MJ)	Process name & units	Required Input
Electricity	8.76E+00	4.01E+00	5.45E-01	0.00E+00	1.33E+01	Electricity (kwh)	1.26E+00
Oil fuels	1.56E-01	6.36E+00	8.37E-02	2.86E+01	3.51E+01	fuel oil (MJ)	6.44E+00
Other fuels	3.12E-01	6.03E+00	1.94E-02	2.30E+01	2.93E+01	nat gas (MJ)	6.04E+00
Totals	9.23E+00	1.64E+01	6.48E-01	5.15E+01	7.78E+01	Total (MJ)	1.70E+01

The APME LCI emission data is also presented in four separate categories: fuel production and delivery, fuel use, transportation, and processing. Because the energy requirements of the modified data sets are met by requiring process inputs, the modified emission outputs omit those associated with energy production, transport, and use. The modified data of emissions from the plastic production process are calculated as the sum of the emissions from transport and processing (converted to kg). Table 3.3 shows the original APME data and the modified data of emissions from the plastic production process. Only those inventory flows that are included in this study (based on the criteria for included outputs) are listed in the table.

Table 3.3 Original and modified output data for low density polyethylene production process.

APME Original Data					Modified Data
Emission	From fuel prod'n (mg)	From fuel use (mg)	From transport (mg)	From process (mg)	Process output (kg)
CO	1.52E+03	4.68E+02	9.55E+00	4.46E+02	4.56E-04
CO ₂	8.27E+05	7.28E+05	6.95E+03	1.43E+05	1.50E-01
SO _x	3.51E+03	9.14E+02	1.25E+02	4.07E+02	5.33E-04
NO _x	2.11E+03	1.11E+03	3.87E+01	1.54E+02	1.93E-04
N ₂ O	9.46E-04	3.07E-04	0.00E+00	1.41E-04	1.41E-10
CH ₄	5.61E+03	1.90E+02	0.00E+00	3.40E+03	3.40E-03
VOC ^a	4.46E-02	0.00E+00	0.00E+00	4.93E+02	4.93E-04

The modified data in the far right columns of Table 3.2 and Table 3.3 are used as the inputs and outputs associated with the production of low density polyethylene for this study.

Insulation Production Process Data

The production process data for the insulation is also presented as an LCI. The emissions due to electricity use are not presented separately, so the information is entered as it is given per kilogram of mineral wool produced. The electricity source is based on a standard US electricity grid.¹⁸ Table 3.4 Original and modified data for BEES mineral wool production process shows the original BEES data based on the 0.91 kg functional unit used in the BEES database, and the final process data set created for this study based on the 1 kg functional unit. See Appendix A for these values entered in this study.

Table 3.4 Original and modified data for BEES mineral wool production process.

	BEES Original Data Set (g or MJ per 0.91 kg)		Modified Data Set (kg or MJ per kg)
	Raw	Manufacturing	Total
Total Primary Energy	2.13335	10.7479	14.06574
Carbon dioxide	56.8455	392.227	0.490367
Carbon monoxide	0.071937	0.209326	0.000307
Nitrous oxide	0.004016	0.1065	0.000121
Methane	0.13288	1.5481	0.001836
Nitrogen oxides	0.326275	1.35918	0.00184
VOC	0	0	0
Particulates, < 10um	1.40124	2.48207	0.00424
Sulfur dioxide	0.1864	2.22667	0.002635

Electricity Production Process Data

The electricity production process data is from the US GREET version 1.6 database for power plant energy use and emissions per kWh of electricity available at user sites for stationary use. Table 3.5 shows the assumptions used to create this average US energy mix.

Table 3.5 Average US Electricity production mix and conversion efficiency.

	Generation Mix for Stationary Applications	Combustion Technology Shares for A Given Fuel	Power Plant Energy Conversion Efficiency
Residual Oil-Fired Power Plants	1.0%		35.0%
Utility boiler: current		20.0%	35.0%
Utility boiler: future		80.0%	35.0%
Natural Gas-Fired Power Plants	14.9%		38.8%
Utility boiler: current		8.0%	34.0%
Utility boiler: future		32.0%	35.0%
Simple-cycle gas turbine: current		8.0%	34.0%
Simple-cycle gas turbine: future		32.0%	35.0%
Combined-cycle gas turbine: current		20.0%	55.0%
Combined-cycle gas turbine: future		0.0%	55.0%
Coal-Fired Power Plants	53.8%		35.1%
Utility boiler: current		19.0%	32.0%
Utility boiler: future		76.0%	35.5%
Advanced tech. with combined cycle		5.0%	41.5%
Nuclear Power Plants	18.0%		100.0%
Other Power Plants (hydro, wind, etc.)	12.3%		100.0%

Cost Input Data

Table 3.6 shows the specific costs of each process required for the construction of the two storage design options. The gravel pit data comes from “High Performance—Low Cost Seasonal Gravel/Water Storage Pit” by Pfeil & Koch.¹⁹ These costs are entered as required environmental inputs for each process first phase process and are used to calculate the total cost of each storage system.

Table 3.6 Specific costs for construction of the storage system designs

Process	Source	Specific Cost	Cost per KG
Excavation	Pfeil & Koch	\$12.90 per m ³	
Gravel-filling	Pfeil & Koch	\$32.25 per m ³	\$0.02
Plastic Lining	Pfeil & Koch	\$68.92 per m ²	\$19.14
Pipe System	McMaster-4884K13	\$29.40 per 100'x1" Dia.	\$1.21
Mineral Wool +10%, Installation	McMaster-9332K65	\$13.72 per 30 lbs	\$1.01 \$1.11
Stainless Steel +10%, Installation	McMaster-8983K14	\$185.17 per .048"x8'x36"	\$8.68 \$9.55
Concrete	McMaster - 76805T91	\$4.42 per 60 lb bag	\$0.16

Transportation Input Data

The long-distance transportation requirements (in ton-miles/kg) for each process are determined from the 2002 US census Commodity Flow Survey. Each process is assigned the most appropriate commodity category (3-digit SCTG description). The transportation is represented as three modes of travel: truck, rail, and barge. For the long-distance requirements, no water transportation is required, so it is omitted from Table 3.8 and Table 3.9. Each mode of travel is a process requiring fuel and outputting vehicle emissions per ton-mile. The average ton-mile value is calculated from the commodity flow survey's ton-miles in each transportation mode divided by total mass (converted

from traditional tons to metric kg) for each process category. An example of this calculation is shown in Table 3.7. The five left-hand columns are original data from the commodity flow survey. The shaded column is the final value that is then entered in Table 3.8 (listing all the long-distance transportation requirements for each process).

Table 3.7 Calculation example of transportation requirements for LDPE pipes.

Code	SCTG Description	Modes of transportation	Tons 2002 (thousands)	Ton-miles 2002 (millions)	Average Ton-miles/kg
331	Pipes, tubes, and fittings	All Modes	44,753	14,156	0.3487
331	Pipes, tubes, and fittings	Truck (3)	39,956	10,220	0.2517
331	Pipes, tubes, and fittings	For-hire truck	26,530	8,282	0.2040
331	Pipes, tubes, and fittings	Private truck	13,271	1,891	0.0466
331	Pipes, tubes, and fittings	Rail	2,391	2,221	0.0547

Table 3.8 Transportation requirements from Commodity Flow Survey in ton-miles per kg.

Process	Code	SCTG Description (3-Digit)	Truck	Private Truck	Rail
Insulation	319	Other nonmetallic mineral products	0.0548	0.0247	0.0197
Concrete	local		on-site	0	0
LDPE pipes	331	Pipes, tubes, and fittings	0.204	0.0466	0.0547
Gravel	local	local	0	0	0
Polypropylene	242	Manmade fibers and plastics basic shapes and articles	0.4401	0.0507	0.032
Stainless steel	322	Flat-rolled products of iron or steel	0.1702	0.0376	0.1114
Hydraulic digging	NA	local	0	0	0
LDPE	241	Plastics in primary forms, rubber in primary forms or sheets	0.2256	0.0257	0.4498
Lubricating Oil	191	Lubricating oils and greases	0.1108	0.0595	0.1006
Formaldehyde	204	Phenols, phenol-alcohols, aldehydes, cyclic polymers of aldehydes	0.0795	0.0071	0.2202
Basalt	139	Other nonmetallic minerals	0.1702	0.0203	0.2369
Portland Cement	local	local			
Bauxite	139	Other nonmetallic minerals	0.1702	0.0203	0.2369
Ferrochromium	141	Iron ores and concentrates			0.7025
Ferronickel	141	Iron ores and concentrates			0.7025
Iron, scrap	411	Metallic waste and scrap	0.062	0.011	0.0768
Limestone	139	Other nonmetallic minerals	0.1702	0.0203	0.2369
Feldspar	139	Other nonmetallic minerals	0.1702	0.0203	0.2369
Diesel, at storage	171	Included in GREET	0	0	0
Sand, at mine	local	local	0	0	0
Clinker	319	Other nonmetallic mineral products	0.0548	0.0247	0.0197

The local distances from the distribution sites to the construction site are calculated as shown in Table 3.9. Each local distance is included in the travel requirements for the first phase materials. Each distribution location address is from the nearest location each process material can be purchased. The default address used for the pipe and insulation is the closest US post office to the Fauntleroy ferry dock. The ferry distance is calculated from ferry speeds divided by travel times posted by Washington State Ferries.²⁰

Table 3.9 Local transportation calculations for construction process materials in miles.

Process	Distribution Location	DL to Fautleroy Ferry Dock	Vashon Ferry Dock to Greenhouse	Truck Distance	Ferry Distance
Gravel	6829 SW 248th, Vashon	NA	NA	5.08	NA
Cement	5900 W. Marginal Way SW	4.59	5.77	10.36	4.99
Steel	3223 Sixth Avenue S,	6.17	5.77	11.94	4.99
Pipe (ldpe)	2116 Taylor Way, Tac	31.14	5.77	36.91	4.99
PP Liner	4412 California Ave SW	2.99	5.77	8.76	4.99
Insulation	4413 California Ave SW	2.99	5.77	8.76	4.99

Table 3.10 shows the total transportation requirements for each of the first phase processes. These values are the sum of the general and local requirements from Table 3.8 and Table 3.9.

Table 3.10 Total transportation requirements for 1st phase materials in ton-miles/kg.

Process	Truck	Rail	Ferry/Barge
Insulation	0.0859	0.0197	0.0055
Concrete	NA	NA	NA
LDPE pipes	0.2913	0.0547	0.0055
Gravel	0.0056	0.0000	0.0055
Polypropylene	0.4972	0.0320	0.0055
Stainless steel	0.2210	0.1114	0.0055
Portland cement	0.0114	0.0000	0

Transportation Process Data

The commercial and private truck requirements are both assumed to be class 8 trucks with an average payload of 20 tons. For long-range trucking, a backhaul rate of 70% is assumed, with 30% of the full trucks making an empty truck return trip requiring 68% of the fuel. This assumption results in a 1.2 backhaul factor (the long-range distances are multiplied by 1.2). For the local distances, all the trucks are assumed to make an empty return trip, so the local distances are multiplied by 1.68. The rail process is for a US freight train from GREET, and the ferry process is assumed to be a barge with an average payload of 1500 tons. The backhaul for the ferry is assumed to be zero since the return

trips are made regardless of the front haul load. See Appendix A for the transportation process data.

3.3.2 Unit Process Description

The general process life cycle diagram shown in

Figure 3.3 represents two phases upstream of construction. The following list outlines the processes required for each option three phases upstream from construction.

However, some of the third phase processes may require more upstream processes. The 30 separate processes included in this study are listed in Table 3.11.

Design Option 1: Concrete tank

Construction requires:

- Hydraulic Digging
 - Requires:
 - Hydraulic Digger
 - Diesel Fuel, at storage
 - Lubricating oil
 - ⇒ Electricity, NG burned, diesel at storage
- Mineral Wool Insulation, LCI
- Polypropylene Liner, LCI
 - Plus:
 - Electricity
 - ⇒ Electricity
 - Heavy fuel oil burned
 - ⇒ Electricity
 - Diesel burned
 - ⇒ Diesel at storage, lubricating oil
- LDPE Pipe Production
 - Requires:

Design Option 2: Gravel-Water Pit

Construction requires:

- Hydraulic Digging (listed left)
- Mineral Wool Insulation, LCI
- Stainless Steel Liner
 - Requires:
 - Ferrochromium Production
 - ⇒ Hydraulic digger, bauxite production, electricity, NG burned, heavy fuel oil burned.
 - Ferronickel
 - ⇒ Limestone packing, limestone extraction, diesel burned, electricity, NG burned, heavy fuel oil burned.
 - Iron Scrap
 - ⇒ Diesel burned, electricity
 - Electricity
- Gravel (listed left)
- Concrete

- LDPE, LCI
 - Electricity
 - Gravel
 - Requires:
 - Electricity
 - Diesel burned
 - Light fuel oil burned
 - ⇒ Electricity
- Requires:
 - Gravel (listed left)
 - Diesel burned (listed left)
 - Portland Cement
 - ⇒ Electricity, clinker production.
 - Electricity
 - Light Fuel oil burned
 - Heavy Fuel oil burned

Table 3.11 shows the process data quality scores for each process. These scores are based on EcoInvent or other process data source metadata, data that describes the data (standard deviation, number of samples, high and low values, etc.), and on how well the technology matches the design requirements. A five in the comment column indicates that the metadata suggests not using the module if it is important in the inventory. Two insulation production processes received a failing score (above 3); therefore, the alternative data set from the BEES software is used. However, the BEES data is life cycle inventory data (cradle to grave), so the energy use assumptions may be different. Therefore, both the EcoInvent and BEES mineral wool production processes are incorporated into the study. The final life cycle inventories and analyses are compared for both storage design options using both insulation process data sets.

Table 3.11 Data Quality Scores for Processes (scale 1 to 5 with 1 being best).

Production Process	Source	Time	Geography	Representativeness	Data Uncertainty	Data Source	Comments	Mean
Rock Wool	EcolInvent v1.1	2	4	2	3	4	5	3.50 ^a
Foam glass	EcolInvent v1.1	1	3	4	4	5	5	3.67 ^b
BEES Mineral Wool	BEES v 3.0 ¹⁴	2	2	3	3	3	3	2.67
Concrete	EcolInvent v1.1	2	3	1	3	2	3	2.33
PE Pipes	EcolInvent v1.1	3	3	2	3	3	3	2.83
Gravel	EcolInvent v1.1	2	3	2	2	3	3	2.50
PP	APME ¹³	3	4	2	4	1	3	2.83
Hydraulic digging	EcolInvent v1.1	2	3	3	3	2	5	3.00
Stainless Steel	EcolInvent v1.1	2	3	3	4	3	3	3.00
LDPE	APME ¹³	3	4	2	4	1	3	2.83
Hydraulic digger	EcolInvent v1.1	2	3	3	2	2	5	2.83
Electricity Production	GREET 1.6	2	2	1	4	3	3	2.50
Natural gas, burned	GREET 1.6	2	2	2	4	3	3	2.67
Lubricating Oil	EcolInvent v1.1	2	2	1	3	3	3	2.33
Diesel, burned	GREET 1.6	2	2	1	4	3	3	2.50
Diesel, at storage	GREET 1.6	2	2	1	4	3	3	2.50
Heavy Fuel Oil, burned	EcolInvent v1.1	2	3	1	4	3	3	2.67
Light Fuel Oil, burned	EcolInvent v1.1	2	3	1	4	3	3	2.67
Portland Cement	EcolInvent v1.1	2	3	1	3	3	3	2.50
Bauxite	EcolInvent v1.1	2	3	1	3	3	3	2.50
Ferrochromium	EcolInvent v1.1	1	2	1	3	2	3	2.00
Ferronickel	EcolInvent v1.1	1	2	1	4	2	3	2.17
Iron, scrap	EcolInvent v1.1	2	3	1	4	4	4	3.00
Limestone	EcolInvent v1.1	2	3	1	2	4	3	2.50
Natural Gas, HP @ user	GREET 1.6	2	3	2	3	2	3	2.50
Limestone, loose	EcolInvent v1.1	3	3	1	2	4	2	2.50
Limestone, at mine	EcolInvent v1.1	3	3	2	2	3	2	2.50
Clinker, at plant	EcolInvent v1.1	3	4	2	3	3	3	3.00
Truck	GREET 1.6	2	2	3	4	3	3	2.83
Rail	GREET 1.6	2	2	2	4	3	3	2.67
Barge	GREET 1.6	2	3	3	4	3	3	3.00
Ocean Freighter	EcolInvent v1.1	2	4	3	3	3	3	3.00

^a Narrowly failed process, to be included and compared to alternative data.
^b Failed processes deleted from study

3.3.3 Calculation Procedure

All computations in this study are performed in Excel according to the basic linear, steady-state model presented in “The Computational Structure of Life Cycle Assessment” by Heijungs and Suh.²¹ The data for each process is entered as a process vector with inputs represented as negative values and outputs represented as positive values. Each

process vector makes up one column in the process matrix. Because each process requires different inputs and delivers different outputs, zeros make up much the matrix. Many process outputs like electricity are required as input by several other processes; therefore, each process vector must use the same units for the same flows. The following assumptions are made to keep all mass units in kilograms (kg) and all energy units in megajoules (MJ), except electricity which is in kilowatt-hours:

1. The density of Gravel is 1682 kg/m^3 ²²
2. The density of LDPE is 900 kg/m^3 ²³
3. The density of crude oil is 870 kg/m^3 ²⁴
4. The energy density of crude oil is 45 MJ/kg
5. The energy density of coal is 31 MJ/kg ²⁵
6. The energy density of natural gas is 38.4 MJ/Nm^3 ²⁶

The process matrix is organized into the “technology matrix,” A , that contains the economic flows, and the “intervention matrix,” B , which contains all the environmental flows. The square technology matrix represents a set of linear equations describing the storage system, 18 for the gravel pit design, and 26 for the concrete tank design.

The inverse is calculated in order to scale the technology matrix for each process to supply the proper amount of material for the final demand vector (vector listing the required process outputs for the construction of the storage unit). The scaling vector is calculated using the formula:²⁷

51

$$A = f * s$$

Or,

$$s = A^{-1} * f$$

Equation 3.1

where

A = Technology matrix

f = Demand vector

s = Scaling vector

The total inputs and outputs are represented by the “inventory vector,” g , which is calculated according to the formula:²⁸

$$g = B * s$$

Equation 3.2

where

B = Intervention matrix

This final inventory vector lists all the required inputs and emissions for the life cycle of each storage design. See Appendix A for the process matrix, demand vector, and scaling vector for each design. The inventory vector results are presented in the next section.

3.3.4 Results

The final inventory vectors for each design option are shown in Table 3.12 and Table 3.13 below. Table 3.12 shows the inputs and Table 3.13 shows the outputs. Only the inputs of interest are shown in the table, energy use that affects environmental impact, and the cost. The inventory vector results are negative for inputs and positive for outputs; however, the inputs are shown as positive values in the table for easier comparison. The percent difference between the two design options for the EcoInvent insulation process

data is shown in the second to right column. The percent difference between the two design options for the BEES insulation LCI data is shown in the farthest right column.

Table 3.12 Inventory analysis results for required inputs.

		EcolInvent-US Adjusted			BEES		
Inventory Name	Units	Gravel Pit	Concrete Tank	Percent Difference	Gravel Pit	Concrete Tank	Percent Difference
US Dollars (2005)	\$	\$872,740	\$797,135	9%	\$872,740	\$797,135	9%
Total Energy	MJ	1.76E+08	2.60E+08	-33%	4.05E+06	5.74E+06	-29%

A positive value in the difference columns indicates that the gravel-water pit result is larger than the concrete tank result. For example, the steel and concrete water tank requires 29-33% more energy to produce than the gravel pit. In both tables, negative differences are prevalent, suggesting that the concrete tank has a higher environmental impact. However, since the gravel pit output is higher for some of the inventories (carbon monoxide, methane, etc.), it is possible that the gravel pit option might have a greater overall impact. These particular inventory outputs could weigh more heavily on the environment, resulting in higher overall environmental impact for the gravel pit storage system. The method used to determine this overall impact, the impact assessment, is described in the next section.

Table 3.13 Inventory analysis results for outputs.

		EcolInvent-US Adjusted			BEES		
Inventory Name	Units	Gravel Pit	Concrete Tank	Percent Difference	Gravel Pit	Concrete Tank	Percent Difference
Carbon Dioxide	kg	2.42E+06	3.76E+06	-36%	1.91E+05	6.00E+05	-68%
Carbon Monoxide	kg	2.02E+03	3.13E+03	-36%	1.94E+02	4.36E+02	-56%
Nitrous Oxide	kg	3.62E+01	5.49E+01	-34%	2.84E+01	2.44E+01	17%
Methane	kg	1.44E+04	2.12E+04	-32%	5.45E+02	4.36E+02	25%
Nitrogen Oxides	kg	6.20E+03	9.16E+03	-32%	8.87E+02	1.39E+03	-36%
NMVOOC	kg	1.18E+03	1.74E+03	-32%	1.06E+01	4.37E+01	-76%
Particulates, < 10um	kg	2.85E+03	4.94E+03	-42%	9.65E+02	3.27E+03	-70%
Sulfur Dioxide	kg	4.14E+03	6.10E+03	-32%	7.21E+02	1.23E+03	-42%

3.4 Impact Assessment

The inventory vector flows are classified, characterized, and normalized for several impact categories for the flows that are tracked. These categories, obtained from the US EPA TRACI database, include: global warming, photochemical smog, and acidification.⁸ Along with the TRACI categories, total energy use and total cost are also assessed. A single flow in the inventory vector can contribute to multiple impact categories. For example, nitrogen oxides impact both acidification and photochemical smog, but a single NO_x molecule cannot cause smog in the air at the same time that it is causing acid rain. However, the impact assessment does not assign a fraction of a chemical to each of its impact categories. Instead, the total emission value for each flow is assumed to contribute to all applicable impact categories. This provides a conservative estimate because when the flow is emitted, it has the potential for all of the emissions to impact a

single category. Therefore, the impact assessment results give the maximum potential impact value for each impact category.

3.4.1 Classification

The inventory flows that contribute to each impact category listed above are shown in Table 3.14 below. Every chemical output is classified under the impact category according to the TRACI database. If a chemical did not have an equivalency value in the database, it was assumed to have zero impact in that category.

Table 3.14 Classification of inventory flow outputs to each impact category.

Global Warming	Photo-chemical Smog	Acidification
Carbon dioxide	Carbon monoxide ^a	Nitrogen oxides
Nitrous oxide	Methane ^a	Sulfur dioxide
Methane	Nitrogen oxides	
	VOCs	
^a Negligible equivalency factor		

3.4.2 Characterization

The inventory vector, g , from the inventory analysis and impact equivalency factors, q , from TRACI are used to calculate the total impact, h , according to the equation:²⁹

$$h_i = \sum_j [q_{ij} g_j]$$

Equation 3.3

where

h = 1xm row vector with each value representing the total impact for each category

i = Category (column number) from 1 to m

q = $n \times m$ matrix containing the equivalency factors

g = $n \times 1$ column inventory vector

j = Chemical output (row number) from 1 to n

m = Total number of categories

n = Total number of chemical outputs

The sum of each chemical emission value multiplied by that chemical's equivalency factor for a particular category is taken in order to get the total impact for the entire system for each impact category. The equivalency factor data is obtained by looking up each chemical from the inventory vector, g_j , in the TRACI database. If there are no entries for the chemical, all synonyms are searched before assuming the chemical has no impact in any category. This assumption could cause significant error because chemicals created after the latest update of the database could have a significant environmental impact that would be assumed to be zero. In the case of this study, the included inventory flows are all in the database. The equivalency factors obtained from TRACI are entered in the j th chemical row and the i th category column. Each chemical only contributes to (has an equivalency factor for) 1-4 categories, so a zero is entered for the remaining categories. The equivalency factors for each inventory flow (the q matrix) are shown in Table 3.15.

Table 3.15 Equivalency factors from TRACI database (*g* matrix).

Name	Global Warming	Photochemical Smog	Acidification
Carbon dioxide	1	0	0
Carbon monoxide	0	0.017	0
Nitrous Oxide	296	0	0
Methane	23	0.004	0
Nitrogen oxides	0	1.24	40.04
VOCs	0	1.86	0
SOx	0	0	50.79

3.4.3 Normalization

The impact assessment gives a number that indicates how much each storage system impacts each category, but the number does not really give any insight unless it has some context. It does allow comparison of the two systems analyzed in this study, but how do they compare to other heating systems, or the world itself? One kilogram of CO₂ equivalent may affect global warming much less than one kilogram of NO_x affects photochemical smog. The only way to tell if these systems have an impact on the world (or a benefit) is to compare them with a standard like the effect of burning the amount of fuel it would take to supply the same amount of heat that these systems store over their lifetime.

The impacts of the heat systems are normalized to burning natural gas or diesel. The natural gas and diesel impact normalization values are obtained by demanding the amount of heat each system will store in its 20-year life, 28.8 million MJ, as diesel burned or natural gas burned in an industrial furnace. Both these processes and their

upstream processes are already included in this study's heat storage LCA model; therefore, the change in the demand vector will result in impact assessment results of burning the fuel. The final normalized values are calculated as the heat system h vector divided by each normalization vector to get the final percentage values.

3.4.4 Results

Table 3.16 compares the impact values (the h vector) for the two storage design options using the EcoInvent insulation process data. The concrete tank design has higher impact values for all impact categories.

Table 3.16 Life cycle impact assessment normalization and characterization results for EcoInvent Insulation.

Impact Category		Total Value		Normalized to Natural Gas		Normalized to Diesel	
Name	Units	Gravel Pit	Conc. Tank	Gravel Pit	Conc. Tank	Gravel Pit	Conc. Tank
Global Warming	kg CO ₂	3.68E+05	7.39E+05	15%	31%	12%	24%
Photochemical Smog	kg NO _x	1.23E+03	1.83E+03	51%	76%	1.0%	1.4%
Acidification	moles H+	8.64E+04	1.27E+05	114%	167%	2.1%	3.0%

Table 3.17 compares the impact values (the h vector) for the two storage design options using the BEES insulation process data. Again, the concrete tank design has higher impact values for all impact categories.

Table 3.17 Life cycle impact assessment normalization and characterization results For BEES Insulation.

Impact Category		Total Value		Normalized to Natural Gas		Normalized to Diesel	
Name	Units	Gravel Pit	Conc. Tank	Gravel Pit	Conc. Tank	Gravel Pit	Conc. Tank
Global Warming	kg CO ₂	2.18E+05	6.26E+05	9%	26%	7%	20%
Photochemical Smog	kg NO _x	1.14E+03	1.75E+03	47%	73%	0.9%	1.4%
Acidification	moles H+	7.56E+04	1.19E+05	99%	157%	1.8%	2.8%

The results presented in Figure 3.4 compare the two storage design options using each insulation process data set, for the evaluation metrics specified in the scope of the study. Both the energy use and global warming values are normalized with respect to natural gas. From the figure it is clear that both storage options have much lower energy use and global warming impact than the natural gas alternative heating source. The gravel pit impacts are lower than the concrete tank impacts even when comparing the lower concrete tank impact value to the higher gravel pit impact value. The BEES results have higher energy use, but lower global warming impact than the EcoInvent results. This is likely due to the high carbon dioxide emissions from the EcoInvent process data. The different upstream energy use may also contribute to this discrepancy.

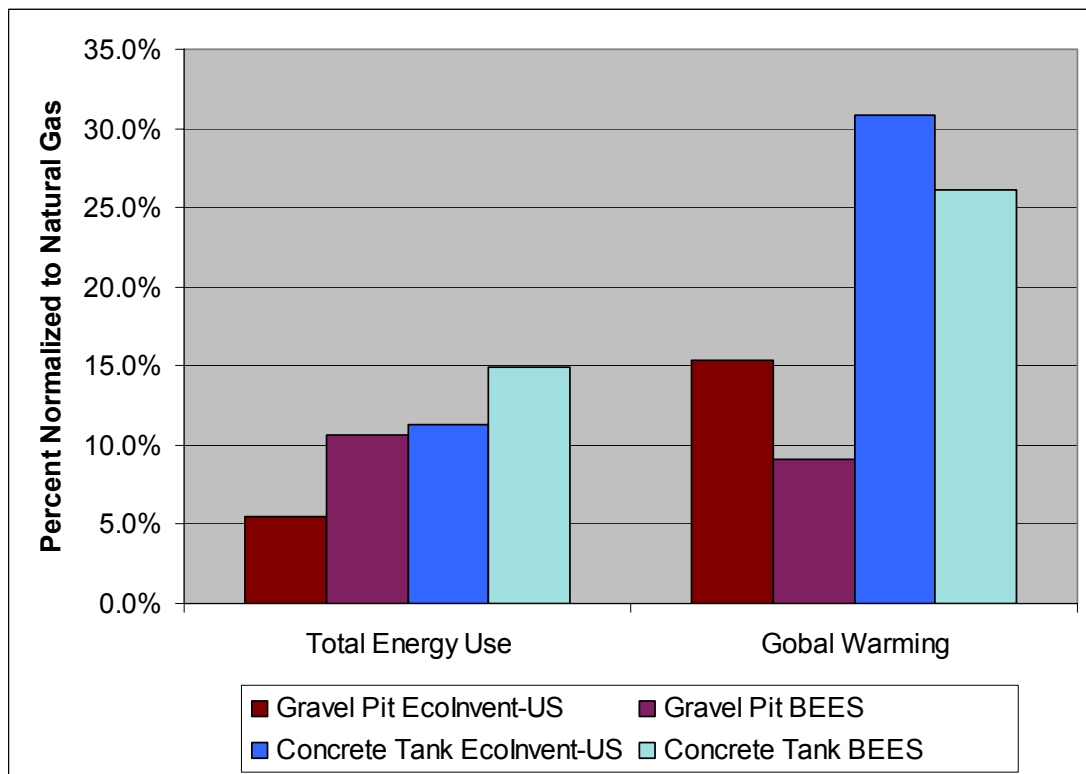


Figure 3.4 Normalized heating system comparison for each insulation data set.

The global warming impact calculations and results are shown in Table 3.18. The global warming emissions from the flows that are tracked during the life cycle of each storage system are less than a third of those that would result from supplying the same amount of stored heat by burning natural gas. The gravel pit design has significantly less global warming impact than the concrete tank design, with less than half of the global warming impact value. Since this environmental impact category is most important as defined in the goal and most reliable as mentioned in the description of the equivalency factors, the contribution to global warming breakdown for each system is described in the next section.

Table 3.18 Global Warming Impact to supply 400 MWh for 20 years in kg CO₂ Equivalents.

					Ecolnvent-US Adjusted		BEES	
Inventory Name	Eq. Factor	Nat Gas	Diesel	Electricity	Gravel Pit	Concrete Tank	Gravel Pit	Concrete Tank
Carbon dioxide	1	2.32E+06	3.11E+06	6.72E+06	3.62E+05	7.33E+05	3.62E+05	7.33E+05
Methane, fossil	23	1.23E+04	6.26E+03	2.51E+04	7.03E+02	1.47E+03	7.03E+02	1.47E+03
Nitrous Oxide	296	1.88E+05	8.27E+04	2.10E+03	4.60E+03	4.82E+03	4.60E+03	4.82E+03
Total		2.52E+06	3.20E+06	6.74E+06	3.68E+05	7.39E+05	3.68E+05	7.39E+05
Normalized to Diesel		78.8%	100.0%	210.7%	11.5%	23.1%	11.5%	23.1%
Normalized to Natural Gas		100.0%	126.9%	267.3%	14.6%	29.3%	14.6%	29.3%

The two storage designs compare more closely in the remaining impact categories as illustrated in Figure 3.5. The gravel pit design has lower impact values for these categories as well. These impacts are shown normalized relative to diesel because diesel affects these impact categories much more than the clean-burning natural gas. The low

percentage values emphasize how insignificant the storage impacts are compared to the effects of burning diesel.

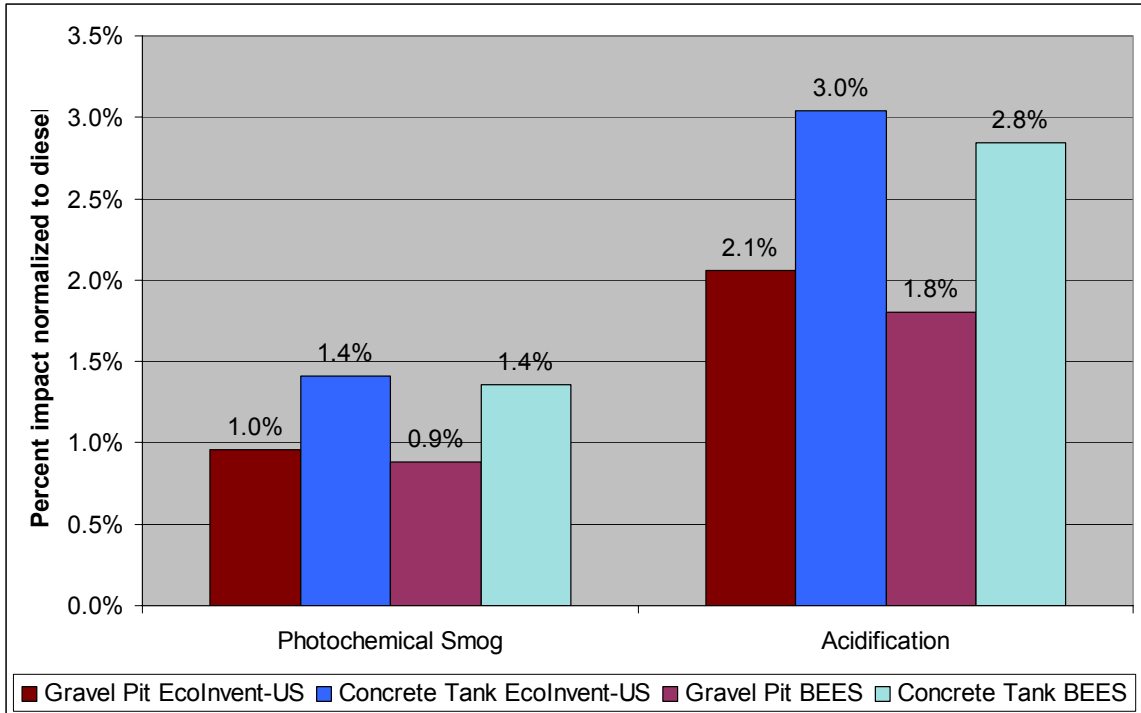


Figure 3.5 Normalized impact comparison to Diesel.

3.5 Interpretation

This section evaluates the results of the life cycle study for completeness, sensitivity, and consistency of the data. The contribution and perturbation analyses in the following sections describe the sensitivity of the model. The consistency of the data is uniform in that most of it is from EcoInvent. However, the electricity and fuel processes from GREET, the BEES insulation LCI, and the APME LCI data impair the consistency. Also, not all of the EcoInvent data sets are created using the same methods and assumptions, which also weakens the consistency. Both storage designs use GREET and the insulation LCI, so the largest inconsistency is from using the APME LCI for only the gravel pit design.

3.5.1 Contribution Analysis

The contribution analysis of each system's components to global warming impact for the flows that are tracked is shown in Figure 3.6 and Figure 3.7. Only the results based on the EcoInvent insulation process data are shown, because the breakdown is very similar. The overwhelming dominance of the insulation contribution to the gravel pit design and its much smaller contribution to the water-tank design stands out. Referring back to the material requirements (Table 3.1) for each system helps explain this difference. The gravel pit is one and a half times larger in volume (in order to store an equal amount of heat), so it has significantly more surface area (115% of the concrete tank) requiring insulation. Another large difference in the two systems is the lining materials. The concrete tank lining consists of stainless steel and concrete which require much higher amounts of energy to process than plastic. Also, the required mass of concrete and steel is much higher in order to provide structural support. The gravel in the water pit design supports the walls of the pit.

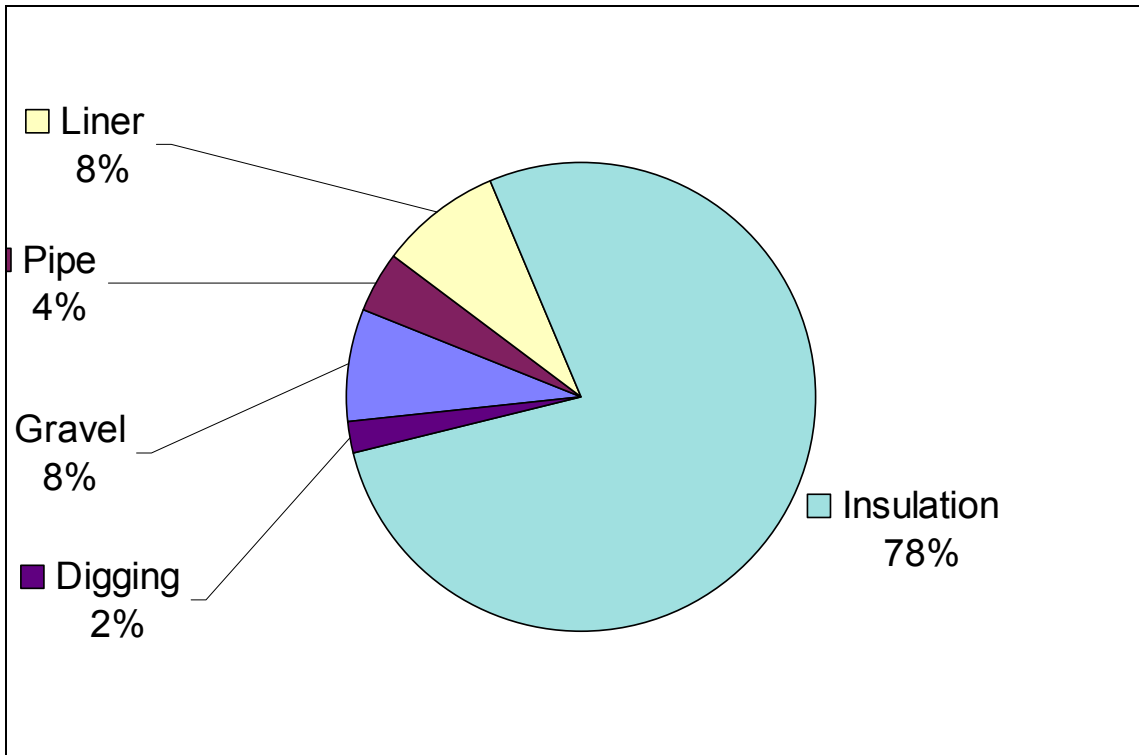


Figure 3.6 Global warming contribution analysis of gravel-water pit storage.

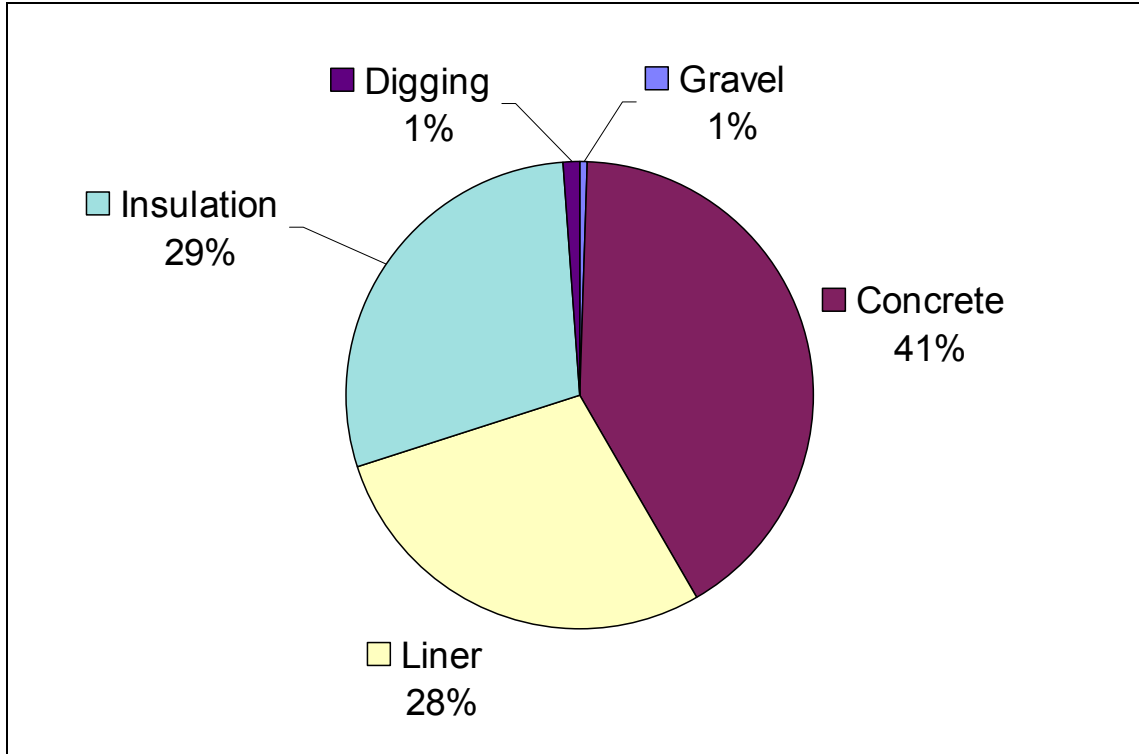


Figure 3.7 Global warming contribution analysis of concrete tank heat storage.

3.5.2 Perturbation Analysis

The perturbation analysis is performed by increasing the amount of each component by 1%, and calculating the percent increase in the final inventory vector. Table 3.19 shows the results for the gravel pit analysis. The majority change is in bold for each inventory flow. Each row's percent increases add up to a one percent increase as would be expected. Insulation increases the final inventory the most for most of the flows as would be expected.

Table 3.19 Percent change of inventory vector with 1% increase of each required input.

Inventory Vector Flow	Gravel	Pipe	Liner	Insulation	Digging
Carbon dioxide	0.08%	0.04%	0.08%	0.77%	0.02%
Carbon monoxide	0.00%	0.00%	0.00%	0.98%	0.00%
Nitrous Oxide	0.06%	0.03%	0.06%	0.79%	0.05%
Methane	0.03%	0.06%	0.19%	0.65%	0.06%
Nitrogen oxides	0.07%	0.02%	0.04%	0.52%	0.34%
VOC	0.02%	0.02%	0.01%	0.93%	0.01%
Particulates, < 10um	0.01%	0.01%	0.02%	0.94%	0.00%
Gravel (in ground)	0.99%	0.00%	0.00%	0.00%	0.00%
Oil, crude, in ground	0.33%	0.09%	0.26%	0.00%	0.31%
Coal, hard, unspecified, in ground	0.44%	0.34%	0.21%	0.00%	0.00%
Gas, natural, in ground	0.44%	0.34%	0.21%	0.00%	0.00%
inputs for other (BTU)	0.00%	0.00%	0.00%	0.99%	0.00%
residual oil (BTU)	0.44%	0.34%	0.21%	0.00%	0.00%
uranium (BTU)	0.44%	0.34%	0.21%	0.00%	0.00%
US Dollars (2005)	0.14%	0.01%	0.33%	0.29%	0.24%

3.5.3 Discernibility

The inventory analysis and impact assessment indicate that the gravel pit design has lower environmental impact than the water-tank design. However, it is important to consider the uncertainty of the data when comparing these differences. Standard deviation, maximum value, and minimum value uncertainty data are available for much of the EcoInvent data, but not for the other data sources. A conservative estimate of 30% uncertainty for the final global warming impact assessment results is used to determine if

the global warming impact results for the two storage systems are truly different. Figure 3.8 shows the global warming impact results for each inventory changed by the 30% uncertainty. The energy use uncertainty bars overlap for the BEES data; therefore, no clear conclusion can be drawn that the gravel-water pit design has lower energy use. However, the global warming uncertainty ranges do not overlap. The difference in global warming impact of the two systems is large enough to conclude that the gravel pit design has lower global warming.

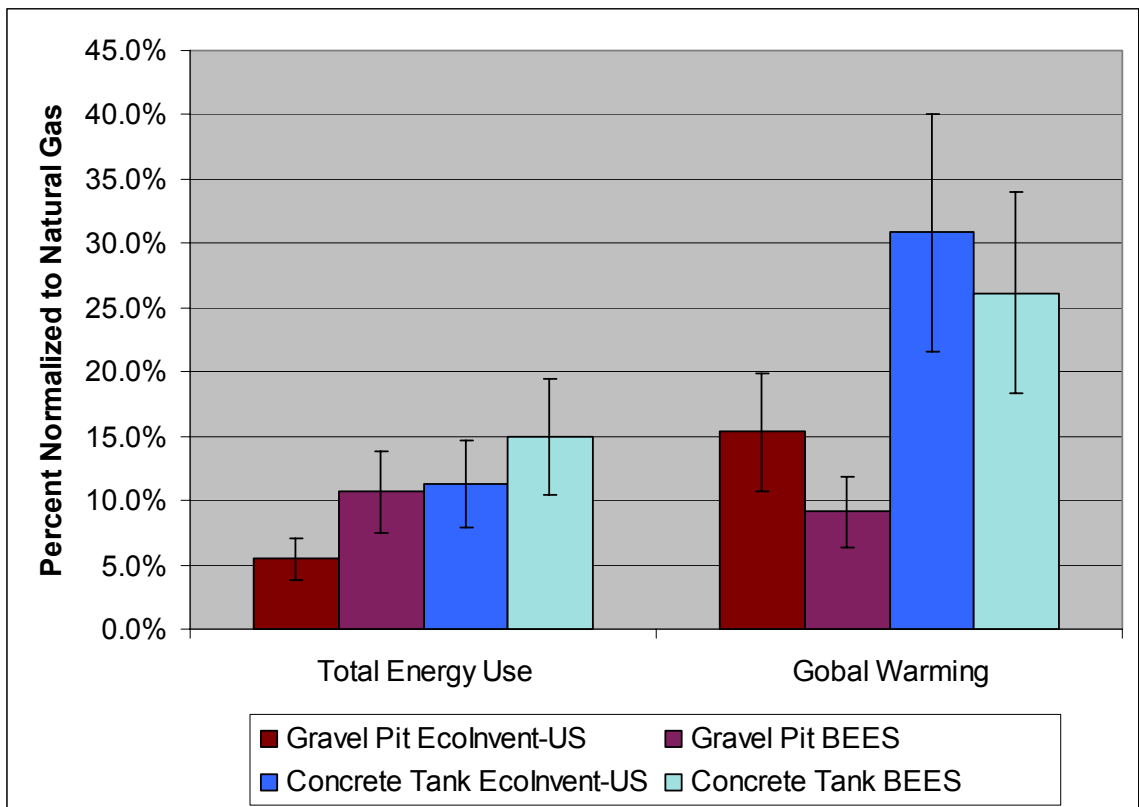


Figure 3.8 Energy use and global warming comparison with 30% uncertainty.

For the impact categories of photochemical smog and acidification, the gravel pit design results in lower impact values. However, for some of these values the difference may not be large enough to be discernible. Figure 3.9 shows a 30% uncertainty range of the two

options for each impact category. The error bars for both impact categories overlap.

Therefore, no conclusions can be made regarding which storage option would have lower impact on these categories. The cost estimates are also too close, only 8.7% different, to conclude with certainty that one system will cost more than the other.

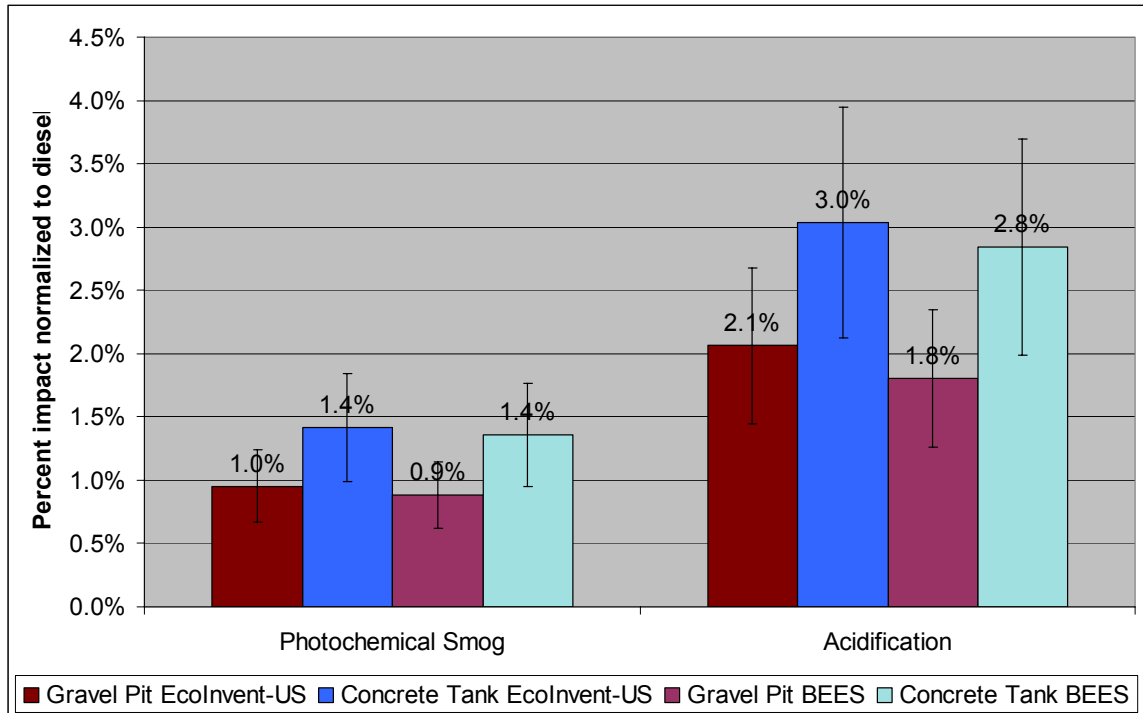


Figure 3.9 Environmental impact with 30% uncertainty range shown.

3.6 Conclusions

The results show that the environmental impact of the gravel pit storage design option is lower than that of the concrete tank design option. When the uncertainty of the cost calculations are considered, the final cost values are too close to be discernable.

Therefore, the gravel pit storage system is selected to be incorporated into the final design. This life cycle study not only provides an environmental impact comparison of these two systems, but also reveals opportunities to decrease the environmental impact

during the detailed design phase. The clearest opportunity for pollution prevention in the gravel pit storage design is to minimize insulation use and to choose an insulation type with low energy use in the production process.

Notes to Chapter 3

¹ International Standards Organization, “Environmental Management Life cycle Assessment Principles and Framework” (ISO 14040, 1997) 2.

² ISO, “Environmental Management Life cycle Assessment Goal and Scope Definition and Inventory Analysis,” (ISO 14041, 1998).

³ Burch, J., J. Salasovich, and T. Hillman, “Cold-Climate Solar Domestic Water Heating Systems: Life-Cycle Analyses and Opportunitites for Cost Reduction,” paper delivered to ISES Solar World Congress sponsored by NREL, Orlando, Florida, August 6-12, 2005, 10 Jan 2006 <<http://www.osti.gov/bridge>>; Ardente, Fulvio, Giorgio Beccali, Maurizio Cellura, and Valerio Lo Brano, “Life cycle assessment of a solar thermal collector.” Renewable Energy 30 (Science Direct 2005) 1031-1054; Mathur, J. and N. K. Bansal, “Energy Analysis of Solar Water Heating Systems in India,” International Journal of Life Cycle Assessment 4 (2) (1999) 113-116.

⁴ Lottner, Volkmar and Mangold, Dirk, “Status of Seasonal Thermal Energy Storage In Germany” (Stuttgart, Germany: Terrastock 2000).

⁵ Schmidt, T., “Central solar heating plants” 167.

⁶ Schmidt, T., D. Mangold, H. Müller-Steinhagen. “Seasonal Thermal Energy Storage in Germany.” paper delivered to ISES Solar World Congress sponsored by the German Federal Ministry for Economy and Technology. Göteborg, Sweden (2003) 3-4.

⁷ Heijungs, R. & S. Suh, Computational Structure of Life Cycle Assessment (The Netherlands: Kluwer Academic Publishers, 2000).

⁸ United States, Environmental Protection Agency, “Tool for the Reduction and Assessment of Chemical and Other Environmental Impacts (TRACI),” EPA: Research & Development: Risk Management Research: Sustainable Technology: Systems Analysis Research, 14 May 2005 <<http://www.epa.gov/ORD/NRMRL/std/sab/traci/>>; Bare, Jane C., Gregory A. Norris, David W. Pennington, and Thomas McKone, “TRACI: The Tool for the Reduction and Assessment of Chemical and Other Environmental Impacts,” Journal of Industrial Ecology 6 (3-4) (The MIT Press 2003) 49-78, 12 July 2005 <http://mitpress.mit.edu/journals/pdf/jiec_6_3_49_0.pdf>.

⁹ GREET 1.6 GUI Beta Release II (Systems Assessment Section Center for Transporation Research Argonne National Laboratory, May 2004).

¹⁰ Cooper, J. S. Lecture on Goal and Scope Definition, ME 599-Life Cycle Assessment, University of Washington, Seattle, WA, Spring 2005. See Appendix B for copy.

¹¹ Heijungs 15.

¹² EcoInvent v1.2 (Swiss Centre for Life Cycle Inventories, 2004).

¹³ Association of Plastic Manufacturers in Europe (APME) 10 July 2005
<http://www.apme.org/media/public_documents/20011009_164930/lca_summary.htm&title=LCA:+Summary+of+topics>.

¹⁴ BEES 3.0 (National Institute of Standards and Technology, October 2002).

¹⁵ United States, Environmental Protection Agency, Compilation of Air Pollutant Emission Factors, Vol 2: Mobile Sources (AP-42) (1991).

¹⁶ United States, Census Bureau, Transportation, Commodity Flow Survey, 2002 Economics Census 2004.

¹⁷ Pfeil, Markus and Holger Koch, "High Performance—Low Cost Seasonal Gravel/Water Storage Pit," Solar Energy 69 (6) (2000) 466, Science Direct 18 Apr. 2005
<http://www.sciencedirect.com/science?_ob=MIimg&_imagekey=B6V50-41SCBB9-5-9&_cdi=5772&_user=582538&_orig=browse&_coverDate=12%2F31%2F2000&_sk=999309993&view=c&wchp=dGLbVtz-zSkWb&md5=7840bdf76a05b3ec8c5bb173ae615053&ie=/sdarticle.pdf>.

¹⁸ Lippiatt, Barbara C., "Building for Environmental and Economic Sustainability Technical Manual and User Guide," Office of Applied Economics, Building and Fire Research Laboratory, National Institute of Standards and Technology (Gaithersburg, MD October 2002) 8.

¹⁹ McMaster-Carr Supply Company. McMaster-Carr on-line catalog. 16 Jan 2006
<<http://www.mcmaster.com>>.

²⁰ United States, Washington State Department of Transportation, Washington State Ferries, "M/V Tillikum: Vessel Information," Washington State Ferries: Vessel Information: M/V Tillikum, 12 July 2005
<http://www.wsdot.wa.gov/ferries/your_wsf/our_fleet/index.cfm?vessel_id=43>.

²¹ Heijungs 11.

²² "SiMetric bulk material density," 10 July 2005
<http://www.simetric.co.uk/si_materials.htm>.

²³ Mateiciuc, "Polyethylene hoses LDPE-PELD, pipelines, water-service pipes, water pipes" MAT: Products: PE Water Pipes, 5 July 2005 <<http://www.mat-plasty.cz/en/pe-trubky-ldpe.php>>.

²⁴ Hydro, "Crude oil Canada – Hydro," Hydro: Oil and gas products: Crude oil production international: Crude oil Canada, 10 July 2005
<http://www.hydro.com/en/our_business/oil_energy/sales_distribution/products/crude_oil_canada.html>.

²⁵ Wilson, R. and W. J. Jones. Energy, Ecology, and the Environment (Academic Press. 1974) 88.

²⁶ Annual Energy Review 2004, Report No. DOE/EIA-0384 (2004), 10 July 2005
<http://www.eia.doe.gov/aer/append_a.html>.

²⁷ Heijungs 17.

²⁸ Heijungs 18.

²⁹ Heijungs 162.

Chapter 4: Heat Transfer Simulation

A detailed heat transfer simulation is performed on the heating system in order to simulate the diurnal temperature and heat transfer changes of each sub-system in the solar-thermal heating system: the collector system, the storage system, and the greenhouse heating delivery system. In the preliminary model, the three sub-systems were treated separately. The calculated total heating demand for the year was used to provide an estimate of the required storage and collector size, but this does not accurately reflect how the integrated heating system works. In reality, the collector will continuously increase the tank temperature, and the greenhouse heating demand will continuously decrease the temperature. This constant, gradual charging and discharging of the storage system needs to be simulated in order to design the heating system to perform within specific operating parameters (boundary conditions).

Section 4.1 describes the physical model, including sub-system component selection, assumptions, and operating parameters. Section 4.2 presents the heat transfer equations used to model the characteristics and simulate the temperatures of each sub-system: 4.2.4 Collector Hourly Heat Gain, 4.2.5 Storage System Hourly Temperatures, 4.2.6 Heat Delivery System (sections 4.2.1 to 4.2.3 describe the Greenhouse Hourly Heat Demand). Section 4.3 describes the simulation code that solves the set of heat transfer equations described in section 4.2 . The simulation code lists the required inputs and solves the heat transfer equations for each sub-system for each hour of the year. The design of the heating system is optimized for minimum cost by calculating the cost of the system for a range of insulation thicknesses. The code automatically solves for the collector area,

storage size, and initial temperatures that balance the energy entering and leaving the storage system for each insulation thickness. Section 4.4 presents the final heating system design and the simulation code results that describe its performance.

4.1 Physical Model

Figure 4.1 shows the physical model of the system with temperature nodes, heat transfer, and fluid flow. The storage tank is divided into 3 nodes to simulate the temperature stratification. Each node has a different storage volume, surface area, and temperature associated with it.

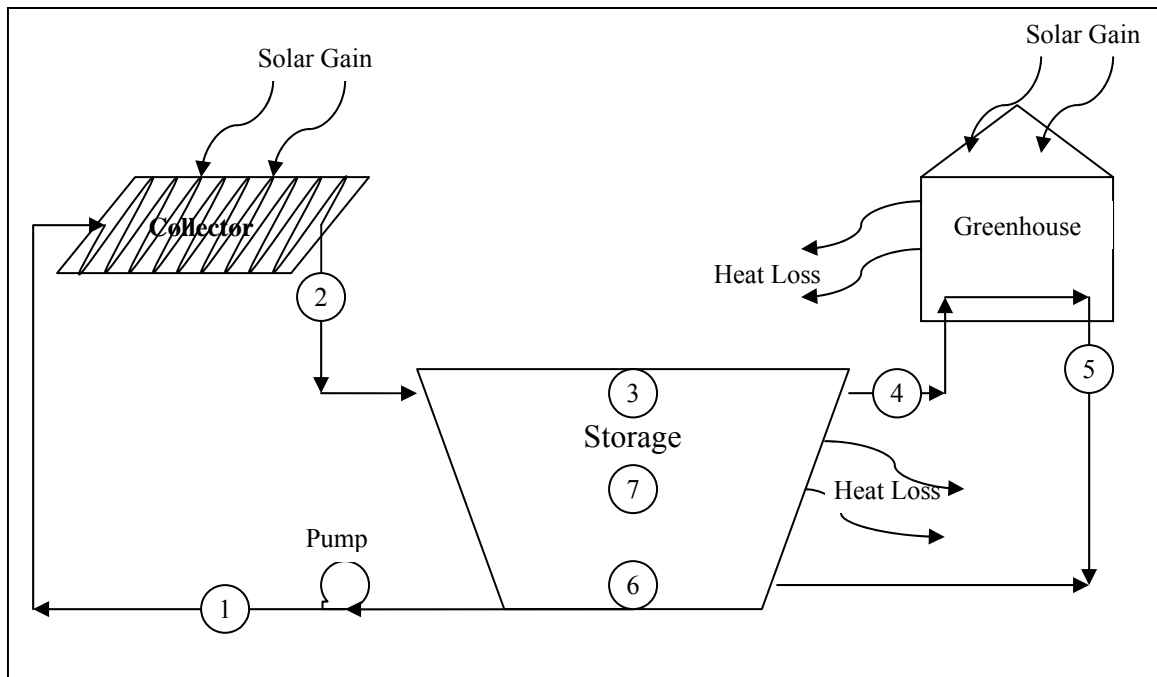


Figure 4.1 Diagram of physical model with temperature nodes.

4.1.1 Component Selection

In order to accurately simulate each component in the system, each one needs to have all of its characteristics defined. Different types of collectors or heat delivery systems have different characteristics; therefore the specific type of component needs to be selected for each part of the heating system. Each component must be selected as an off-the-shelf

unit or designed to meet the specific needs of the heating system. The component selections and their justifications are shown in Table 4.1.

Table 4.1 Heating system component selection and justification

Sub-system	Selection/Design Decision	Justification
Collector	Thermomax Mazdon vacuum-tube flat plate collector	High inlet temperatures require maximum heat resistance in collectors. MAZDON has the lowest-sloped efficiency curve of SRCC certified flat plate collectors. ¹
Greenhouse Heat Delivery	Cross-linked polyethylene (PEX) with aluminum layer tubing in soil bed.	Provides most efficient heating directly where plants need it most. ² Allows for custom design of extra tubing to minimize storage tank return temperature. Aluminum provides oxygen barrier. ³
	Maintain average soil surface temperature at 22 C	Results in ideal plant temperature for flowering roses (about 18 C). ⁴
Gravel-Water Storage Pit	Indirect heat exchange from collector to storage with cross-linked PE tubing using a tubing length to storage volume ratio of 6.36 m tube/m ³ storage ⁵	For storage volumes less than 10,000 m ³ water equivalent, the cost benefit of direct exchange is not worth the risk of opening for pump access required at bottom of tank. ⁵ Indirect exchange means a glycol can be used in collector according to manufacturer's requirement.
	Double-layer flexible polypropylene storage pit lining	Provides redundancy and vacuum control seal and 90 C maximum pit temperature.
	Mineral wool blankets	Low cost, moisture permeability.

4.1.2 Assumptions

Many of the assumptions for the detailed simulation are the same as for the preliminary analysis. However, there are several assumptions that must be changed to simulate the system more accurately. The most significant of these is using hourly TMY2 data for Seattle instead of the monthly average daily meteorological data. The TMY2 (Typical Meteorological Year) "data sets were produced by the National Renewable Energy Laboratory's (NREL's) Analytic Studies Division under the Resource Assessment Program . . . derived from the 1961-1990 National Solar Radiation Data Base

(NSRDB).”⁶ This difference not only gives more up-to-date and specific data, but it changes the form of many of the solar radiation gain equations as well.

The tank losses are modeled based on variable storage temperatures, external surface area, and insulation thickness rather than approximating those values. The specific heat values for water are calculated from a second-order function of temperature at each temperature node and for each time-step. The collector efficiency is determined according to the efficiency equation for the “Thermomax Mazdon Collector System” published by the Solar Rating and Certification Corporation.¹ Another important difference is that instead of assuming an average greenhouse temperature of 20 C, the temperature range is set at a minimum temperature of 18 C and a maximum temperature of 24 C. When the temperature reaches 24 C, increased ventilation is assumed to maintain the temperature.

4.1.3 Operating Parameters

Table 4.2 lists each temperature point and any design limits placed on it. The system operating parameters are as follows:

1. Maintain greenhouse temperatures in the range of 18 to 24 C
2. Maintain maximum storage temperature less than 90 C to prevent degradation of lining material
3. Balance collector size to provide the same amount of heat to storage as is needed for the greenhouse heating demand and loss through insulated storage walls
4. Control mass flow rates to meet minimum and maximum requirements of collectors and heating delivery tubing

Table 4.2 Temperature point operating parameters.

Point	Location	Temp (C)	Description	
T1	Collector Inlet	88	Maximum	to transfer heat from collector
T2	Collector Outlet	90	Set	to maximize storage temperature change over year
T3	Storage, top	90	Maximum	to prevent lining deterioration
T4	Greenhouse Inlet	32	Minimum	to transfer heat to greenhouse
T5	Greenhouse Outlet	30	Set	to maximize storage temperature change over year
T6	Storage, bottom	90	Maximum	to prevent lining deterioration
T7	Storage, mid	90	Maximum	to prevent lining deterioration
Th	Greenhouse, air	18-24	Set range	to optimize plant growth ⁷
Ts	Soil, at top surface	22	Set average	to optimize plant growth

4.2 Heat Transfer Equations

Like the assumptions, many of the heat transfer equations used to calculate solar radiation gain and heat loss are the same for the detailed heat transfer simulation as for the preliminary analysis. However, each equation now results in a 1x8,760 vector for each hour of the year, rather than a 1x12 vector for each month of the year. For this reason, a sample day of January 7th is used for an example of the calculation results.

4.2.1 Greenhouse Hourly Heat Loss

The hourly heat loss from the greenhouse is calculated based on the heat loss rate given in Equation 2.2 integrated over one hour to give the total hourly heat loss:

$$H_L = \frac{MJ}{10^6 J} (UA)_h (Th - Ta) \Delta t$$

Equation 4.1

where

H_L = Hourly heat loss from greenhouse in MJ

Th = Greenhouse temperature of 18 C

Ta = Ambient temperature in C

Δt = Time change per hour time step, 3600 seconds

The greenhouse heat loss coefficient UA_h value of 11,299W/C from the preliminary analysis is the same value used in Equation 4.1. Again, only positive answers to the equation result in a heat loss value. The ambient temperature is input as a 1x8,760 vector in excel, and the equation outputs a 1x8,760 vector of the heat loss for each hour in the year. Table 4.3 shows the results of Equation 4.1 for the sample day.

Table 4.3 Heat Loss for January 7th

Hour	Temp (C)	Heat Loss (MJ)	Hour	Temp (C)	Heat Loss (MJ)
1	3.3	598	13	8.9	370
2	3.9	574	14	8.9	370
3	3.3	598	15	8.3	395
4	3.3	598	16	7.8	415
5	3.3	598	17	6.1	484
6	3.9	574	18	5.6	504
7	3.3	598	19	5.0	529
8	3.9	574	20	5.0	529
9	3.9	574	21	4.4	553
10	5	529	22	3.9	574
11	6.7	460	23	2.2	643
12	7.8	415	24	1.7	663

4.2.2 Greenhouse Hourly Solar Heat Gain

The solar radiation gain equations for the hourly time step are based on the same isotropic diffuse assumption as the monthly heat gain, but several of the average monthly values from the preliminary assessment must be calculated for each hour. The total heat gain is still defined as the sum of the product of the specific heat gain on each surface multiplied by the area of that surface. The specific solar radiation gain equation has the same form as Equation 2.7 in the preliminary assessment but with hourly variables:⁸

$$S = I_B R_B (\tau\alpha)_B + I_D (\tau\alpha)_D \frac{1 + \cos \beta}{2} + I_{\rho_G} (\tau\alpha)_G \frac{1 - \cos \beta}{2}$$

Equation 4.2

where

S = Hourly absorbed radiation in Wh/m²

I = Hourly radiation on a flat surface in Wh/m²

In this case the bars over the variables indicating monthly averages have been removed and the daily radiation variable H has been replaced with the hourly radiation variable I . The diffuse radiation values I_D are no longer estimated based on a clearness index as in the preliminary assessment, but are input as vectors from the TMY2 data for diffuse radiation on a flat plate. The beam radiation on a flat plate I_B is still calculated as the difference between the total and the diffuse radiation on a flat plate, $I_B = I - I_D$. The diffuse and ground reflected geometry factors and transmittance-absorptance products do not depend on the sun angle, therefore they remain the same as for the preliminary assessment and constant throughout the year. As with the monthly average R_B and $(\tau\alpha)_B$ values, the hourly R_B and $(\tau\alpha)_B$ values are dependent on the angle of the sun. However, now this angle changes for each hour, so R_B is based on δ , ω , and ϕ calculated for each hour instead of the monthly average δ , ω_s , and ϕ values. The hourly R_B value is calculated according to the equation:⁹

$$R_B = \frac{\cos(\phi - \beta) \cos(\delta) \cos(\omega) + \sin(\phi - \beta) \sin(\delta)}{\cos(\phi) \cos(\delta) \cos(\omega) + \sin(\phi) \sin(\delta)}$$

Equation 4.3

where

δ = Declination angle in degrees

ω = Hour angle from the local meridian in degrees

The declination angle is determined based on the day of the year according to the equation:

$$\delta = 23.45 * \sin(360 * (284 + \text{day})/365 * \text{PI}()/180)$$

Equation 4.4

The hour angle is defined based on the time of day according to the equation:

$$\omega = (\text{solartime} - 12) * 15$$

Equation 4.5

The $\frac{(\overline{\tau\alpha})_b}{(\overline{\tau\alpha})_n}$ ratios are still determined from figure 5.6.1 of Duffie-Beckman based on the incident angle θ . However, the incident angle is calculated for each hour, rather than determined from a figure. Since there are too many data points to read the figure for each hour, a ratio is assigned for 9 ranges of the incident angle, which is calculated according to the equation:

$$\theta = \arccos[\cos(\phi - \beta) \cos(\delta) \cos(\omega) + \sin(\phi - \beta) \sin(\delta)]$$

Equation 4.6

The calculation of hourly heat gain for January 7th is shown in Table 4.4. The R_B , S , and θ values for the south wall are not shown, but the value in the heat gain column includes both the roof and the south wall.

Table 4.4 Hourly heat gain on south roof and wall for January 7th.

Hour	I	I _D	I _B	δ	Solar Time	ω	R _B	θ	$\frac{(\bar{\tau}\alpha)_b}{(\bar{\tau}\alpha)_n}$	S _R	Heat Gain
Units:	Wh	Wh	Wh	°	hrs	°	NA	°	NA	MJ/m ²	MJ
1	0	0	0	-22	0.45	-173	0.90	144	0.000	0	0
2	0	0	0	-22.4	1.45	-158	0.88	139	0.000	0	0
3	0	0	0	-22.4	2.45	-143	0.82	130	0.000	0	0
4	0	0	0	-22.4	3.45	-128	0.71	118	0.000	0	0
5	0	0	0	-22.4	4.45	-113	0.52	106	0.000	0	0
6	0	0	0	-22.4	5.45	-98	0.13	93	0.000	0	0
7	0	0	0	-22.4	6.45	-83	0.00	79	0.400	0	0
8	0	0	0	-22.4	7.45	-68	0.00	65	0.720	0	0
9	52	28	24	-22.4	8.45	-53	6.75	52	0.900	101	424
10	126	42	84	-22.4	9.45	-38	3.78	38	0.980	210	874
11	207	35	172	-22.4	10.45	-23	3.12	24	0.990	343	1426
12	284	35	249	-22.4	11.45	-8	2.90	13	0.999	461	1914
13	265	60	205	-22.4	12.45	7	2.89	12	0.999	392	1628
14	212	73	139	-22.4	13.45	22	3.08	23	0.990	294	1222
15	128	94	34	-22.4	14.45	37	3.68	36	0.980	117	485
16	78	50	28	-22.4	15.45	52	6.08	50	0.900	115	483
17	5	5	0	-22.4	16.45	67	0.00	64	0.720	2	9
18	0	0	0	-22.4	17.45	82	0.00	78	0.400	0	0
19	0	0	0	-22.4	18.45	97	0.07	91	0.000	0	0
20	0	0	0	-22.4	19.45	112	0.49	105	0.000	0	0
21	0	0	0	-22.4	20.45	127	0.70	117	0.000	0	0
22	0	0	0	-22.4	21.45	142	0.81	129	0.000	0	0
23	0	0	0	-22.4	22.45	157	0.87	138	0.000	0	0
24	0	0	0	-22.4	23.45	172	0.90	144	0.000	0	0

4.2.3 Greenhouse Hourly Heat Demand

An energy balance on the greenhouse is performed to determine the hourly heat demand of the greenhouse. Unlike the preliminary analysis, this is not assumed to be steady-state. On an hourly basis, the change in energy of the system cannot be assumed to be zero because of fluctuations in the greenhouse temperature. Assuming all variables to be constant over one hour and that the heating demand is set to maintain the greenhouse at a constant temperature, the temperature change over one hour can be calculated:

$$\Delta Energy_{sys} = Energy_{in} - Energy_{out}$$

$$Cap(Th^{n+1} - Th^n) = F_{c,D}H_D + H_G - H_L$$

$$Th^{n+1} = Th^n + F_{c,S}(F_{c,D}H_D + H_G - H_L)/Cap$$

Equation 4.7

where

H_D = Heat demand in MJ

H_G = Solar heat gain in MJ

H_L = Heat loss in MJ

$F_{c,S}$ = Control function to set a maximum storage temperature

$F_{c,D}$ = Control function for heating demand

Cap = Effective capacitance of the building, 0.418 MJ/C

Th^{n+1} = Greenhouse temperature at the end of the hour in C

Th^n = Greenhouse temperature at the beginning of the hour in C

The effective capacitance is calculated assuming a concrete floor thickness of 0.2 meters and a thermal capacitance for the concrete of 2.06 MJ/m³-C.¹⁰ The control function for the storage $F_{c,S}$ is used to set a maximum limit to the temperature of the greenhouse. If this limit is not set, the thermal storage capacity would be infinite. The use of the function assumes that ventilation is used to dump excess energy when the greenhouse temperature is above the set temperature of 24 C. When Th^k is less than 24, $F_{c,S}$ is one; when Th^k is greater than 24 and the heat gain is less than the heat loss, $F_{c,S}$ is one; and when Th^k is greater than 24 and the heat gain is greater than the heat loss, $F_{c,S}$ is zero.

The control function for the heating demand $F_{c,D}$ is set to one when the greenhouse temperature is less than 18 C, and 0 otherwise. This allows the thermal capacitance of the building to compensate for the heat loss when the greenhouse is above its minimum allowable temperature of 18 C. Because the heating delivery system is set to keep the

greenhouse temperature constant, there is no temperature change or thermal storage to account for when calculating the heating demand, so the same assumption applies as in Equation 2.1. The difference is that the control function sets the heating system to only supply heat when the greenhouse temperature demands it.

$$H_D = F_{c,D}(H_L - H_G)$$

Equation 4.8

The results of Equation 4.7 and Equation 4.8 are shown in Table 4.5 and Figure 4.2. The internal thermal storage change shown in the figure reflects the difference between the thermal mass temperature and the previous hour's temperature. It is calculated by multiplying the temperature difference by the greenhouse heat storage capacity. The temperature of the thermal mass increases steadily during sunny days and decreases during the evening. This decrease in stored thermal energy offsets the losses through the exterior windows. This means there is no need for heat supplied by the active heating system until late at night, in this case until after midnight. Figure 4.3 shows a 5 day period in autumn to give an idea of typical diurnal behavior.

Table 4.5 Heat Demand for January 7th.

Hour	Heat Gain (MJ)	Heat Loss (MJ)	Thermal Mass Temperature (C)	Internal Energy Change (MJ)	Heat Demand (MJ)
1	0	598	17.9	0	679
2	0	574	17.9	0	655
3	0	598	17.9	0	679
4	0	598	17.9	0	679
5	0	598	17.9	0	679
6	0	574	17.9	0	655
7	0	598	17.9	0	679
8	0	574	17.9	0	655
9	424	574	17.9	0	231
10	874	529	18.3	345	0
11	1426	460	19.5	966	0
12	1914	415	21.4	1,500	0
13	1628	370	22.9	1,258	0
14	1222	370	24.0	852	0
15	485	395	24.0	0	0
16	483	415	24.0	0	0
17	9	484	23.2	-475	0
18	0	504	22.4	-504	0
19	0	529	21.6	-529	0
20	0	529	20.8	-529	0
21	0	553	20.0	-553	0
22	0	574	19.1	-574	0
23	0	643	18.1	-643	0
24	0	663	17.1	-663	0

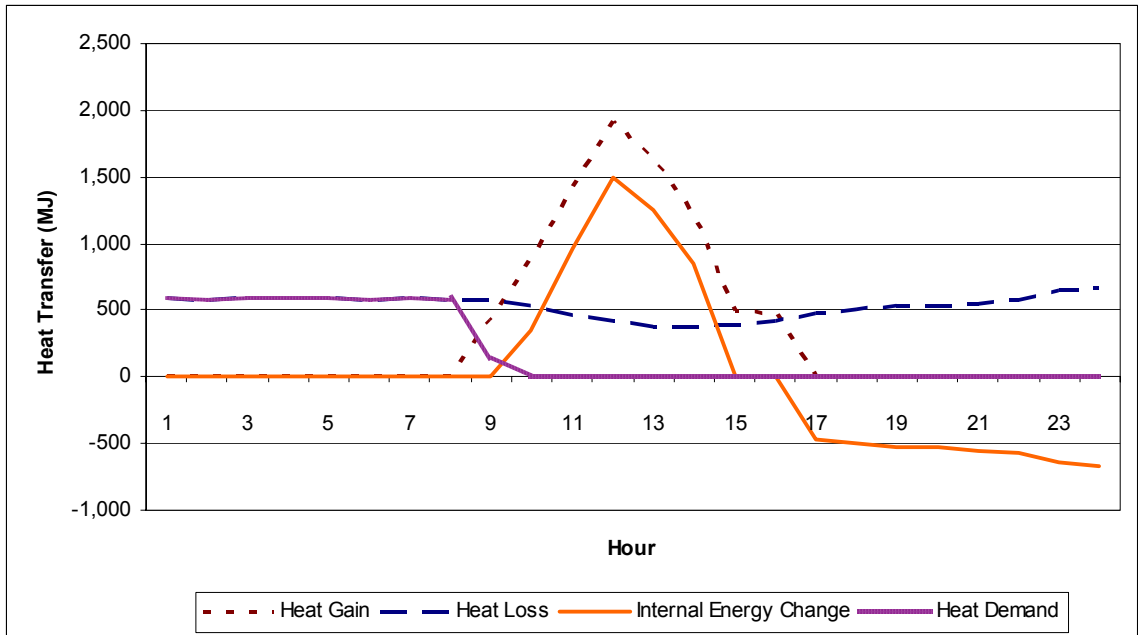


Figure 4.2 Greenhouse heat profile during the 24 hour period of January 7th.

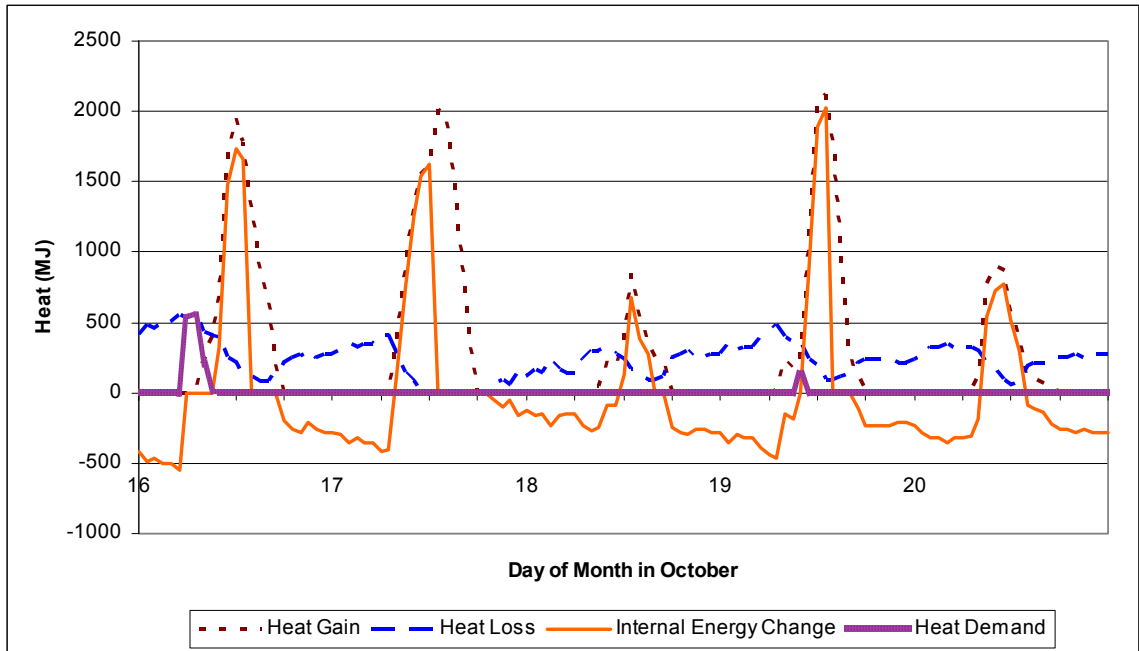


Figure 4.3 Hourly greenhouse heat profile over 5 days in October

4.2.4 Collector Hourly Heat Gain

Tilt Angle Optimization

In most cases the optimum tilt angle for solar-thermal collectors equals the latitude angle (in this case, 47.5 degrees). However, because of the high number of overcast days during the Seattle winter, the optimum tilt angle is lower. This lower tilt angle takes advantage of higher summer radiation, which is stored for later use. Figure 4.4 shows the solar heat gain for one year from the collectors as a function of the tilt angle. The simulation code generates this figure by simulating the heat collected for one year over a range of tilt angles, keeping all other input parameters constant (listed in section 4.3.1 Input Parameters). It is important to optimize the tilt angle based on the simulation in order to account for the variation of the collector inlet temperature throughout the year. The optimum tilt angle of 33 degrees is used in Equation 4.11 to calculate the incident radiation on the collectors.

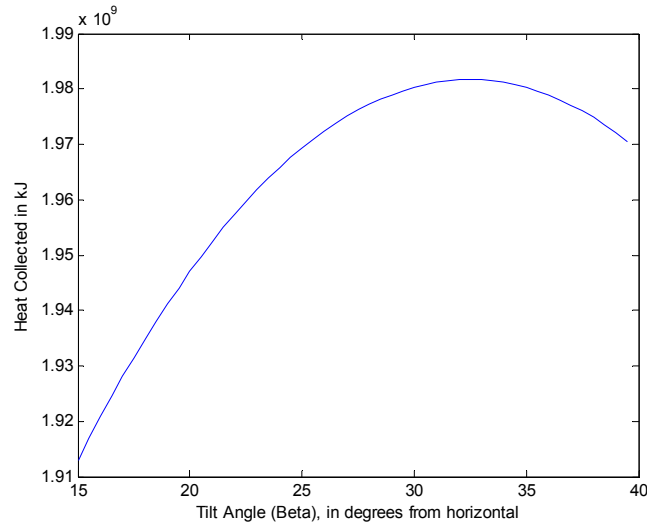


Figure 4.4 Collector heat gain as a function of the tilt angle, beta.

Collector Heat Gain Calculation

The total heat gain from the collectors is calculated based on technical information equations (for efficiency and incident angle modifier) published by the Solar Collector Rating and Certification Corporation (SRCC).¹ These equations come from performance test data conducted in certified laboratories. The hourly heat collected is calculated based on collector efficiency and the incident radiation:

$$H_{Cl} = \eta K_{\tau\alpha} I_T A_C \frac{10^6 \text{ MJ}}{\text{J}} \frac{3600 \text{ s}}{\text{h}}$$

Equation 4.9

where

H_{Cl} = Heat collected in MJ

η = Efficiency of collector

$K_{\tau\alpha}$ = Incident angle modifier

I_T = Incident radiation on the tilted collector surface in kWh/m²

A_C = Area of collector in m²

The efficiency is calculated according to the equation:

$$\eta = 0.525 - 0.8858 \frac{(T_1 - T_a)}{I_T} - 0.0074 \frac{(T_1 - T_a)^2}{I_T}$$

Equation 4.10

where

T_I = Inlet temperature to collector

T_a = Ambient temperature

and ¹¹

$$I_T = I_B R_B + I_D \frac{1 + \cos \beta}{2} + I_{\rho_G} \frac{1 - \cos \beta}{2}$$

Equation 4.11

The total incident radiation is calculated based the same isotropic diffuse model as the total absorbed radiation described for the greenhouse heat gain, without the transmittance-absorptance products. These values, as well as the heat losses and heat removal efficiency of the collector are accounted for in the efficiency equation. The dependence of the transmittance-absorptance product on the incident angle is accounted for using the incidence angle modifier:

$$K_{\tau\alpha} = 1 - 0.1441(S) - 0.0948(S)^2$$

Equation 4.12

where

$$S = \frac{1}{\cos(\theta)} - 1$$

Equation 4.13

4.2.5 Storage System Hourly Temperatures

The temperature of the tank at each node needs to be calculated for each hour in order to simulate the amount of heat being stored. The energy balance on the storage tank results in a differential equation as follows:

$$\Delta E_{\text{sys}} = E_{\text{in}} - E_{\text{out}}$$

$$MassCp \frac{DT}{dt} = H_{\text{Coll}} - H_{\text{Dem}} - H_{\text{Loss}}$$

Equation 4.14

Similarly to calculating the temperature change for the greenhouse, assuming that the variables remain constant over one hour results in an equation that can be solved for the storage temperatures at the end of the hour. The temperature equations for each node of the tank are given below. These equations account for the heat losses through the walls as well as water flowing between nodes and into and out of the tank. Figure 4.5 presents a diagram of the stratification model with the three temperature nodes. A dashed line represents the control volume around each node; straight arrows show the water flow and curved arrows show the heat flow crossing each control boundary. The temperature at node 4 is assumed to be equal to that at node 3.

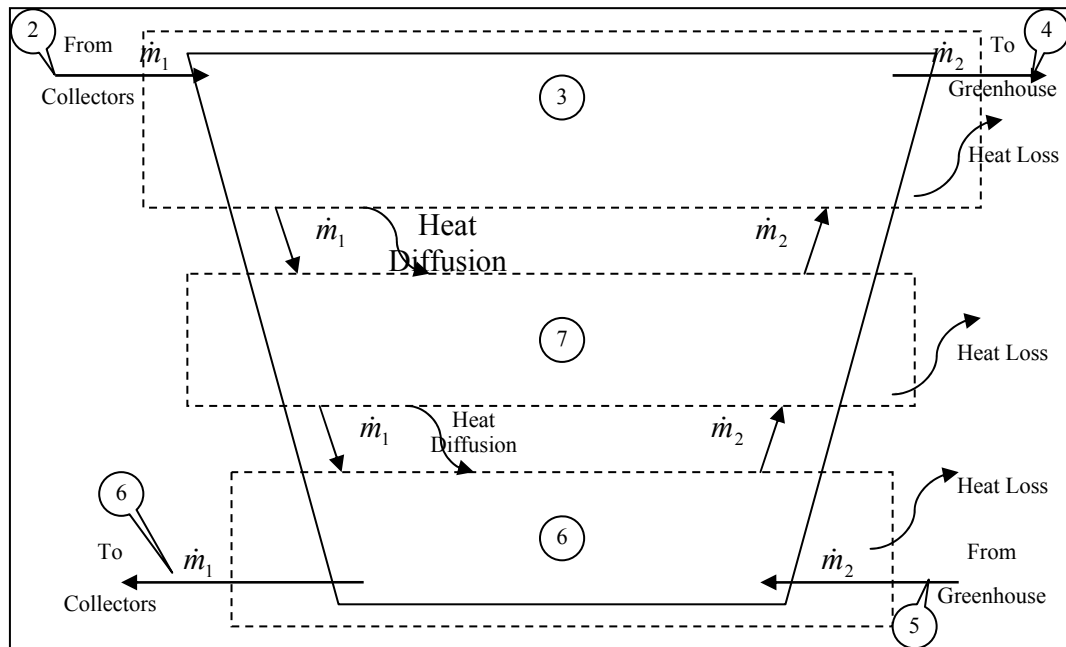


Figure 4.5 Storage tank stratification showing heat and water flow.

$$T_3^{n+1} = T_3^n + \frac{\Delta t}{M_{eq,3} Cp_3} \left[\dot{m}_1 (Cp_2 T_2 - Cp_3 T_3) + \dot{m}_2 (Cp_7 T_7 - Cp_3 T_3) \right] - \frac{k_w A_{mt}}{L} (T_3 - T_7) - U_i S A_3 (T_3 - T_g)$$

Equation 4.23

where

T_3^{n+1} = Temperature of node 3 at end of hour in C

T_3^n = Temperature of node 3 at beginning of hour in C

Δt = Change in time during 3600 second timestep

$M_{eq,3}$ = Equivalent mass of node 3 in kg H₂O

Cp_3 = Specific heat of water at T_3^k in J/kg-C

\dot{m}_1 = mass flow rate of collector in kg/s

\dot{m}_2 = Mass flow rate of heat delivery to greenhouse in kg/s

k_w = conductivity of water in W/m-K

A_{mt} = Cross sectional area between the top and middle sections of the tank in m²

L = Distance between nodes (1/3 of inner tank height) in m

U_t = Tank heat loss coefficient (based on insulation thickness) in W/m²-K

SA_3 = Surface area of node 3 in m²

T_g = Temperature of ground, 10 C

It is important to note that the water temperature and properties are based on conditions at the beginning of the hour. Also, the numbered subscripts indicate values at that numbered node. Variables with the same symbol, but different subscript as defined above are not redefined.

$$T_7^{n+1} = T_7^n + \frac{\Delta t}{M_{eq,7} Cp_7} \left[\dot{m}_1 (Cp_3 T_3 - Cp_6 T_6) + \dot{m}_2 (Cp_6 T_6 - Cp_3 T_3) + \frac{k_w A_{mt}}{L} (T_3 - T_7) - \frac{k_w A_{mb}}{L} (T_7 - T_6) - U_t SA_7 (T_7 - T_g) \right]$$

Equation 4.24

where

A_{mt} = Cross sectional area between the middle and bottom sections of the tank in m²

$$T_6^{n+1} = T_6^n + \frac{\Delta t}{M_{eq,6} Cp_6} \left[\dot{m}_1 (Cp_7 T_7 - Cp_6 T_6) + \dot{m}_2 (Cp_5 T_5 - Cp_6 T_6) + \frac{k_w A_{mb}}{L} (T_7 - T_6) - U_t SA_6 (T_6 - T_g) \right]$$

Equation 4.25

There are no control functions in these equations to dictate whether there is a heating demand to be supplied to the greenhouse or if there is heat gain from the collectors. The control comes from the mass flow rate values. The mass flow rate of the collector is zero when there is negligible heat gain on the collectors; otherwise, it is adjusted to supply a constant return temperature T_2 of 90 C. Likewise, the mass flow rate for the greenhouse heating is set to supply a return temperature T_5 of 30 C. It is set to zero when the flow rate required to reach 30 C is less than the minimum recommended flow rate in the heat delivery tubing. The mass flow rates for the collector system and the heat delivery system are calculated from an energy balance around each system:

$$\dot{m}_1 = \frac{H_{Cl}}{Cp_2T_2 - Cp_1T_1}$$

Equation 4.26

$$\dot{m}_2 = \frac{H_D}{Cp_4T_4 - Cp_5T_5}$$

Equation 4.27

where

H_{Cl} = Heat collected in MJ from Equation 4.9

H_D = Heat demand in MJ from Equation 4.8

4.2.6 Heat Delivery System

The heat to the greenhouse is supplied though one inch PEX-AL-PEX tubing embedded in the plant beds. Four inches of wet sand over the tubing will distribute the heat evenly and effectively.¹² The selection of the diameter of the tubing is based on the maximum required flow rate to meet the heat demand and the maximum allowable flow rate for the tubing. The recommended minimum and maximum flow rates for 1" PEX-AL-PEX tubing are 5.2 and 10.4 gpm respectively.¹³ This converts to a minimum flow rate of 0.32

kg/s and maximum of 0.65 kg/s. The maximum value limits the noise and the minimum value ensures that air bubbles are entrained. In order to have a more uniform temperature in the beds and to stay within the maximum allowed flow rate, 4 heating circuits will be run each with an inlet temperature equal to the top tank temperature and an outlet temperature equal to the design parameter of 30 C. The limiting conditions for the maximum flow rate are in March, when the top tank temperature is near its lowest value and the heating demand can still reach high values. Under these conditions the small temperature change from inlet to outlet combined with the large heat load result in the highest flow rate requirement. The maximum allowable flow rate out of the tank is four times that in each circuit, or 2.6 kg/s. For this limiting condition and the top tank temperature T_4 equal to 55 C, the maximum heat demand that can be met is q_{dem} equal to 272 kW.

The minimum allowable flow rate limits the minimum amount of heat that can be delivered to the greenhouse at a given inlet temperature (top tank temperature). If the heat demand is lower than this minimum value, the flow rate is set to zero and the heat demand is accumulated from one hour to the next until the total demand is higher than the minimum heat rate.

The length of the tubing required to reach the desired return under the limiting condition of the maximum inlet temperature must be calculated. For high inlet temperatures, the flow rate is set at the minimum value. An energy balance performed on a finite element of the tubing is of the form:

$$T_m^i Cp\dot{M}_2 - T_m^{i+1} Cp\dot{M}_2 - q_{out} = 0$$

Equation 4.28

where

T_m^i = Inlet temperature of element i in C

T_m^{i+1} = Outlet temperature of element i in C

Cp = Specific heat of water at T_m^i in J/kg-C

\dot{M}_2 = maximum flow rate in kg/s

and

$$q_{out} = \frac{\frac{1}{2}(T_m^i + T_m^{i+1}) - T_s}{R_t}$$

Equation 4.29

where

T_s = Average soil temperature at surface, 22 C

R_t = Total resistance from water to sand surface, $R_t/L = 0.185$ C-m/W

Equation 4.28 can be solved for the exit temperature of the water as shown in Equation 4.30. Then the element number i is increased by one and the exit temperature becomes the inlet temperature for this next element. The heat transfer through the walls of the pipe is calculated and summed for each element. When the total heat transfer out of the pipe is greater than the heating demand, the i loop breaks and the total length is output as the number of elements multiplied by the 0.5 meter element length.

$$T_m^{i+1} = \frac{T_m^i Cp\dot{M}_2 R_t + T_s - \frac{1}{2} T_m^i}{\frac{1}{2} + Cp\dot{M}_2 R_t}$$

Equation 4.30

Determining the Total Resistance, R_t

The total resistance from the center of the water flow to the surface of the sand is the sum of three thermal resistances from: convection from the water flow to the pipe, conduction through the pipe wall, and conduction through the sand according to the equation:

$$R_t = \frac{1}{\pi D_i L h} + \frac{\ln\left(\frac{D_o}{D_i}\right)}{2\pi L k_p} + \frac{\ln\left(\frac{D_s}{D_o}\right)}{2\pi L k_s}$$

Equation 4.31

where

D_i = Inner diameter of pipe, 0.0219 m

D_o = Outer diameter of pipe, 0.0286m

D_s = Equivalent diameter to average temperature point on sand surface, 0.23 m

k_p = Conductivity of pipe, 1.23 W/m-C¹⁴

k_s = Conductivity of wet sand, 2.25 W/m-C¹⁵

k_w = Conductivity of water at 330K, 0.65 W/m-K¹⁶

h = Convection coefficient for pipe, 5.55 W/m²-C

The calculations and property values for these variables are shown in Appendix D:

Greenhouse Heat Transfer Function Code on page 129.

4.3 Simulation Code Description

The heat transfer simulation is performed in MatLab using the explicit Euler method.

The differential equations that describe the rate of temperature change are discretized into a finite one-hour time step as shown in Equation 4.7, Equation 4.23, Equation 4.24, and Equation 4.25. In a *for* loop, the set of heat transfer equations for the entire system is solved. The hour number, n , is used to retrieve the correct hour of TMY2 hourly meteorological data. By the end of the loop the temperatures are updated and the hour increases by one before this n loop is repeated for each of the 8,760 hours in the year.

See Appendix D for a copy of the MatLab simulation code and all its functions.

4.3.1 Input Parameters

The code's required set of input parameters and initial conditions is as follows:

1. Height of Tank in meters, H =*optimized parameter*

2. Time step in seconds, $\Delta t=3600$
3. Greenhouse return temperature in C, $T_5=30$
4. Collector return temperature in C, $T_2=90$
5. Collector area in m^2 , $A_c=optimized\ parameter$
6. Slope of tank walls in degrees, $slope=70^\circ$
7. Thickness of insulation in meters, $th=variable\ parameter$
8. Initial temperature of top tank in C, $T_4=optimized\ parameter$
9. Initial temperature of mid tank in C, $T_7=optimized\ parameter$
10. Initial temperature bottom tank in C, $T_6=optimized\ parameter$
11. Initial temperature of greenhouse in C, $T_h=optimized\ parameter$
12. Initial flow rates in kg/s, \dot{m}_{1} and \dot{m}_{2}

The characteristics of each component of the system are also included in the simulation code. The collector performance equations are used to determine the heat gained from the collector. The heat delivery system is modeled in a separate function to determine the required length of tubing to achieve the set return temperature. The storage system geometry is also calculated in a separate function.

4.3.2 Storage Geometry

The volume, external surface area, and cross-sectional area of each node in the tank are determined from the storage geometry function. The input parameters for the function are the height of the tank, slope of the side walls, and insulation conductivity and thickness. The function outputs the geometric characteristics of each node as well as the total material requirements for the storage construction. One of the design requirements is to install the storage system within the footprint of the greenhouse. Therefore, the length and width of the pit are equal to the length and width of the greenhouse. A finite element model approximates the total volume and area values. The height of the storage

volume is divided into 5,000 elements each representing a rectangular prism. The volume and external surface area is calculated for each element. The length and width of the element is updated at the end of each loop based on the slope of the pit walls.

Appendix D: Storage Geometry Function shows the details of this model.

4.3.3 Energy Balance

The initial storage temperatures should be the same at the end of the year as at the beginning of the year. However, this does not happen automatically, the initial temperatures and collector area must be adjusted to achieve an energy balance for the year. If the tank temperature ends lower than it begins, it follows that more heat was removed from the storage (lost through walls and delivered to the greenhouse) than heat was added to the storage from the collectors. Correspondingly, if the tank temperatures end higher, more heat was added to the tank than removed. In reality the tank will store extra heat some years and supply extra heat in others, but an energy balance should be achieved for the average TMY2 year. In order to reach this energy balance, another *for* loop is added to the MatLab code, the *k loop*. This loop adjusts the collector area and initial temperatures for the year. The collector area changes based on the energy balance for the year according to the equation:

$$Ac^{k+1} = Ac^k - \Delta E_{in-out} / 10^6$$

Equation 4.32

This results in the area of the collector increasing slightly if more energy needs to be added to the tank and decreased slightly if less energy needs to be added to the tank. The initial temperatures are adjusted in a similar manner. If the tank temperatures increased from the start of the year to the end, the initial temperature inputs are increased slightly

and vice-versa. With about 1.7 TJ of energy delivered to the greenhouse every year, the energy balance is not expected to reach precisely zero. An energy balance tolerance is set so the energy balance condition is met when the difference between the energy coming into the system and the energy leaving the system can be considered negligible. This negligible difference point is set to less than 0.03% of the heat demanded by the greenhouse value, 500 MJ. A tolerance is also set for the difference between the year's starting and ending temperature of 0.25 C. The k loop stops when the energy balance and temperature difference tolerances are met. Figure 4.6 shows the annual temperature change and energy balance as a function of the number of k loop iterations.

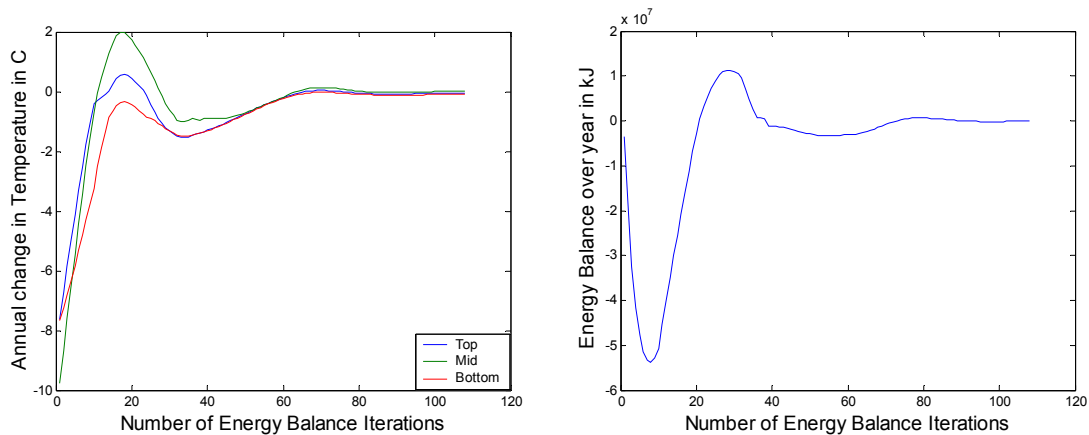


Figure 4.6 Annual temperature change and energy balance.

4.3.4 Storage Size Minimization

The simulation code and the storage geometry function require the tank height as an input parameter. However, it is desirable to use the smallest storage size possible while maintaining required system performance levels. When the storage thermal mass is below the acceptable level, either the bottom tank temperature T_6 gets too hot and approaches the collector return temperature T_2 of 30 C or the top tank temperature T_4 gets

too cool and approaches the set greenhouse return temperature T_5 of 90 C. When this happens, the mass flow rate equations (Equation 4.26 and Equation 4.27) do not solve properly. The mass flow rate can get much too large if the temperatures are close enough that the denominator approaches zero or it can become negative if the tank temperatures surpass the set return temperature, if $T_6 > T_2$ or $T_4 < T_5$. Therefore, boundary conditions are set on the storage pit temperatures. The simulation stops if either the top or bottom storage temperature comes within 2 C of the set return temperature of the system it is feeding, if $T_6 + 2 > T_2$ or $T_4 < T_5 + 2$. If these conditions are met, the storage system cannot meet the demands of the other two sub-systems because it is too small.

The minimum required storage volume is found based on this boundary condition. The initial tank height is intentionally input lower than the expected solution. Another *for* loop, the *i loop*, is added to the code that increases the tank height by 0.1 meters if the storage temperatures approach (within 2 C) the return temperatures. The lowest height at which the storage temperatures remain within the boundary conditions (*i loop* does not break) is the minimum storage pit height. The internal loops, the *n loop* and *k loop*, continue to run until the energy balance tolerances are met. The program then outputs the minimum tank height required for the system and the other system characteristics.

4.3.5 Cost Minimization

The goal of determining the component sizes is to minimize the total cost of the heating system while maintaining performance standards and design constraints. The key design variables for this are insulation thickness and the tank height. The tank height determines the size and therefore cost of the storage system, and the cost of the insulation is based on

the insulation thickness. The code automatically solves for the minimum storage height for the given input parameters, but the input parameter of insulation thickness is variable. Higher insulation thickness results in a smaller tank size as well as lowers the required collector area. However, there is a point when increasing the insulation thickness increases the cost of the system, because the insulation cost is not trivial. Figure 4.7 shows the cost as a function of storage insulation thickness. The large abrupt changes in cost from one thickness to another are the result of the storage size variation. From the cost breakdown on the right-hand side of the figure, it is clear that the storage construction costs play a key role in determining the optimum cost point. The input parameters that correspond to the minimum cost point are used for the final design of the greenhouse heating system. The optimum insulation thickness is 0.86 meters.

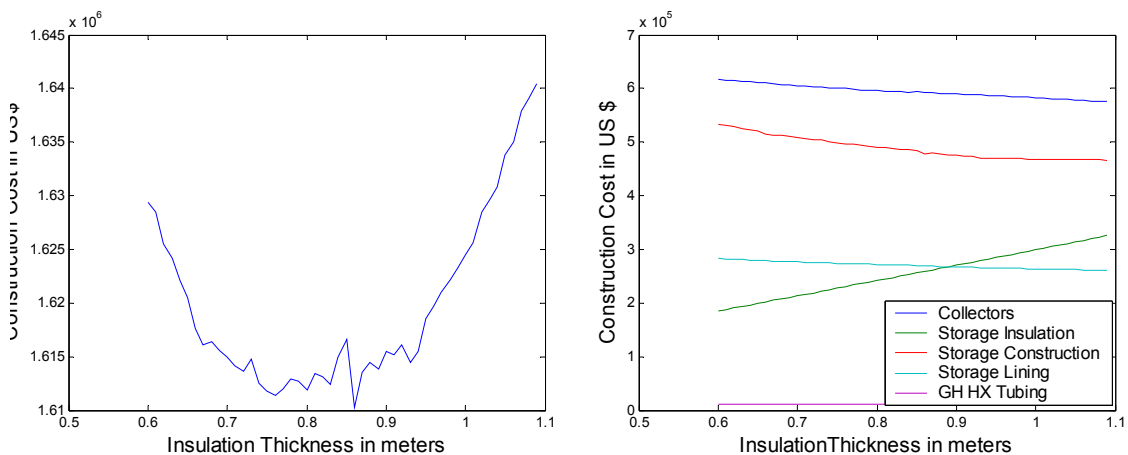


Figure 4.7 Heating system cost versus insulation thickness.

Determining the Heating System Cost

The total cost of the heating system is calculated from the specific costs of each component multiplied by the amount or size required for each. Table 4.6 shows the

specific cost of each component. After the simulation has solved for the minimum storage size, it outputs the total cost according to the equation:

$$Cost = c_{coll} A_c + c_{ins} V_{ins} + c_{st} V_{Eq} + c_{lin} SA_{lin} + c_{tub} L_{tub}$$

Equation 4.33

where

$$V_{Eq} = (M_{eq,6} + M_{eq,7} + M_{eq,4}) / 1000 m^3 / kg$$

Equation 4.34

The water equivalent storage volume is used rather than the actual storage volume, because the storage system costs are based on water-equivalent storage volume in the source.¹⁹

Table 4.6 Specific costs of heating components.

Component	Variable Name	Spec. Cost	Units
Collectors	c_{coll}	\$568.60 ¹⁷	US \$/m ²
Insulation	c_{ins}	\$71.07 ¹⁸	US \$/m ³
Exc+grav+pipng sys	c_{st}	\$77.39 ¹⁹	US\$/m ³
Lining	c_{lin}	\$68.92 ¹⁹	US\$/m ²
Heat Delivery Tubing	c_{tub}	\$ 5.35 ³	US\$/m

4.4 Simulation Code Results and Final Design

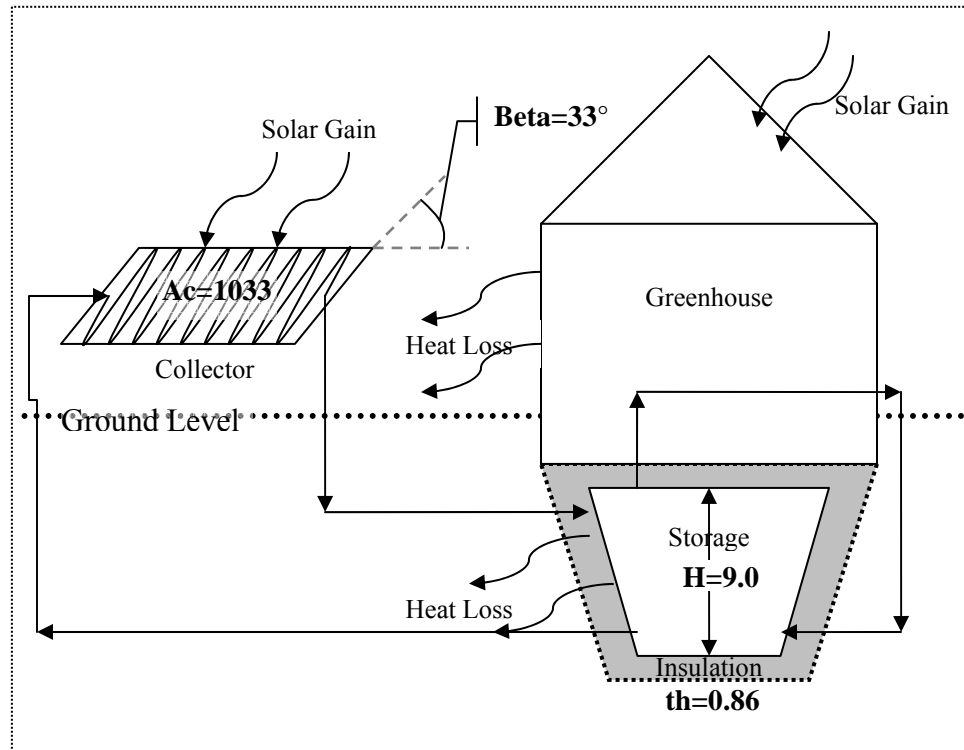


Figure 4.8 Physical model of solar-thermal heating system.

Table 4.7 shows the design parameters and system performance for the final, optimized design. The design parameters specify the optimal sizing for each system component. The system performance value outputs verify that the system is operating within the specified constraints. The maximum storage temperature is below the recommended 90 C for the flexible polypropylene lining. The energy balance and annual temperature change are satisfied well below the set tolerances. The final cost value is minimized using the optimum values for insulation thickness, collector area, and tank size.

Table 4.7 Simulation Results.

Design Parameters	Value	Units
Insulation Thickness	0.86	m
Area of Collector	1033	m ²
Tilt Angle	33	°
Storage Height	8.9	m
Storage Volume (Actual)	9589	m ³
Storage Volume (Eq.)	6393	m ³
Delivery Tubing Length	2104	m
System Performance		
Min Tank Temp	30.2	C
Max Tank Temp	84.3	C
Temp Change-Top	0.09	C
Temp Change-Mid	0.24	C
Temp Change-Bottom	0.21	C
Final Temp-Top	63.6	C
Final Temp-Mid	53.3	C
Final Temp-Bottom	41.2	C
Heat Gain	1960	GJ
Heat Delivered	1697	GJ
Heat Loss Storage	258	GJ
Heat Gain-Heat Out	0.356	GJ
Cost	1.610E+06	\$

The total heat delivered to the greenhouse for the year calculated from the simulation of 1,697 GJ compares closely with the estimate from chapter 2 of 1,439 GJ. The 18% higher value from using hourly time-steps is expected because the estimation in chapter 2 used monthly average values for daily radiation, which do not account for excess heat being vented during warm days. The storage system size and insulation thickness also compare closely between the estimates in chapter 2 and the simulation results. The required volume of water for the storage system approximated in chapter 2 was 7,821m³. This estimate assumes a 10% heat loss from the storage system and an average temperature difference between fully charged and fully discharged of 50 C. The water equivalent volume calculated from the simulation is 6,393 m³. This value is limited by the temperature operating parameters listed in Table 4.2. This difference is mostly due to

the assumption of a 50 degree temperature change from fully charged to fully discharged in the preliminary estimate. The limiting parameters in the detailed design allow the tank to vary between 90C and 30 C, and the difference between the simulated maximum tank temperature and minimum tank temperature is 54 C. The optimized insulation thickness of 0.86 m is significantly lower than the estimate from chapter 2, but the 10% heat loss from the tank limitation was too stringent. For the optimized design the percentage of heat loss is 13%. The simulated temperature of the storage system varied between a low of 30 C and a high of 84 C. However, this range does not reflect the average temperature of the entire storage volume. Figure 4.9 shows the temperature profile of the storage pit at each node. The low temperatures reach the limit in March and the high temperatures in November.

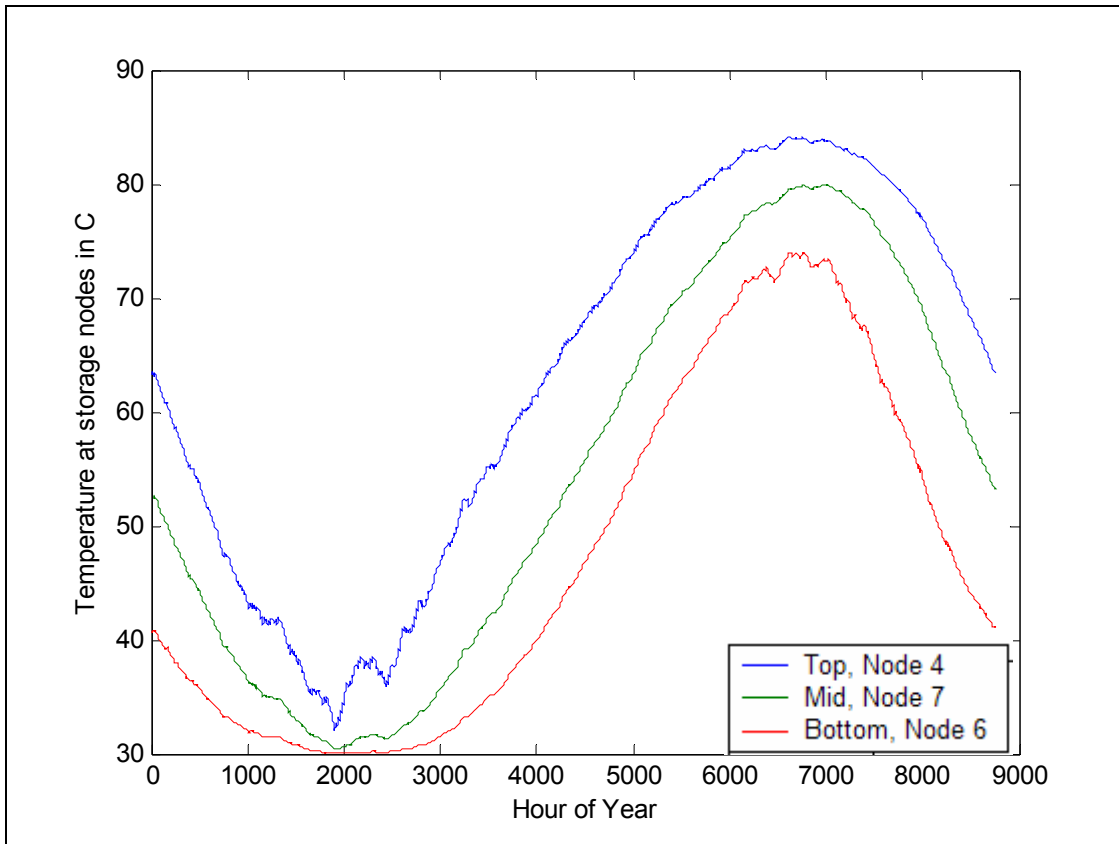


Figure 4.9 Temperature profile of storage tank throughout year

The collector area estimation of 929m^2 determined in chapter 2 is 10% lower than the required collector area for the optimized system of 1033 m^2 . The large collector field area calculated in the simulation is necessary because the high inlet temperatures decrease the efficiency of the collectors. The selection of the vacuum tube collectors to minimize the heat loss from the collector surface minimizes the effect of these high temperatures as much as possible. Figure 4.10 shows the heat transfer to and from the storage system for the year. The heat loss through the storage walls is entirely dependant on storage temperature, so it has the same profile as the temperature curves. The columns in the collector heat supply and greenhouse heat demand represent the diurnal cycling of heat collected during the days and heat delivered to the greenhouse at night.

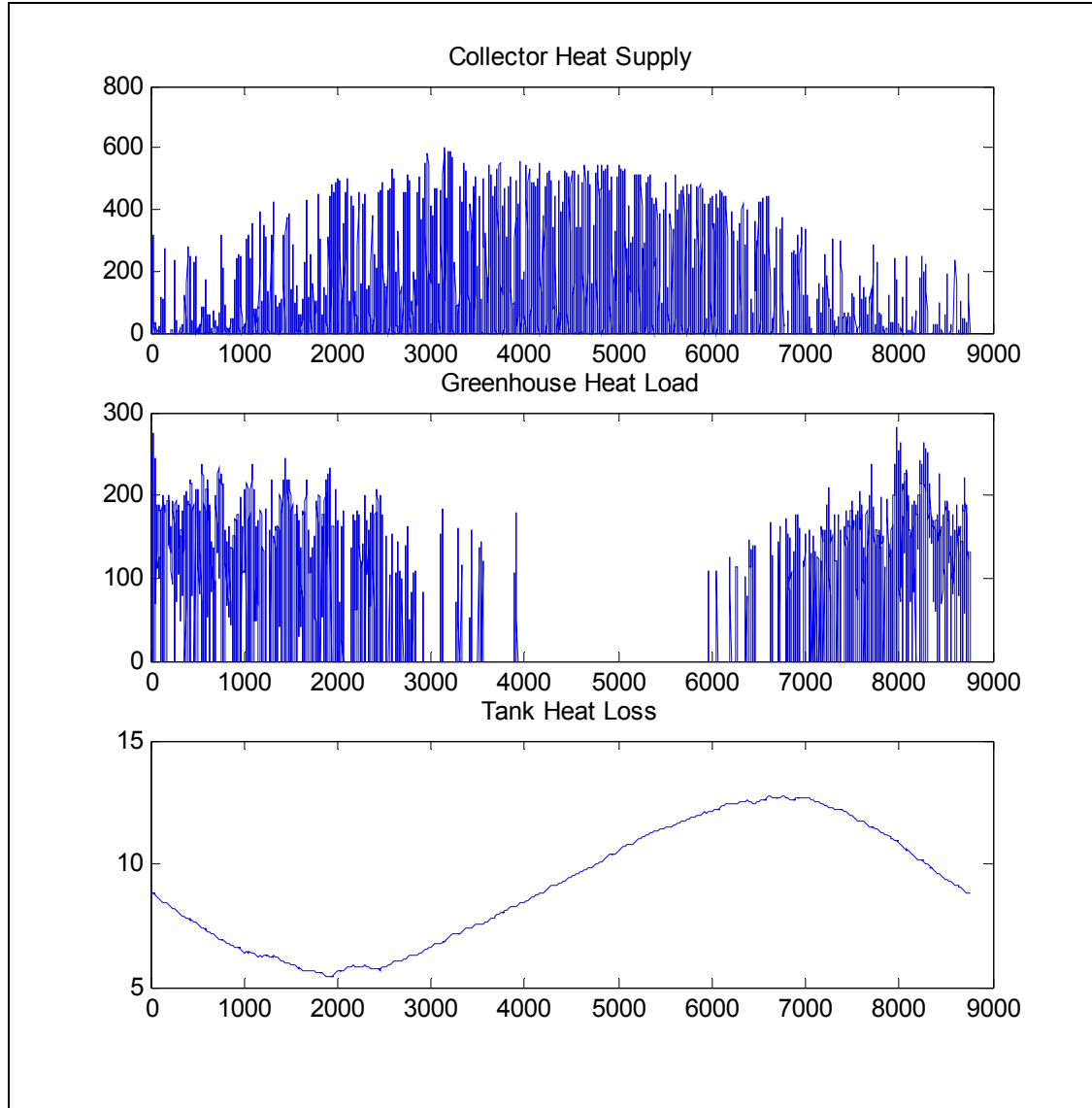


Figure 4.10 Heat gain and loss from storage system throughout year in kJ.

Notes to Chapter 4

¹ Solar Rating and Certification Corporation, Directory of SRCC Certified Solar Collector Ratings. (Cocoa, FL: SRCC 2005)131. See Appendix C for copy

² In-bed heating most efficient

³ PexSupply.com, “Mr. PEX (PEX-AL-PEX) Pex Tubing - PEX Tubing - PEX-al-PEX - Aluminum PEX,” 10 Jan. 2006
<<http://www.pexsupply.com/categories.asp?cID=389&brandid=>>.

⁴ Walls, Ian G. The complete book of the greenhouse, (London: Ward Lock 1988) 47.

⁵ Pfeil 465.

⁶ Marion, William and Ken Urban, “User's Manual for TMY2s” Jan. 1995, 2 Jan. 2006
<http://rredc.nrel.gov/solar/pubs/tmy2/tmy2_index.html>.

⁷ Byrne, Thomas G, “Lowering Rose Greenhouse Temperatures May be False Economy,” Flower & Nursery Report for commercial growers (Fall 1980) 2-3, University of California, Cooperative Extension 6 Feb 2006
<http://ohric.ucdavis.edu/Newsltr/fn_report/FNReportF80.pdf>.

⁸ Duffie 235.

⁹ Duffie 26.

¹⁰ Australia, Australian Greenhouse Office, Department of the Environmental Heritage, Chris Reardon, Caitlin McGee, and Geoff Milne, “Thermal Mass: Thermal Mass Properties,” Fact sheets: Passive Design 10 Jan 2006
<<http://www.greenhouse.gov.au/yourhome/technical/fs17.htm>>.

¹¹ Duffie 95.

¹² Bartok, John W. “Root Zone Heating Systems,” Greenhouse Management May 2005, (University of Massachusetts Amherst, Massachusetts 2003) 3 Feb. 2006
<http://www.umass.edu/umext/floriculture/fact_sheets/greenhouse_management/jb_root_zone_heat.htm>.

¹³ Siegenthaler, John, “Hydronic Fundamentals: Part 1” (PM Engineer, 2004 BNP Media).

¹⁴ Vanguard System Inc., “Compax-L PEX-Aluminum-PEX (PAX) Tubing” 4 Jan. 2006 <<http://www.vanguardpipe.com/paxtechdata.htm>>.

¹⁵ Hendrickx, Jan M. H., Remke L. van Dam, Brian Borchers, John Curtis, Henk A. Lensen, and Russell Harmon, “Worldwide distribution of soil dielectric and thermal properties,” Detection and remediation technologies for mines and minelike targets VIII, Proceedings of the SPIE, Ed. Harmon, R.S., Holloway, J. H., and Broach, J.T., volume 5089: 1158-1168; Saur et al, “Errors In Heat Flux Measurement By Flux Plates Of Contrasting Design And Thermal Conductivity,” Vadose Zone Journal 2 (2003): 580-588.

¹⁶ Incropera, Frank P., and David P. DeWitt, Fundamentals of Heat and Mass Transfer, 5th ed. (New York: John Wiley & Sons, 2002): 924.

¹⁷ SolarThermal, “Mazdon Solar Collector System: US Price List-2004” 24 Oct. 2005 <www.SolarThermal.com>.

¹⁸ McMaster-Carr Supply Company, McMaster-Carr on-line catalog 3307, 16 Jan 2006 <<http://www.mcmaster.com>>

¹⁹ Pfeil 466.

Chapter 5: Economic Analysis

The economic feasibility and opportunities for cost reduction are described in this chapter. Section 5.1 presents the calculation and results to determine the price per kWh of heating based on the optimized construction cost calculated in chapter 4. Section 5.2 examines the economic feasibility of this heating system based on the price per kWh. Section 5.3 examines cost reduction opportunities.

5.1 Calculation of Specific Cost per kWh

The economic analysis shown in Table 5.2 presents the system worth, loan payment (subdivided into interest payment and loan deduction), and loan balance in each year's current dollars. The present worth (current dollar) value of the payments, of the total payments, and of the price per kWh are shown in the far-right columns. The assumptions used in these calculations are as follows:

1. Duration of Loan = 20 years
2. Interest rate = 5%
3. Discount rate = 3%
4. Inflation rate = 2.5%

The system worth increases at the inflation rate; the interest payment is calculated by multiplying the interest rate by the loan balance; the present worth values are calculated based on the discount rate. The system worth at year zero is equal to the capital cost of the system shown in Table 5.1.

Table 5.1 Capital cost in US dollars.

Collectors	5.93E+05
Storage Construction	4.79E+05
Storage Insulation	2.59E+05
Storage Lining	2.69E+05
Heat Delivery Tubing	1.14E+04
Total	1.61E+06

Table 5.2 Economic analysis of solar-thermal heating system in thousands of US dollars.

Year	System Worth	Payment	Interest	Loan Deduction	Loan Balance	Payments P- W	Total PW Cost	Price per kWh
0	\$1,610	\$0			\$1,610	\$0	\$0	
1	\$1,651	\$129	\$81	\$49	\$1,562	\$125	\$125	\$0.266
2	\$1,692	\$129	\$78	\$51	\$1,510	\$122	\$247	\$0.262
3	\$1,734	\$129	\$76	\$54	\$1,457	\$118	\$365	\$0.258
4	\$1,777	\$129	\$73	\$56	\$1,400	\$115	\$480	\$0.255
5	\$1,822	\$129	\$70	\$59	\$1,341	\$111	\$592	\$0.251
6	\$1,867	\$129	\$67	\$62	\$1,279	\$108	\$700	\$0.247
7	\$1,914	\$129	\$64	\$65	\$1,214	\$105	\$805	\$0.244
8	\$1,962	\$129	\$61	\$69	\$1,145	\$102	\$907	\$0.240
9	\$2,011	\$129	\$57	\$72	\$1,073	\$99	\$1,006	\$0.237
10	\$2,061	\$129	\$54	\$76	\$998	\$96	\$1,102	\$0.234
11	\$2,113	\$129	\$50	\$79	\$918	\$93	\$1,196	\$0.231
12	\$2,166	\$129	\$46	\$83	\$835	\$91	\$1,286	\$0.227
13	\$2,220	\$129	\$42	\$87	\$748	\$88	\$1,374	\$0.224
14	\$2,275	\$129	\$37	\$92	\$656	\$85	\$1,460	\$0.221
15	\$2,332	\$129	\$33	\$96	\$559	\$83	\$1,543	\$0.218
16	\$2,391	\$129	\$28	\$101	\$458	\$81	\$1,623	\$0.215
17	\$2,450	\$129	\$23	\$106	\$352	\$78	\$1,701	\$0.212
18	\$2,512	\$129	\$18	\$112	\$240	\$76	\$1,777	\$0.209
19	\$2,574	\$129	\$12	\$117	\$123	\$74	\$1,851	\$0.207
20	\$2,639	\$129	\$6	\$123	\$0	\$72	\$1,922	\$0.204
21	\$2,705	\$0	\$0	\$0	\$0	\$0	\$1,922	\$0.194
22	\$2,772	\$0	\$0	\$0	\$0	\$0	\$1,922	\$0.185
23	\$2,842	\$0	\$0	\$0	\$0	\$0	\$1,922	\$0.177
24	\$2,913	\$0	\$0	\$0	\$0	\$0	\$1,922	\$0.170
25	\$2,985	\$0	\$0	\$0	\$0	\$0	\$1,922	\$0.163
26	\$3,060	\$0	\$0	\$0	\$0	\$0	\$1,922	\$0.157
27	\$3,137	\$0	\$0	\$0	\$0	\$0	\$1,922	\$0.151
28	\$3,215	\$0	\$0	\$0	\$0	\$0	\$1,922	\$0.146
29	\$3,295	\$0	\$0	\$0	\$0	\$0	\$1,922	\$0.141
30	\$3,378	\$0	\$0	\$0	\$0	\$0	\$1,922	\$0.136
40	\$4,324	\$0	\$0	\$0	\$0	\$0	\$1,922	\$0.102
50	\$5,535	\$0	\$0	\$0	\$0	\$0	\$1,922	\$0.082

The system is designed to last a minimum of 20 years, but the system may last as many as 50 years. In the latter case, the final cost of heat is 8.2 cents per kWh.

5.2 Economic Feasibility

Even for the 50 year extreme, the cost per kWh is more than the current price of natural gas and is slightly less than that of electric heating (3.9 ¢/kWh and 8.4 ¢/kWh respectively).¹ However, the externality benefits of pollution prevention and the rapidly increasing cost of fossil fuel must be taken into account. Table 5.3 shows the cost of natural gas heating assuming the cost of carbon sequestration to be \$10/ton according to Department of Energy projections² and an annual fuel increase rate of 8.63% (inflation adjusted).³ The present worth price per kWh of heating with natural gas increases over time because the fuel increase rate is greater than the discount rate. Even with this assumption and including the cost of carbon sequestration, the present worth price per kWh of heating with natural gas is still less than that of heating with the solar-thermal heating system for the 20 year design life. The cost of a solar heating system with seasonal storage to provide 100% of the heating demand for only one greenhouse is too great. However, taking advantage of the economy of scale of building a heating system for several greenhouses or the cost reduction from using supplemental heat to optimize the size of the system may result in competitive heating costs.

Table 5.3 Price comparison of solar to natural gas heating with carbon sequestration in US \$.

Year	Solar-thermal System		Natural Gas Heating			
	Total PW Cost	Price per kWh	Total Fuel Cost	CO ₂ seq. cost	Total PW Cost	Price per kWh
0	\$0				\$0	
1	\$125	\$0.266	\$20.4	\$0.3	\$20	\$0.043
10	\$1,102	\$0.234	\$53	\$0.3	\$288	\$0.061
20	\$1,922	\$0.204	\$152	\$0.3	\$901	\$0.096
30	\$1,922	\$0.136	\$436	\$0.3	\$2,209	\$0.156
40	\$1,922	\$0.102	\$1,253	\$0.3	\$5,004	\$0.265
50	\$1,922	\$0.082	\$3,599	\$0.3	\$10,976	\$0.466

5.3 Cost Reduction Opportunities

5.3.1 Cost breakdown

Figure 5.1 shows the percentage cost of each sub-system. The storage system cost is further divided into insulation, lining, and excavation, gravel, and heat exchanger system. The total percentage of the storage system of 65% is the majority by far. Reducing the cost of the storage system offers the clearest opportunity for cost savings. One method to do this is to maximize the volume to surface area ratio by using a circular cross-sectional area rather than the shape of the greenhouse footprint. An inverted frustrum of a cone with a slope of 60 degrees is the ideal geometry presented for the up-scaled Steinfurt project.⁴ Another way to reduce the cost of the storage system is to reduce the cost of the insulation. Innovative insulation techniques have been employed in the Steinfurt gravel-water pit in Germany.⁵ In this case, large bags are filled with granulated recycling glass on site.

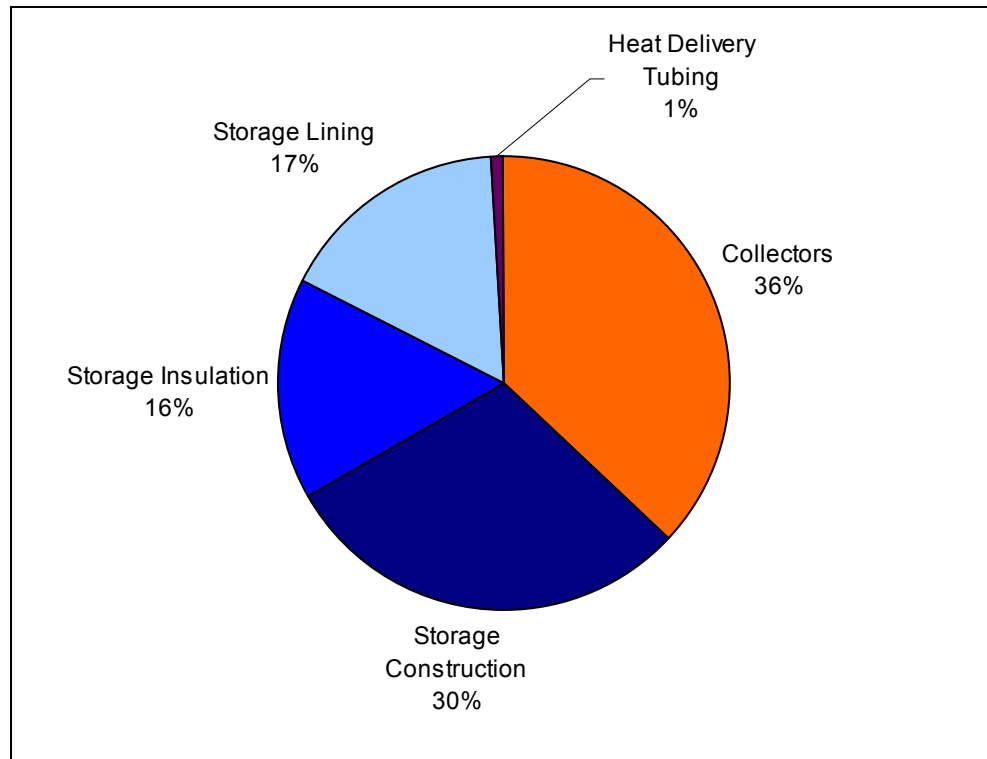


Figure 5.1 Cost breakdown of final solar heating system.

5.3.2 Economy of Scale

The most significant opportunity for cost reduction of solar heating systems with seasonal storage is to take advantage of economy of scale. Creating a heating system for a large group of greenhouses would allow for a single, larger storage system to maximize the volume to surface area ratio. This would not only decrease insulation costs because of less external surface area per unit volume, it would also decrease the specific construction costs for every process and material. From Figure 5.2, the specific cost of seasonal storage seems to reach the point of diminishing return at approximately 20,000 m³ water equivalent. The optimum storage size and corresponding collector area has been simulated to be about 100,000 m³ and 30,000 m², which corresponds to about 300 greenhouses.⁶ This storage volume to collector area ratio is greater than the simulation for this study because the c

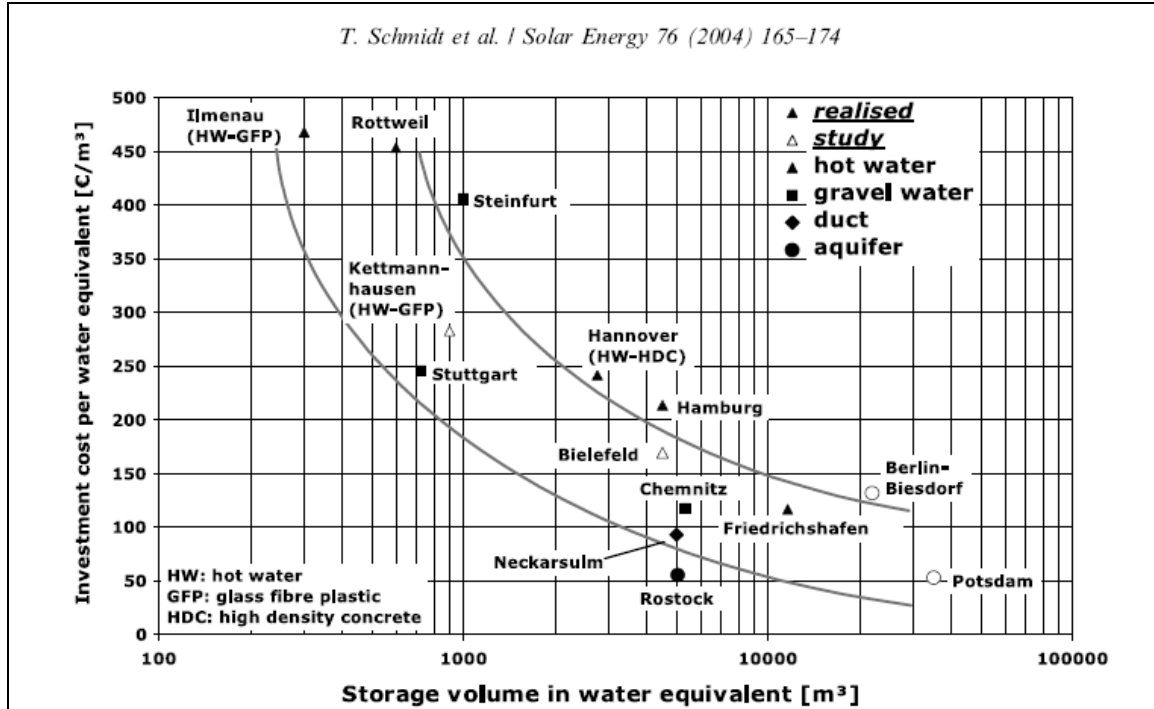


Figure 5.2 Cost of Solarthermie-2000 seasonal storage system per m^3 water equivalent.⁷

5.3.3 Supplemental heating

The addition of a supplemental heating source also presents a significant potential for cost reduction. When the solar heating system is the sole source for heating, the system must have the capacity to meet the highest heating load of the greenhouse. This means that most of the time, the system only utilizes a fraction of its capacity to meet the normal heating loads. Usually, the highest heating demand only happens for a short period, and therefore a small amount of supplemental heating is drawn upon in times of need. All large-scale heating systems currently in operation meet only a fraction of the heating demand with solar energy, usually between 30 and 60 percent.⁷

Notes to Chapter 5

¹ Puget Sound Energy, “Gas Prices Summary for 2005,” 20 Jan 2006
<http://www.pse.com/InsidePSE/ratesDocs/summ_gas_prices_2005_10_01.pdf>.

² United States, Department of Energy, Fossil Energy Office of Communications, “Carbon Sequestration R&D Overview,” DOE: Fossil Energy: Overview of Carbon Sequestration Technology 6 Nov 2005, 2 Feb 2006
<<http://www.fossil.energy.gov/programs/sequestration/overview.html>>.

³ Brown, Merwin, Douglas Huizenga, Eron Jacobsen, Bill Lynn, Phil Malte, Brian Polayge, Michael Richardson, Joseph Salvo, and Rita Schenck, “Pacific Northwest Energy Independent Communities: A 10-year Plan” (Institute for Environmental Research and Education, July 2005) 108, 25 March 2006
<<http://www.iere.org/documents/EnergyIndependentCommunities-10yearplan.pdf>>

⁴ Pfeil 465.

⁵ Pfeil 464.

⁶ Heller, Alfred, “15 Years of R&D in Central Solar Heating in Denmark,” Solar Energy 69 (6) (2000) 437-447.

⁷ Schmidt, T., D. Mangold, H. Müller-Steinhagen, “Central solar heating plants with seasonal storage in Germany,” Solar Energy 76 (2004) 165-174.

Chapter 6: Conclusions

The preliminary analysis in chapter 2 estimates a greenhouse heating demand of 1,429 GJ. The storage system capacity approximation, based on this demand value and a heat loss of 10%, results in 7,821m³ of water required size of the seasonal storage system. The mineral wool insulation thickness necessary to limit the heat loss to 10% is 1.37m. The collector size based on monthly radiation and the required storage capacity is estimated at 929 m².

Chapter 3 presents a comparative life cycle study aimed at determining the seasonal storage design option (gravel-water pit or concrete water tank) with the lowest environmental impact. The storage system capacity and insulation requirement estimated in chapter 2 are used to calculate the amount of materials required to build the two storage design options. The gravel-water pit is 1.5 times larger in volume because of the lower thermal capacitance of the gravel-water mixture, but the concrete structural support of the concrete tank requires more mass of material than the flexible plastic lining of the gravel-water pit. The assessment compares the life cycle environmental impact of building each storage design. The emissions from constructing and manufacturing the materials used in the storage unit, and the upstream processes required to manufacture those materials are calculated in the life cycle inventory analysis. The steel manufacturing in the concrete tank design results in significantly more emissions of chromium, formaldehyde, and lead all of which are harmful to humans and the ecosystem. The impact assessment results reveal that the gravel pit system has lower environmental impact for global warming (35% of tank value). For the impacts on

photochemical smog and acidification, the impact values are too close to discern a difference between the two systems. The gravel-water pit construction cost estimation is 8.7% greater than that of the concrete water tank. This difference is too close to determine a consequential difference between the two systems.

The detailed heat transfer simulation, presented in chapter 4, models the specific characteristics of each sub-system. The gravel-water pit seasonal storage sub-system is characterized in chapter 3. The Thermomax Mazdon vacuum tube collector system is selected because of the high inlet temperatures to the collector sub-system. It is critical that heat loss from the collectors be minimized by using the best insulated collector system possible. The selection of the radiant tube heat delivery system to maximize efficiency and minimize return temperature is also presented at the beginning of chapter 4. The radiation gain and heat loss equations in the detailed analysis are similar to those in the preliminary estimate. The most significant difference is the use of hourly rather than monthly radiation and meteorological data. This means that the set of heat transfer equations is solved 8,760 times (once for each hour) to simulate one year, instead of 12 times (once for each month) as in chapter 2. Because of the large number of calculations, MatLab is used to solve the heat transfer equations. The simulation optimizes the size of each component to finalize the entire system design to meet the specific needs of the Vashon greenhouse. The optimized design has a storage volume of 7,880 m³ water equivalent, a collector area of 1074 m², and a heat delivery tubing length of 2,116 m.

The use of a solar-thermal heating system with seasonal storage instead of natural gas will prevent over 2.2 million kg CO₂ equivalents of greenhouse gasses from being emitted to the environment over the 20-year life of the system. However, at 20.4 cents per kWh, this system does not appear to be economically feasible even when the cost of carbon sequestration is taken into account. The solar-thermal heating system costs more per kWh than natural gas heating with carbon sequestration even for a 50 year system lifetime.

The best opportunity for cost reduction is to maximize the volume to surface area ratio of the storage system by creating a heating system with a circular cross section for a large group of greenhouses rather than just one.

Bibliography

- Annual Energy Review 2004. Report No. DOE/EIA-0384 (2004) July 2005. <http://www.eia.doe.gov/aer/append_a.html>.
- Ardente, Fulvio, Giorgio Beccali, Maurizio Cellura, and Valerio Lo Brano. "Life cycle assessment of a solar thermal collector." Renewable Energy 30 (7) (2005): 1031-1054. Science Direct. 29 Mar. 2005 <http://www.sciencedirect.com/science?_ob=MIimg&_imagekey=B6V4S-4DVVYVG-2-1&_cdi=5766&_user=582538&_orig=search&_coverDate=06%2F01%2F2005&_sk=999699992&view=c&wchp=dGLbVtb-zSkWz&md5=10fdfb0c1d21faed2f918d8c25c30615&ie=/sdarticle.pdf>
- Association of Plastic Manufacturers in Europe (APME). 10 July 2005 <http://www.apme.org/media/public_documents/20011009_164930/lca_summary.htm&title=LCA:+Summary+of+topics>.
- Bartok, John W. "Root Zone Heating Systems." Greenhouse Management. University of Massachusetts May 2005. 3 Feb. 2006 <http://www.umass.edu/umext/floriculture/fact_sheets/greenhouse_management/jb_root_zone_heat.htm>.
- Burch, J., J. Salasovich, and T. Hillman. "Cold-Climate Solar Domestic Water Heating Systems: Life-Cycle Analyses and Opportunitites for Cost Reduction." paper delivered to ISES Solar World Congress sponsored by NREL. Orlando, Florida, August 6-12, 2005. 10 July 2005. 12 Jan. 2006 <<http://www.osti.gov/bridge>>.
- Byrne, Thomas G. "Lowering Rose Greenhouse Temperatures May be False Economy." Flower & Nursery Report for commercial growers (Fall 1980): 2-3. University of California, Cooperative Extension. 6 Feb 2006 <http://ohric.ucdavis.edu/Newsltr/fn_report/FNReportF80.pdf>.
- Canada. Natural Resources Canda (NRCan). "Solar Energy Heating it up in Alberta: Homeowners will benefit from the sun's warmth on cold, cloudy winter days." Natural Elements 2. 27 June 2005. 10 Oct 2005 <http://www.rncan.gc.ca/elements/issues/02/cetc_e.html>.
- Clayton, T. Crowe, John A. Roberson, and Donal F. Elger. Engineering Fluid Mechanics 7th Ed. New York: John Wiley and Sons, 2000.
- Cooper, J. S. Lecture on Goal and Scope Definition. ME 599-Life Cycle Assessment. University of Washington, Seattle, WA. Spring 2005.
- Duffie, John A., and William A. Beckman. Solar Engineering of Thermal Processes. 2nd ed. New York John Wiley & Sons, 1991.

- EcoInvent v1.2. On-line database. Swiss Centre for Life Cycle Inventories 2004. 11 Feb. 2005 <<http://db.ecoinvent.org/ecoquery/index.php?newlanguage=en>>.
- Environmental Protection Agency. Compilation of Air Pollutant Emission Factors Vol 2: Mobile Sources “AP-42” (1991). 18 July 2005 <<http://www.epa.gov/otaq/ap42.htm>>.
- REET 1.6 GUI Beta Release II. Systems Assessment Section Center for Transportation Research. Argonne National Laboratory, May 2004.
- Heijungs, R. and S. Suh, Computational Structure of Life Cycle Assessment. The Netherlands: Kluwer Academic Publishers, 2000.
- Hendrickx, Jan M. H., Remke L. van Dam, Brian Borchers, John Curtis, Henk A. Lensen, and Russell Harmon. “Worldwide distribution of soil dielectric and thermal properties.” Detection and remediation technologies for mines and minelike targets VIII, Proceedings of the SPIE. Ed. Harmon, R.S., Holloway, J. H., and Broach, J.T. volume 5089: 1158-1168.
- HistoryLink. “King County Landmarks: Harrington-Beall Greenhouse Company Historic District (ca. 1885-1989), Vashon, Vashon Island.” 5 July 2005 <www.historylink.org>.
- Hydro. “Crude oil Canada - Hydro.” Hydro: Oil and gas products: Crude oil production international: Crude oil Canada. 10 July 2005 <http://www.hydro.com/en/our_business/oil_energy/sales_distribution/products/crude_oil_canada.html>.
- Incropera, Frank P., and David P. DeWitt, Fundamentals of Heat and Mass Transfer. 5th ed. New York John Wiley & Sons, 2002.
- International Standards Organization. “Environmental Management Life Cycle Assessment Principles and Framework.” (ISO 14040-1997) .
- ISO. “Environmental Management Life cycle Assessment Goal and Scope Definition and Inventory Analysis,” (ISO 14041-1998).
- Lottner, Volkmar and Dirk Mangold. “Status of Seasonal Thermal Energy Storage In Germany” Terrastock 2000 Stuttgart, Germany.
- Macrolux. “Macrolux plastics.” 8 Jan 2006 <<http://www.tapplastics.com/uploads/pdf/Coex8mm.pdf>>.
- Magee, Tim with Ectotope Group. A solar greenhouse guide for the Pacific Northwest. Seattle: the Group, 1979.
- Marion, William and Ken Urban. “User's Manual for TMY2s”. Jan. 1995. 2 Jan. 2006 <http://rredc.nrel.gov/solar/pubs/tmy2/tmy2_index.html>.
- Mateiciuc. “Polyethylene hoses LDPE-PELD, pipelines, water-service pipes, water pipes” MAT: Products: PE Water Pipes. 5 July 2005 <<http://www.mat-plasty.cz/en/pe-trubky-ldpe.php>>.

- Mathur, Jyotirmay and Narendra Kumar Bansal. "Energy Analysis of Solar Water Heating Systems in India" International Journal of Life Cycle Assessment. 4 (2) (1999): 113-116. ScientificJournals.com. 4 Apr. 2005 <<http://www.scientificjournals.com/sj/lca/Pdf/aId/1287>>.
- McMaster-Carr Supply Company. McMaster-Carr on-line catalog. 16 Jan 2006 <<http://www.mcmaster.com>>.
- PexSupply.com. "Mr. PEX (PEX-AL-PEX) Pex Tubing - PEX Tubing - PEX-al-PEX - Aluminum PEX." 10 Jan. 2006 <<http://www.pexsupply.com/categories.asp?cID=389&brandid=> >.
- Pfeil, Markus and Holger Koch "High Performance—Low Cost Seasonal Gravel/Water Storage Pit." Solar Energy. 69 (6) (2000): 461-467. Science Direct. 18 Apr. 2005 <http://www.sciencedirect.com/science?_ob=MIimg&_imagekey=B6V50-41SCBB9-5-9&_cdi=5772&_user=582538&_orig=browse&_coverDate=12%2F31%2F2000&_sk=999309993&view=c&wchp=dGLbVtz-zSkWb&md5=7840bdf76a05b3ec8c5bb173ae615053&ie=/sdarticle.pdf>.
- Power Smart Technical Services & Research. "Technical Potential for Electric Energy Savings from Residential Solar Domestic Water Heating in BC Hydro's Non-Integrated Areas." Prepared for Power Smart Residential Building Operations, June 1994. Private e-mail communication 6 Sept 2005.
- Saur, T.J., D.W. Meek, T.E. Ochsner, A. R. Harris, and R. Horton. "Errors In Heat Flux Measurement By Flux Plates Of Contrasting Design And Thermal Conductivity." Vadose Zone Journal 2 (2003): 580-588. 20 Jan 2006 <<http://vzj.scijournals.org/cgi/content/full/2/4/580>>
- Schmidt, Anders C., Allan A. Jensen, Anders U. Clausen, Ole Kamstrup, and Dennis Postlethwait. "A Comparative Life Cycle Assessment of Building Insulation Products made of Stone Wool, Paper Wool and Flax: Part1: Background, Goal and Scope, Life Cycle Inventory, Impact Assessment and Interpretation." International Journal of Life Cycle Assessment. 9 (1) (2004): 53-66. ScientificJournals.com. 14 Apr. 2005 <<http://www.scientificjournals.com/sj/lca/Pdf/aId/6389>>.
- Schmidt, Anders et. al. "A Comparative Life Cycle Assessment of Building Insulation Products made of Stone Wool, Paper Wool and Flax: Part2: Comparative Assesment." International Journal of Life Cycle Assessment. 9 (1) (2004): 53-66. ScientificJournals.com. 14 Apr. 2005 <<http://www.scientificjournals.com/sj/lca/Pdf/aId/6390>>.
- Schmidt, T., D. Mangold, H. Müller-Steinhagen. "Seasonal Thermal Energy Storage in Germany." paper delivered to ISES Solar World Congress sponsored by the German Federal Ministry for Economy and Technology. Göteborg, Sweden 2003.
- Siegenthaler, John. "Hydronic Fundamentals: Part 1" PM Engineer, BNP Media 2004.

- “Simetric bulk material density.” 10 July 2005
<http://www.simetric.co.uk/si_materials.htm>.
- Solar Rating and Certification Corporation. “Directory of SRCC Certified Solar Collector Ratings.” Cocoa, FL: SRCC, 2005.
- SolarThermal. “Mazdon Solar Collector System: US Price List-2004” 24 Oct. 2005
<www.SolarThermal.com>.
- Trinkl, Christoph, Wilfried Zörner, Claus Alt, Christian Stadler. “Performance of Vacuum Tube and Flat Plate Collectors Concerning Domestic Hot Water Preparation and Room Heating.” paper delivered to the 2nd European Solar Thermal Energy Conference 2005, sponsored by the Bavaria State Ministry of the Environment, Public Health and Consumer Protection. Freiburg, Germany. June 21-22, 2005. 10 July 2005
- United States. Census Bureau. “Transportation, Commodity Flow Survey, 2002 Economics Census.” 2004.
- United States. Department of Energy. Fossil Energy Office of Communications. “Carbon Sequestration R&D Overview.” DOE: Fossil Energy: Overview of Carbon Sequestration Technology. 6 Nov 2005. 2 Feb 2006
<<http://www.fossil.energy.gov/programs/sequestration/overview.html>>.
- United States. Department of Energy. Strategic Environmental Research and Development Program. “Solar Water Heating: Well-Proven Technology Pays off in Several Situations.” Federal Technology Alert. DOE/GO-10098-570, May 1996.
- United States. Washington State Department of Transportation. Washington State Ferries. “M/V Tillikum: Vessel Information.” Washington State Ferries: Vessel Information: M/V Tillikum. 12 July 2005
<http://www.wsdot.wa.gov/ferries/your_wsf/our_fleet/index.cfm?vessel_id=43>.
- Vanguard System Inc. “Compax-L PEX-Aluminum-PEX (PAX) Tubing” 4 Jan. 2006
<<http://www.vanguardpipe.com/paxtechdata.htm>>.
- Walls, Ian G. The complete book of the greenhouse. London: Ward Lock, 1988.
- Wilson, R. and J. Jones. Energy, Ecology, and the Environment. Academic Press, 1974.

Appendix A: LCA Matrices

Process:		Life Cycle Inventory for Gravel Pit Seasonal Storage																				
	unit	Gravel Extraction	Pipe Extrusion	Polypropylene Production	Hydraulic Digging	Diesel burned	Lubricating Oil	Electricity Production (US mix)	Natural Gas-burned	PE Production	Light Fuel Oil-burned	Heavy Fuel Oil-burned	Diesel at storage	Truck	Rail	Barge	Ocean Freighter	wool LCI (from conc.)	BEES	Natural Gas, high pressure at consumer		
Technology Matrix, A	Gravel (kg)	1	0	0	0	0	0	0	0	0	0	0	0	0	0	0	0	0	0	0	0	
	Pipe (kg)	1	0	0	0	0	0	0	0	0	0	0	0	0	0	0	0	0	0	0	0	
	PP Liner (kg)	1	0	0	0	0	0	0	0	0	0	0	0	0	0	0	0	0	0	0	0	
	Hydraulic Digging m ³	1	0	0	0	0	0	0	0	0	0	0	0	0	0	0	0	0	0	0	0	
	Diesel Burned MJ	-4.9	0	0	0	0	0	0	0	0	0	0	0	0	0	0	0	0	0	0	0	
	Lubricating Oil kg	0	0	0	0	0	0	0	0	0	0	0	0	0	0	0	0	0	0	0	0	
	Electricity kWh	-0.54	0	0	0	0	0	0	0	0	0	0	0	0	0	0	0	0	0	0	0	
	Natural Gas-burned MJ	0	0	0	0	0	0	0	0	0	0	0	0	0	0	0	0	0	0	0	0	
	LDPE kg	0	0	0	0	0	0	0	0	0	0	0	0	0	0	0	0	0	0	0	0	
	Light Fuel Oil-burned MJ	0	0	0	0	0	0	0	0	0	0	0	0	0	0	0	0	0	0	0	0	
	Heavy Fuel Oil-burned MJ	-7.29	0	0	0	0	0	0	0	0	0	0	0	0	0	0	0	0	0	0	0	
	Diesel at storage and up KG	0	0	0	0	0	0	0	0	0	0	0	0	0	0	0	0	0	0	0	0	
	Truck ton-mi	-0.01	-0.29	-0.5	0	0	0	-0.17	0	0	0	0	0	0	0	0	0	0	0	0	0	
	Rail ton-mi	0	-0.05	-0.03	0	0	0	-0.1	0	0	0	0	0	0	0	0	0	0	0	0	0	
	Barge ton-mi	-0.01	-0.01	-0.01	0	0	0	0	0	0	0	0	0	0	0	0	0	0	0	0	0	
BEES Min. Wool kg	0	0	0	0	0	0	0	0	0	0	0	0	0	0	0	0	0	0	0	0		
Natural Gas, high pressure at c MJ	0	0	0	0	0	0	0	0	0	0	0	0	0	0	0	0	0	0	0	0		
Intervention Matrix, B	Water kg	-4.82	0	0	0	0	0	0	0	-2.95	0	0	0	0	0	0	0	0	0	-0.16	-1.23	
	Gravel (in ground) kg	0	0	0	0	0	0	0	0	0	0	0	0	0	0	0	0	0	0	0	0	
	Oil, crude, in ground MJ	0	0	0	0	0	0	0	0	0	0	0	0	0	0	0	0	0	0	0	0	
	Coal, hard, unspecified, in gros. MJ	0	0	0	0	0	0	-5.99	0	0	0	0	0	-53.3	0	0	0	0	0	-0.07	0	
	Gas, natural, in ground MJ	0	0	0	0	0	0	-1.5	0	0	0	0	0	0	0	0	0	0	0	-2.15	0	
	Inputs for other (BTU) MJ	0	0	0	0	0	0	-0.48	0	0	0	0	0	0	0	0	0	0	0	-2.23	0	
	residual oil (BTU) MJ	0	0	0	0	0	0	-0.11	0	0	0	0	0	0	0	0	0	0	0	-0.17	-14.1	
	uranium (BTU) MJ	0	0	0	0	0	0	-0.7	0	0	0	0	0	0	0	0	0	0	0	-0.04	0	
	Sodium chloride, in ground kg	0	0	0	0	0	0	0	0	0	0	0	0	0	0	0	0	0	0	-0.25	0	
	Calcite, in ground kg	0	0	0	0	0	0	0	0	0	0	0	0	0	0	0	0	0	0	-0.36	0	
	US Dollars (2005) \$	-19.1	0	0	0	0	0	0	0	0	0	0	0	0	0	0	0	0	0	-1.11	-1.11	
	Heat (waste) MJ	0	0	0	0	0	0	0	0	0	0	0	0	0	0	0	0	0	0	0	0	
	Carbon dioxide, fossil kg	0.42	0.076	0.712	0.057	0.15	0.832	0.124	0.03	0.034	1.22	0.49	0.111665	0	0	0	0	0	0	0	0	0
	Carbon monoxide, fossil kg	5E-04	2E-05	9E-05	4E-05	5E-04	8E-04	2E-04	8E-05	4E-05	0	0	0	0	0	0	0	0	0	0	0	0
	Dinitrogen monoxide, N2O kg	0	4E-07	9E-06	1E-06	1E-10	1E-05	3E-06	7E-07	8E-07	0	0	0	0	0	0	0	0	0	0	0	0
Methane kg	0.003	2E-07	1E-05	1E-06	0.003	0.004	2E-06	1E-06	8E-07	0	0	0	0	0	0	0	0	0	0	0	0	
Nitrogen oxides kg	5E-04	8E-05	8E-04	5E-05	2E-04	0.002	8E-04	8E-04	4E-04	0	0	0	0	0	0	0	0	0	0	0	0	
MIVOC, non-methane volatile kg	2E-05	7E-07	8E-06	3E-06	5E-04	3E-04	4E-05	2E-05	2E-05	0	0	0	0	0	0	0	0	0	0	0	0	
Particulates, < 10um kg	0	3E-06	8E-05	4E-06	0	1E-04	1E-05	2E-05	1E-05	0	0	0	0	0	0	0	0	0	0	0	0	
Sox kg	7E-04	1E-04	0.002	3E-07	5E-04	1E-03	3E-05	5E-05	1E-04	0	0	0	0	0	0	0	0	0	0	0	0	


a = Raw data from Ecoinvent may not be published

Appendix B: UWME DFE laboratory scoring method

ISO14040 Data Quality Indicators	Supporting Information	Scoring Method
(UWME ID DQS1) Time-related coverage (i.e., data age)	<ul style="list-style-type: none"> Start date of valid time span (SPOLD ID 601, 603, 611) End date of valid time span (SPOLD ID 602, 603, 611) 	Deviation from intended period (1) Less than three years difference to the year of study (2) Less than 6 years difference (3) Less than 10 years difference (4) Less than 15 years difference (5) Age of data unknown or more than 15 years of difference
(UWME ID DQS2) Geographical coverage	<ul style="list-style-type: none"> Area and country names (SPOLD ID 662 & 663, 401, 3703) 	Deviation from intended area (1) Data from area under study (2) Average data from larger area in which the area under study is included (3) Data from area under similar production conditions (4) Data from area with slightly similar production conditions (5) Data from unknown area or area with different production conditions
ISO14040 Data Quality Indicators	Supporting Information	Scoring Method
(UWME ID DQS3) Technology coverage	<ul style="list-style-type: none"> Technology description (SPOLD ID 692, 492) Included processes (SPOLD ID 402, 492) Extrapolations (SPOLD ID 726) 	Deviation from intended technology (1) Data from enterprises, processes, and materials under study (2) Data from processes and materials under study but different enterprises (3) Data from processes and materials under study but different technology (4) Data on related process and materials but same technology (5) Data on related process and materials but same technology
(UWME ID DQS4) Precision, completeness, and representativeness of the data	<ul style="list-style-type: none"> Sampling procedure (SPOLD ID 725) Number of samples (SPOLD ID 3792) Absolute sample volume (SPOLD ID 722) Relative sample volume (SPOLD ID 724) Extrapolations (SPOLD ID 726) Uncertainty adjustments (SPOLD ID 727) 	Representativeness for intended process (1) Very high (data represent all aspects of the system under study) (2) High (data represent a majority subset of the system under study) (3) Moderate (data represent a minority subset of the system under study) (4) Low (data represent an example of the system under study) (5) Very low or unknown (the extent to which the data represents the system under study is unknown)
ISO14040 Data Quality Indicators	Supporting Information	Scoring Method
(UWME ID DQS5) Consistency and reproducibility of the methods used throughout the LCA	<ul style="list-style-type: none"> Description of method for data collection and data treatment (SPOLD ID 802, 803) 	(1) Very high (Data are based on direct measurements using a widely accepted test methods or on sound engineering models representing current technology and have been extensively peer reviewed. Also, the source provides a transparent account of the assumptions made.) (2) High (Although the data are based on a generally sound test method or model and the source provides a transparent account of the assumptions made, the data are dated or lack enough detail for adequate validation or have not been extensively peer reviewed.) (3) Moderate (Data are based on an unproven or new methodology or are lacking a significant amount of background information.) (4) Low (Data are based on a generally unacceptable method, but the method may provide an order-of-magnitude value of the flow.) (5) Very low or unknown (Data are based on an unknown method, but the method may provide an order-of-magnitude value of the flow.)
(UWME ID DQS6) Sources of the data and their representativeness	<ul style="list-style-type: none"> References used for data collection and data treatment (SPOLD ID 756-762, 1002-1013, 5615, 5619) 	Type of reference (1) Data from reviewed source (2) Data from public written source (not reviewed) (3) Data from closed written source (not reviewed) (4) Other sources (5) Unknown source
ISO14040 Data Quality Indicators	Supporting Information	Scoring Method
(UWME ID DQS7) Uncertainty of the information	<ul style="list-style-type: none"> Mean value (SPOLD ID 3707) Standard deviation (SPOLD ID 3709) Uncertainty type (SPOLD ID 3708, 3792) Description of strengths and weaknesses (e.g., occurrence of data gaps) 	Coefficient of variance (1) Below 10% (2) 10 – 25% (3) 25 – 50% (4) 50 – 100% (5) Over 100% or unknown

Appendix C: SRCC Collector Certification Page

Thermo Technologies • TMA-600-30

SOLAR COLLECTOR CERTIFICATION AND RATING  SRCC OG-100	CERTIFIED SOLAR COLLECTOR SUPPLIER: Thermo Technologies 5560 Sterrett Place Suite 115 Columbia, MD 21044 MODEL: Mazdon TMA-600-30 COLLECTOR TYPE: Tubular CERTIFICATION #: 100-1998-001A
---	--

COLLECTOR THERMAL PERFORMANCE RATING							
Megajoules Per Panel Per Day				Thousands of Btu Per Panel Per Day			
CATEGORY (Ti-Ta)	CLEAR DAY 23 MJ/m ² ·d	MILDLY CLOUDY 17 MJ/m ² ·d	CLOUDY DAY 11 MJ/m ² ·d	CATEGORY (Ti-Ta)	CLEAR DAY 2000 Btu/ft ² ·d	MILDLY CLOUDY 1500 Btu/ft ² ·d	CLOUDY DAY 1000 Btu/ft ² ·d
A (-5°C)	46	35	23	A (-9°F)	44	33	22
B (5°C)	45	33	22	B (9°F)	42	31	21
C (20°C)	42	30	19	C (36°F)	40	29	18
D (50°C)	35	24	13	D (90°F)	33	23	12
E (80°C)	27	17	6	E (144°F)	26	16	6

A-Pool Heating (Warm Climate) B-Pool Heating (Cool Climate) C-Water Heating (Warm Climate) D-Water Heating (Cool Climate) E-Air Conditioning

Original Certification Date: April 20, 1998

COLLECTOR SPECIFICATIONS

Gross Area:	4.581 m ²	49.31 ft ²	Net Aperture Area:	3.381 m ²	36.39 ft ²
Dry Weight:	89.4 kg	197 lb	Fluid Capacity:	0.7 l	0.2 gal
Test Pressure:	1034 kPa	150 psig	Max. Oper. Temp.:	130 °C	266 °F

COLLECTOR MATERIALS

Frame:	Stainless Steel
Cover (Outer):	Iron Free Glass Vacuum Tube
Cover (Inner):	None
Absorber Material:	Tube - Copper / Plate - Copper Fin
Absorber Coating:	Black Chrome
Insulation (Side):	Vacuum
Insulation (Back):	Vacuum

PRESSURE DROP

Flow		Δ P	
ml/s	gpm	Pa	in H ₂ O
40	0.63	935	3.75
80	1.27	3128	12.56
120	1.90	6492	26.06

TECHNICAL INFORMATION

Efficiency Equation [NOTE: (P) = Ti-Ta]				<u>Y Intercept</u>	<u>Slope</u>
S I Units:	$\eta = 0.525$	$-0.8858 (P)/l$	$-0.0074 (P)^2/l$	0.53	-1.421 W/m ² ·°C
I P Units:	$\eta = 0.525$	$-0.1561 (P)/l$	$-0.0007 (P)^2/l$	0.53	-0.250 Btu/hr·ft ² ·°F

Incident Angle Modifier [(S) = 1/cos θ - 1, 0° ≤ θ ≤ 60°]			
K _{en} = 1.0	-0.1441 (S)	-0.0948 (S) ²	(Linear Fit)
K _{en} = 1.0	-0.24 (S)		

Model Tested:	30
Test Fluid:	Water
Test Flow Rate:	76 ml/s 1.20 gpm

REMARKS: Collector tested with long axis of tubes oriented north-south. IAM perpendicular to the tubes is listed above. IAM parallel to the tubes = 1.0 - 0.28(S)

June, 2005

Certification must be renewed annually. For current status contact:
 SOLAR RATING & CERTIFICATION CORPORATION
 c/o FSEC • 1679 Clearlake Road • Cocoa, FL 32922 • (321) 638-1537 • Fax (321) 638-1010

Appendix D: Heat Transfer Simulation Code

```

C:\MATLAB6p5\work\Simulation.m
%Annual Simulation using Hourly Data
%Explicit Eurler Method
clear
clc
Etol=5e5;      %Energy Balance Tolerance (kJ/year)
Ttol=0.25;     %Temperature Tolerance (C), initial temperature-Final
Temperature for year.
K=200;        %Max Number of annual iterations for Energy
Balance(changing input parameters t6, t7, t4, and Ac, initial temps and
collector area).
I=40;         %Max Number of k-loop iterations to minimize tank size
(changing input parameter H, height of tank).
delt=3600;    %seconds in one hour timestep

H=8.605;     %Initial height of Tank (m).

for i=1:I %i loop increases H until energy balance is satisfied.
    clear t4;clear t7;clear t6;clear dt4;clear dt7;clear dt6;clear
IN_OUT; clear k;clear Th;
    %Input Parameters:
    T5=30;     %Greenhouse return temperature (C)
    T2=90;     %Collector return temperature (C)
    Ac=1050;   %Collector Area (m^2)
    Tg=10;    %Temperature of Ground (C)
    A_f=1783.7; %Floor area of greenhouse (m^2)
    th_f=.203; %Floor thickness of greenhosue (m)
    Cap_c=2.06; %Specific thermal capacity of concrete (MJ/m^3-C)
    CAP_h=Cap_c*th_f*A_f; %Equivalent thermal capacity of greenhouse
(MJ/C)
    k_w=2.50e-3; %Conductivity of Gravel-Water (kW/m-K)
    Beta=33; %Tilt angle of collectors from horizontal (degrees)
    %Specific Pump Work
    w_p=0.35; %kJ/kg typical conservative estimate for flow rates.

    %Tank Geometry
    %Input
    slope=70; %Slope of tank wall from horizontal in degrees
    slp=slope/180*pi; %Slope of tank wall from horizontal (rad)
    k_i=0.0389; %Thermal Conductivity of mineral wool from McMaster
(.27 Btu/hr.-F x in./sq. ft. @75° F)McMaster-9332K65
    th=0.86; %Initial Insulation Thickness
    %Geometry Function Output

[SA4, SA7, SA6, SA, UT, Meq4, Meq7, Meq6, CS67, CS47, Vol_ins]=Geo(th, slp, H, k_i);
    Ut=UT; %U value of insulation (W/m^2)
    Amt=CS47; %Cross Sectional Area of Tank between node 4 and 7 (m^2)
    Amb=CS67; %Cross Sectional Area of Tank between node 6 and 7 (m^2)
    %Other Geometry Output
    h=H-2*th; %Storage Volume Height (m)
    L=h/3; %Distance between nodes (m)

```

```

%Initial Temperatures
delbottom=15;
deltop=13;
T7=57; %Mid Tank Temperature (C)
T4=T7+deltop; %Top Tank Temperature (C)
T6=T7-delbottom; %Bottom Tank Temperature (C)
T1=T6; %Pump Outlet Temperature (C)
Thi=18; %Greenhouse initial temperature (C)

%Initial Flow rates
mdot1=.1; %Flow rate to collectors (kg/s)
mdot2=.1; %Flow rate to greenhouse (kg/s)

for k=1:K %k loop adjusts initial temperatures and collector area
until energy balance is satisfied.
    t=1; %Initial Time in Hours from 12:00 am 01/01 (start time is
1:00am 01/01 )
    %Temperatures at year start
    Ti4=T4;
    Ti7=T7;
    Ti6=T6;
    Th=Thi;
    for n=1:8760
        %Specific Heat of water at each node at current time from
Specific
        %Heat as a second order function of Temperature in kJ/kg-C.
        [Cp2]=SpH(T2); [Cp4]=SpH(T4); [Cp5]=SpH(T5);
[Cp6]=SpH(T6); [Cp7]=SpH(T7);
        %COLLECTOR
        [HCl]=coll_new(t,T1,Beta); %Heat collection rate (kW/m^2)
        Q_c=HCl*Ac; %Heat collection rate (kW)
        %set mass flow rate for constant collector temperature output
        if Q_c<10
            mdot1=0;
        else
            mdot1=Q_c/(T2*Cp2-T1*Cp6);
        end
        %Temperature increase from pump
        if mdot1>0.1
            T1=T6+w_p/(Cp6*mdot1);
        else
            T1=T6;
        end
        HEATg(n)=Q_c*delt; %Heat Gain in kJ per timestep

%%%%%%%%%%%%%%%%%%%%%%%%%%%%%%%%%%%%%%%%%%%%%%%%%%%%%%%%%%%%%%%%%%%%%%%%
%%%%%%%%%%%%%%%%%%%%%%%%%%%%%%%%%%%%%%%%%%%%%%%%%%%%%%%%%%%%%%%%%%%%%%%%
        %GREENHOUSE HEAT DEMAND
        [hl,Th]=hload__(t,Th,CAP_h); %Heat load rate (MJ/hour)
        if mdot2==0
            Q_L=Q_L+hl*10^3/3600; %Heat load rate (kW) including
previously unmet timesteps' load
        else
            Q_L=hl*10^3/3600; %Heat load rate (kW)

```

```

end
%set mass flow rate for constant greenhouse temperature
output
if Q_L/(T4*Cp4-T5*Cp5)>0.3226
    mdot2=Q_L/(T4*Cp4-T5*Cp5);
else
    mdot2=0;
end
Q_D=mdot2*(T4*Cp4-T5*Cp5); %Heat delivery rate to load in kW
HEATL(n)=Q_L*delt; %Heat load in kJ per timestep
HEATD(n)=Q_D*delt; %Heat delivered to load in kJ per timestep

%%%%%%%%%%%%%%%%%%%%%%%%%%%%%%%%%%%%%%%%%%%%%%%%%%%%%%%%%%%%%%%%%%%%%%%%
%%%%%%%%%%%%%%%%%%%%%%%%%%%%%%%%%%%%%%%%%%%%%%%%%%%%%%%%%%%%%%%%%%%%%%%%
%STORAGE TANK
%Explicit Euler method solving DT/dt Differential Equations
(1 hour timestep)
T4=T4+delt/(Meq4*Cp4)*(mdot1*Cp2*T2+mdot2*Cp7*T7-
mdot1*Cp4*T4-mdot2*Cp4*T4-k_w*Amt/L*(T4-T7)-Ut*SA4*(T4-Tg)/1000);
T7=T7+delt/(Meq7*Cp7)*(mdot2*(Cp6*T6-Cp7*T7)+mdot1*(Cp4*T4-
Cp7*T7)+k_w*Amt/L*(T4-T7)-k_w*Amb/L*(T7-T6)-Ut*SA7*(T7-Tg)/1000);
T6=T6+delt/(Meq6*Cp6)*(mdot1*(Cp7*T7-Cp6*T6)+mdot2*(Cp5*T5-
Cp6*T6)+k_w*Amb/L*(T7-T6)-Ut*SA6*(T6-Tg)/1000);
Qsla=Ut*(SA4+SA7+SA6)/1000*(T7+T6+T4-3*Tg); %Approximate
storage tank heat loss rate (kW)
Qsl=Ut/1000*(SA6*(T6-Tg)+SA7*(T7-Tg)+SA4*(T4-Tg));

%%%%%%%%%%%%%%%%%%%%%%%%%%%%%%%%%%%%%%%%%%%%%%%%%%%%%%%%%%%%%%%%%%%%%%%%
%%%%%%%%%%%%%%%%%%%%%%%%%%%%%%%%%%%%%%%%%%%%%%%%%%%%%%%%%%%%%%%%%%%%%%%%
%n Loop Heat and Temperature Arrays
%L_(n)=L;
HL(n)=hl;
QL(n)=Q_L;
QD(n)=Q_D;
QC(n)=Q_c;
QSL(n)=Qsl;
Hour(n)=t;
Temp1(n)=T1;
Temp2(n)=T2;
Temp4(n)=T4;
Temp5(n)=T5;
Temp6(n)=T6;
Temp7(n)=T7;
Temph(n)=Th;
CFlow(n)=mdot1;
LFlow(n)=mdot2;
HEATlt(n)=Qsl*delt;
TM(n)=T4-T7;
MB(n)=T7-T6;
t=t+1;
if (T4<T5+2)
    n
    break
end

```

```

        if (T6+2>T2)
            n
            break
        end
    end
end
%k Loop Heat and temperature Arrays
Heat_Gain=sum(HEATg);
Heat_toLoad=sum(HEATD);
Heat_outTank=sum(HEATlt);
Heat_outTotal=Heat_toLoad+Heat_outTank;
IN_OUT(k)=Heat_Gain-Heat_outTotal;
dt4(k)=T4-Ti4;
dt6(k)=T6-Ti6;
dt7(k)=T7-Ti7;
TEMP4(k)=T4;
TEMP7(k)=T7;
TEMP6(k)=T6;
DT=max(abs(dt7(k)),max(abs(dt6(k)),abs(dt4(k))));
if (DT<Ttol)&(abs(IN_OUT(k))<Etol)
    break
end
if n<8760
    k
    Ac
    break
end
t7(k)=Ti7-dt7(k)/7;
if (dt4(k)<-.2)&(abs(dt7(k))<.75);
    delbottom=delbottom*(1+dt4(k)/150);
    deltop=deltop*(1+dt4(k)/175);
end
if (dt6(k)<-.2)&(abs(dt7(k))<.75);
    deltop=deltop*(1-dt6(k)/150);
    delbottom=delbottom*(1-dt6(k)/150);
end
if (dt4(k)>.2)&(abs(dt7(k))<.75);
    delbottom=delbottom*(1+dt4(k)/150);
    deltop=deltop*(1+dt4(k)/175);
end
if (dt6(k)>.2)&(abs(dt7(k))<.75);
    deltop=deltop*(1-dt6(k)/150);
    delbottom=delbottom*(1-dt6(k)/150);
end
t4(k)=t7(k)+deltop;
t6(k)=t7(k)-delbottom;
Ac=Ac-IN_OUT(k)/1e6;
AC(k)=Ac;
T4=t4(k);
T7=t7(k);
T6=t6(k);
end
if (n<8760)
    H=H+0.01
else

```

```

        break
    end
end
end
%%%%%%%%%%%%%%%%%%%%%%%%%%%%%%%%%%%%%%%%%%%%%%%%%%%%%%%%%%%%%%%%%%%%%%%%
%=====cost calc=====
%input
    c_coll=568.6; %specific cost of collector ($/m^2)
    c_ins=71.068; %specific cost of insulation ($/m^3)
    c_st_=77.39; %specific cost of storage, excavation, gravel, and
    piping sys ($/m^3)
    c_lin=68.92; %specific cost of lining ($/m^2)
    c_tub=5.35; %specific cost of tubing ($/m)

%Simulation input
Vol_Eq=(Meq6+Meq7+Meq4)/1000;
[L]=ghHX_(T5,Temp4);
L_tub=L;
%calculation
cost=c_coll*Ac+c_ins*Vol_ins+c_st_*Vol_Eq+c_lin*SA+c_tub*L_tub;
%%%%%%%%%%%%%%%%%%%%%%%%%%%%%%%%%%%%%%%%%%%%%%%%%%%%%%%%%%%%%%%%%%%%%%%%

%=====OUTPUT=====
Ac
Min_Tank_Temp=min(min(Temp6),min(Temp7))
Max_Tank_Temp=max(max(Temp4),max(Temp7))
Heat_Gain=sum(HEATg)
Heat_toLoad=sum(HEATD)
Heat_outTank=sum(HEATlt)
Heat_outTotal=Heat_toLoad+Heat_outTank
Heat_in_out=IN_OUT(k)
Top_Temp_Change=dt4(k)
Mid_Temp_Change=dt7(k)
Bottom_Temp_Change=dt6(k)
Final_Temp_top=Temp4(8760)
Final_Temp_mid=Temp7(8760)
Final_Temp_bottom=Temp6(8760)
H
k
MinStratification=min(min(abs(min(TM)),abs(min(MB))))
MaxStratification=max(max(TM),max(MB))
Vol_Eq
HeatingTubeLength=L
cost
figure (1);
subplot(3,1,1);plot(Hour,Temp4);title('Tank Temp Top');
subplot(3,1,2);plot(Hour,Temp7);title('Tank Temp Mid');
subplot(3,1,3);plot(Hour,Temp6); title('Tank Temp Bottom');
figure (2);
subplot(3,1,1);plot(Hour,QC);title('Collector Heat Supply');
subplot(3,1,2);plot(Hour,QD);title('Greenhouse Heat Load');
subplot(3,1,3);plot(Hour,QSL);title('Tank Heat Loss');
figure (3);
subplot(2,1,1);plot(Hour,CFlow);title('Collector Flow Rate');

```

```

subplot(2,1,2);plot(Hour,LFlow);title('Load Flow Rate');
it=1:k-1;
its=1:k;

figure (5)
plot(AC)
figure(6)
plot(its,dt4,its,dt7,its,dt6);
figure (7)
plot(its,TEMP4,its,TEMP7,its,TEMP6)
figure (8)
plot (IN_OUT)
figure (4)
plot(it,t4,it,t7,it,t6)

```

Storage Geometry Function Code

```

function
[SA4,SA7,SA6,SA,UT,Meq4,Meq7,Meq6,CS67,CS47,V_ins]=Geo(th,slp,H,k_i);
%tank geometry calculator
%all units in meters
%given input:
L=73.152;
W=24.384;

%Initial value calculations
h=H-2*th; %storage volume height
l=L-2*th; %storage volume length
w=W-2*th; %storage volume width

I=5000; %number of elements
dh=H/I; %incremental height
thH=round(th/dh); %number of height increments in thickness

for i=1:I
    a=w*i; %incremental storage cross section area
    csa(i)=w*i; %incremental storage cross section area array
    v(i)=a*dh; %incremental storage volume
    psa(i)=dh*(2*w+2*i); %incremental storage perimeter area
    A=W*L; %incremental pit cross section area
    V(i)=A*dh; %incremental pit volume
    l=l-2*dh/tan(slp); %updated storage length
    w=w-2*dh/tan(slp); %updated storage width
    L=L-2*dh/tan(slp); %updated pit length
    W=W-2*dh/tan(slp); %updated pit width
end
HV=sum(V); %hole volume

```



```

SV=sum(v(1+thH:I-thH)); %storage volume
Meq=SV/1.5*1000; %water equivalent storage mass of gravel-water mix
PSA=sum(psa(1+thH:I-thH)); %perimeter surface area of storage volume
i_t=1+thH; %array number at top of storage volume
i_b=I-thH; %array number at top of storage volume
SA=PSA+csa(i_t)+csa(i_b); %Total surface area of storage volume
i_47=round((I-2*thH)/3)+thH; %array number for one third distance from top of storage
volume
i_67=I-thH-round((I-2*thH)/3); %array number for one third distance from bottom of
storage volume
CS47=csa(i_47); %cross sectional area between nodes 4 and 7
CS67=csa(i_67); %cross sectional area between nodes 6 and 7
SA4=sum(psa(1+thH:i_47))+csa(i_t); %tank to ground surface area of node 4
SA7=sum(psa(i_47+1:i_67)); %tank to ground surface area of node 7
SA6=sum(psa(i_67+1:I-thH))+csa(i_b); %tank to ground surface area of node 6
SV4=sum(v(1+thH:i_47)); %storage volume of node 4
SV7=sum(v(i_47+1:i_67)); %storage volume of node 7
SV6=sum(v(i_67+1:I-thH)); %storage volume of node 6
Meq4=SV4/1.5*1000; %water equivalent storage mass of gravel-water mix at node 4
Meq7=SV7/1.5*1000; %water equivalent storage mass of gravel-water mix at node 7
Meq6=SV6/1.5*1000; %water equivalent storage mass of gravel-water mix at node 6
V_ins=HV-SV; %Volume of insulation
UT=k_i/th; %U value of insulation

```

Specific Heat Function Code

```

function [Cp]=SpH(T)

Cp=9E-06*T^2 - 0.0006*T + 4.1882;

```

Heat Collected Function Code

```

function [HCl]=coll_new(t,T1);
I_T=[1x8760 array];
Temp_a=[1x8760 array];
Theta=[1x8760 array];
G=I_T(t);
Ta=Temp_a(t);
Theta=min(60,theta(t));
S=1/cos(Theta/180*3.14159265359)-1;
Kappa=1.0-.1441*S-0.0948*S^2;
if G>0
    Eff=max(0,0.525-0.8858*(T1-Ta)/G-.0074*(T1-Ta)^2/G);
else

```

```

    Eff=0;
end

```

```

HCl=G*Eff*Kappa/1000; %Heat gain from collector to storage tank in kW

```

Heat Load Function Code

```

function [hl,Th]=hload(t,Th,CAP_h)
%All heat values in MJ
Hg=[1x8760 array];
Hl=[1x8760 array];
Th_i=Th;
if Th<18.1
    hl=max(0,Hl(t)-Hg(t));
else
    hl=0;
end
if Th>24
    Th=Th+min(0,Hg(t)-Hl(t)+hl)/(CAP_h);
else
    Th=Th+(Hg(t)-Hl(t)+hl)/(CAP_h);
end

```

Greenhouse Heat Transfer Function Code

```

function [L]=ghHX_(T5,Temp4)
%Heat Delivery Design, Determine length of tubing needed using finite element explicit
%euler method with 0.1m finite length size
T4=max(Temp4);
l=.5;
Ts= 22;
N=4; %number of loops
[Cp4]=SpH(T4);
[Cp5]=SpH(T5);
Mdot2=0.3226; %minimum flow rate
Q_ =Mdot2*(N*(T4*Cp4-T5*Cp5)); %heat out loop for minimum flow rate and
maximum temperature drop
W=9/12/3.28083989501; %Spacing of tubing (m), set at 9 inches
D_i=0.02192; %Inner diameter of pipe (m)
D_o=0.028575; %Outer diameter of pipe (m)
D_s=((W/4)^2+(4/12/3.28083989501)^2)^.5*2; %Diameter surface corresponding to 4"
of sand and 9" spacing
k_p=1.23; %Conductivity of pipe (W/m-C) from Vanguard Piping Systems, Inc., 2004
k_s=2.25; %Conductivity of wet sand (W/m-C) from Hendrickx.

```

```

k_w=0.65; %Conductivity of water at 330K (W/m-K) from Incropera and DeWitt pg 924
rho=984.25; %Density of water at 330K (kg/m^3) from Incropera and DeWitt pg 924
mu=4.89e-4; %Dynamic viscosity of water at 330K (Ns/m^2) from Incropera and
DeWitt pg 924
Pr=3.15; %Prandtl number for water flow at 330K from Incropera and DeWitt pg 924
Ai=pi*D_i^2/4; %Inner area of tube (m^2)
u=Mdot2/(rho*Ai); %mean velocity of water flow (m/s)
Re=rho*u*D_i/mu; %reynolds number of water flow
f=(.79*log(Re)-1.64)^-2; %Friction factor for pipe from Eqn 8.21 of Incropera and
DeWitt
Nu_D=(f/8*Re*Pr)/(1.07+12.7*(f/8)^.5*(Pr^(2/3)-1)); %Nusult number from Eqn 8.62
of Incropera and DeWitt
h_in=Nu_D*k_w/D_i; %Convection coefficient for pipe
if h_in<10;
    h_in=10;
end
Ri=1/(h_in*pi*D_i); %Thermal Resistance of convection from water to pipe
Rp=log(D_o/D_i)/(1*2*pi*k_p); %Thermal Resistance through pipe wall
Rs=log(D_s/D_o)/(1*2*pi*k_s); %Thermal Resistance through wet sand
R_t=Ri+Rp+Rs;
%R_t=2.339404862;

%Initial Temperature
Tm=T4;

for i=1:10000
    T_l(i)=Tm;
    Length(i)=i*1*N;
    [Cp]=SpH(Tm)*1000;
    Tm=(Tm*Cp*Mdot2*R_t+Ts-Tm/2)/(1/2+Cp*Mdot2*R_t);
    q(i)=((Tm+T_l(i))/2-Ts)/R_t;
    Q=sum(q);
    if Q>Q_/N*1000
        break
    end
end
end
L=i*1*N;

```